Signalling pathways regulating re-epithelialisation and scar-free regeneration of cutaneous wounds in *Danio rerio*

Inaugural-Dissertation

zur
Erlangung des Doktorgrades
der Mathematisch-Naturwissenschaftlichen Fakultät
der Universität zu Köln
vorgelegt von

Manuel Metzger
aus Lindau (Bodensee)

Berichterstatter: Herr Prof. Dr. Matthias Hammerschmidt

Herr Prof. Dr. Mats Paulsson

Vorsitzender der

Prüfungskommission: Herr Prof. Dr. Ulrich Baumann

Tag der mündlichen Prüfung: 07.05.18

1 Abstract

Cutaneous wounds must be closed rapidly to avoid infection. Fish close their epidermal barrier by re-epithelialisation. This work shows that their wounds are closed independent of proliferation by both transforming growth factor beta (TGF-ß) and integrin dependent active cell migration of basal keratinocytes or rhoA associated kinase (ROCK) and jun N-terminal kinase (JNK) regulated cell elongation and intercalation, most likely initiated by the planar cell polarity pathway protein dishevelled. Further the results of this work show that the wounds are initially perceived by the influx of hypotonic medium, which leads to an activation of the phosphoinositide-3 kinase (PI3K) and protein kinase B (AKT) signalling axis that might contribute, possibly in conjunction with TGF-ß, to a relocation of integrins to the lamellipodia of leading-edge keratinocytes or a calcium-dependent activation of actin and myosin.

The result of wound healing in mammals is very often the formation of a scar, which is composed of a collagen network that is not degraded completely during tissue repair and can have a detrimental influence on tissue stability and function. Interestingly, wound healing in teleosts rarely results in fibrosis or scarring. A new putative recruitment pathway of wound fibroblasts via fibroblast growth factor (FGF) was investigated in zebrafish. Thus far, FGF signalling was described to have a direct effect on other processes of wound healing but a direct fibroblast activation has not yet been described. Previously, it was demonstrated that both FGF signalling and immune suppression lead to a lack of granulation tissue and here it is demonstrated that constitutive FGF signalling can overcome simultaneous immune suppression. This supports the hypothesis that leukocytes in the wound secrete FGF to stimulate fibroblast migration and proliferation.

In mammals it was shown that wound fibroblasts are stimulated by resistin-like molecule alpha (Relm-α) to express *plod2* (Lysyl hydroxylase 2). This enzyme leads to a type of collagen crosslinking (dihydroxy-lysinonorleucin, DHLNL) usually found in harder tissues such as bone, cartilage and tendons. Zebrafish lack Relm-α in their genome and their granulation tissue shows no signs of DHLNL crosslinks. Wounding of fish with transient ectopic expression of *plod2b* showed a larger amount of remaining collagen fibrils compared to wild type siblings. These observations suggest a central role of wound fibroblasts in determining the character of the collagen matrix and thereby the decision between rapid tissue repair or regeneration.

2 Zusammenfassung

Hautwunden müssen schnellstmöglich geschlossen werden, um Infektionen zu verhindern. Fische verschließen die epidermale Barriere durch Re-epithlialisierung. Diese Arbeit zeigt, dass ihre Wunden unabhängig von Zellteilung entweder durch TGF-ß- und Integrin-abhängige Zellwanderung von basalen Keratinozyten oder durch ROCK und JNK regulierte Zellstreckung und -Interkalation geschlossen werden. Letzteres wird wahrscheinlich durch das planare Zellpolaritäts-Signalwegsprotein Dishevelled initiiert. Weiterhin demonstrieren die Ergebnisse, dass die Wunden anfänglich durch das Einströmen von hypotonischem Medium wahrgenommen werden, welches zu einer Aktivierung des PI3K und AKT Signalweges führt. Dieser trägt womöglich (vielleicht sogar im Zusammenwirken mit TGF-ß) zu einer Verlagerung von Integrinen an die Lamellipodien der Keratinozyten an der Wundkante bei oder führt zu einer Calcium-abhängigen Aktivierung von Aktin und Myosin.

Das Ergebnis der Wundheilung von Säugern ist häufig die Bildung von Narbengewebe, welches aus einem Kollagen-Netzwerk besteht das während der Gewebe-reparatur nicht abgebaut wurde. Narbengewebe kann drastische Auswirkungen auf die Stabilität und die Funktion von Geweben haben. Interessanterweise resultiert die Wundheilung von Fischen selten in Narben. Ein möglicher neuer Signalweg zur Rekrutierung von Fibroblasten durch FGF wurde in Zebrabärblingen untersucht. Bisher war lediglich bekannt, dass FGF andere Prozesse der Wundheilung direkt beeinflusst aber eine direkte Aktivierung von Fibroblasten konnte noch nicht beschrieben werden. Zuletzt wurde demonstriert, dass sowohl die Unterdrückung von FGF Signalen als auch des Immunsystems zum Fehlen von Granulationsgewebe führt und hier wird gezeigt, dass konstitutive FGF Signale die Auswirkungen von gleichzeitiger Immunsuppression überwinden können. Dies unterstützt die Hypothese, dass Leukozyten in der Wunde FGF sekretieren um Fibroblasten-Wanderung und -Teilung zu stimulieren.

In Säugetieren wurde gezeigt, dass Wund-Fibroblasten durch Relm-α zur Expression von *plod2* (Lysyl Hydroxylase 2) angeregt werden. Dieses Enzym führt zu einer Art von Kollagen-Vernetzung (Dihydroxy-Lysinonorleucin, DHLNL), die üblicherweise nur in härteren Geweben wie Knochen, Knorpel oder Sehnen zu finden sind. Zebrabärblinge tragen kein Relm-α in ihrem Genom und ihr Granulationsgewebe zeigt keine Anzeichen für DHLNL-Vernetzung. Wundheilungs-Experimente mit Fischen, die transient und ektopisch *plod2b* exprimieren, zeigen eine höhere Menge von übrigem Kollagen im Vergleich zu Wildtypen. Diese Beobachtung legt eine zentrale Rolle der Fibroblasten bei der Festlegung der Kollagen-Matrix Eigenschaften und daher der Entscheidung zwischen schnellstmöglicher Gewebereparatur oder Regeneration nahe.

3   Introduction

3.1   <u>Skin function and structure of mouse and fish</u>

The skin is the interface of organisms with their outside environment. Thus, its main function is to protect the body from potential harm and external influences like pathogen infection, chemical or physical damage and - especially vital for land-living animals - desiccation [1]–[3]. Several similarities and differences can be found in the skin of both mammals and teleosts. While the overall structure is comparable, minor details characterise the skin of the different classes.

3.1.1   <u>*The epidermis is the barrier to the outside world*</u>

The epidermis is the outermost compartment of the skin and is the main tissue responsible for this protection against the outside. In adult mammalian organisms, the epidermis is a stratified epithelium and consists of the basal keratinocytes, the spinous and the granular layer and the outermost cornified layer (Fig. 1.1). The basal keratinocytes are responsible for the balance between shed corneocytes from the outermost layer and supply of new keratinocytes as replacement, as they are the only cells with proliferative potential within the epidermis. This balance is known as epidermal homeostasis [4], [5]. After asymmetric cell division of a basal keratinocyte the daughter cell loses contact to the basement membrane, enters the spinous layer and starts terminal differentiation. This includes loss of proliferative potential, a switch in keratin gene expression and the formation of a more stable intermediary filament, which is interconnected with desmosomes to neighbouring keratinocytes [5]. Keratinocytes continue to differentiate as they get pushed further towards the outside and the cornified envelope is formed. For this purpose, structural proteins like periplakin, envoplakin and involucrin are expressed and form heterotrimers. These are localised to the plasma membrane in a calcium-dependent manner and form a thin intracellular filament, which is crosslinked by transglutaminases. In the granular layer, the cells start to form lamellar bodies that contain a high amount of lipids, which are transported to the plasma membrane and secreted to the extra-cellular space [5], [6]. Among those lipids are long-chain ceramides that replace the plasma membrane over time and are connected to the layer of structural proteins (periplakin, envoplakin and involucrin) on the inner side of the cell membrane by transglutaminases. Simultaneously, organelles, microtubules and microfilaments as well as desmosomes and other cell junctions are degraded, leaving a dead cell body behind. The corneocytes in the outermost epidermal layer then only consist of lipids, intermediary filaments (keratins) and the aforementioned structural proteins [6].

The adult teleost epidermis differs from mammalian epidermis in several important aspects. The stratification is not as complex as in mammals. Instead of four distinct layers, there are just three distinguishable layers in zebrafish: the basal, the intermediate and the surface layer (Fig. 1.1). While mostly less differentiated keratinocytes dominate the teleost epidermis, more specialised cells can be found in addition, such as ionocytes (osmotic regulation), club cells (secretion of alarm substances) and mucus cells (secretion of mucus to the cell surface, Fig. 1.1, green). In contrast to the mammalian epidermis, not only basal cells are proliferative in zebrafish, but also cells of the intermediate layer. Distinct cellular phenotypes due to

progressive states of cell differentiation, like degradation of organelles or cell shape changes, are not detectable throughout the intermediate layer. Hence, a subdivision into spinous or granular layer is not possible in zebrafish. Genetic markers for terminal differentiation of keratinocytes in mammals are not detectable in teleosts. For example, differential keratin expression, loss of p63 (a basal keratinocyte-specific marker in the mouse epidermis) as well as activated expression of periplakin, involucrin and other structural proteins have not been described in the zebrafish intermediate epidermal layer so far. Periplakin and involucrin are not represented in the fish genome at all according to ZFIN gene database (zfin.org). Another prominent difference is the lack of cornification and keratinisation of the fish epidermis. The adult zebrafish epidermis consists exclusively of living cells that are metabolically active (with exception of the specialised keratinised structures called breeding tubercles). Hence, it resembles the embryonic mouse skin during mid-gestation stages [7]–[9]. The outermost layer of the epidermis in fish consists of superficial cells that are flattened and have a characteristic pattern of furrows and ridges on their apical surface. It has been described that these microridges are caused by the actin-cytoskeleton and required for proper attachment of the mucus to the cell surface [10], [11].

3.1.2 *The dermis provides flexibility, mechanical resistance and nutrient supply*

In contrast to the mammalian epithelial barrier, which provides an impenetrable and water-tight outer body surface, the underlying dermis is more flexible and necessary for the tensile strength of the skin. It is mainly composed of extracellular matrix components and, to a smaller degree, of fibroblasts and immune cells. The extracellular matrix (ECM) consists mainly of collagen type I, III and V, but other components such as fibrillin and elastin additionally contribute to stretch resistance of the skin. The importance of individual components can be concluded from diseases such as Marfan syndrome, induced by mutations in the gene encoding for fibrillin, or Ehlers-Danlos syndrome, caused by impaired collagen processing [12]. Marfan syndrome manifests mainly in musculoskeletal and cardiovascular symptoms, but also includes skin and connective tissue abnormalities (i.e. hyperflexible joints, translucent skin, easy bruising). It is caused by mutations in the gene encoding Fibrillin-1, a major component of the extracellular matrix. Fibrillin has not only structural functions, but also an important role in binding the latent form of the transforming growth factor beta (TGF-ß). Hence, interference with TGF-ß signalling can lead to overlapping phenotypes such as dystrophic scars for example [13]. Ehlers-Danlos syndrome belongs to the group of marfanoid disorders and it exists in several subtypes. It manifests mainly in hyperflexible joints or hyperextensible skin. The underlying molecular cause is assumed to be a deficiency of either of the collagen processing enzymes lysyl hydroxylase and lysyl oxidase or mutations in collagen itself. Both influence the nature of collagen crosslinks in skin, bone and cartilage by changing it to a more flexible and less rigid network [14]–[16].

Cells are mostly found in the upper layer of the dermis, the so-called papillary dermis as well as surrounding areas of blood vessels. The lower compartment of the dermis – the reticular dermis – contains mostly collagen fibres of increased thickness, branching elastic fibres and, to a lesser extent, fibroblasts. The fibroblast is the predominant cell type in the dermis and is derived from the mesenchyme. The main

task of these cells is the synthesis and continuous remodelling of the extracellular matrix. Fibroblasts can alter their gene expression as well as their proliferative or migratory behaviour rapidly and extensively upon different external stimuli, e.g. due to injury. During injury their main task is to lay down a provisory collagen matrix to facilitate a faster migration of other cell types (leukocytes, endothelial cells, and keratinocytes). Fibroblasts have been described to respond to TGF-ß, hepatocyte growth factor (HGF) and several Interleukins (ILs), for example by upregulation of collagen expression, processing or more general cellular behaviours like proliferation.

There are morphologically distinguishable, tissue-resident immune-cell types in the dermis: dendritic cells and monocyte-macrophage lineage-derived cells. Dermal dendrocytes are located in the papillary dermis and around blood vessels [12]. They share markers with phagocytic mononuclear cells (macrophages). In addition to phagocytosis, they can also present antigens for further immune response [17]. Dermal macrophages are derived from bone marrow and start their differentiation program once migrated to the dermis. There, they take over antigen presentation, phagocytosis of microbes or malignant cells as well as the secretion of growth factors and cytokines [12]. The interplay of macrophages and fibroblasts during wound healing is especially of interest for this thesis as it was postulated by Eming *et al.* that a perturbation of this signalling axis might be the cause for 'non-healing conditions and excessive scarring' [18]. This topic will be described in more detail in chapter 3.2.3.

The dermis composition of teleosts is highly similar to mammalian dermis. The superficial dermal layer, called stratum laxum, contains mainly loose collagen matrix with numerous fibroblasts, nerves, pigment cells, blood vessels and – in the case of zebrafish - elasmoid scales [9], [19]. The lower layer of the teleost dermis is called stratum compactum and composed mainly of dense collagen-matrix organised in a plywood-like fashion. Vertical bundles of collagen fibres and the special structure of horizontal collagen fibres are assumed to increase the resistance to tensile forces on the skin [9].

3.1.3 *The hypodermis serves as insulation, pressure protection and energy storage*

The last component of mammalian skin, located underneath the dermis, is the hypodermis. This tissue is composed of loose collagen and provides thermal insulation, pressure protection and energy supply. The hypodermis consists mainly of subcutaneous adipose tissue, regulated by energy homeostasis molecules like leptin. The adipocyte number and the lipid content change throughout life. In contrast to mammals, in which melanocytes are located in the epidermis [12], melanocytes in fish are located in the dermis and hypodermis [9].
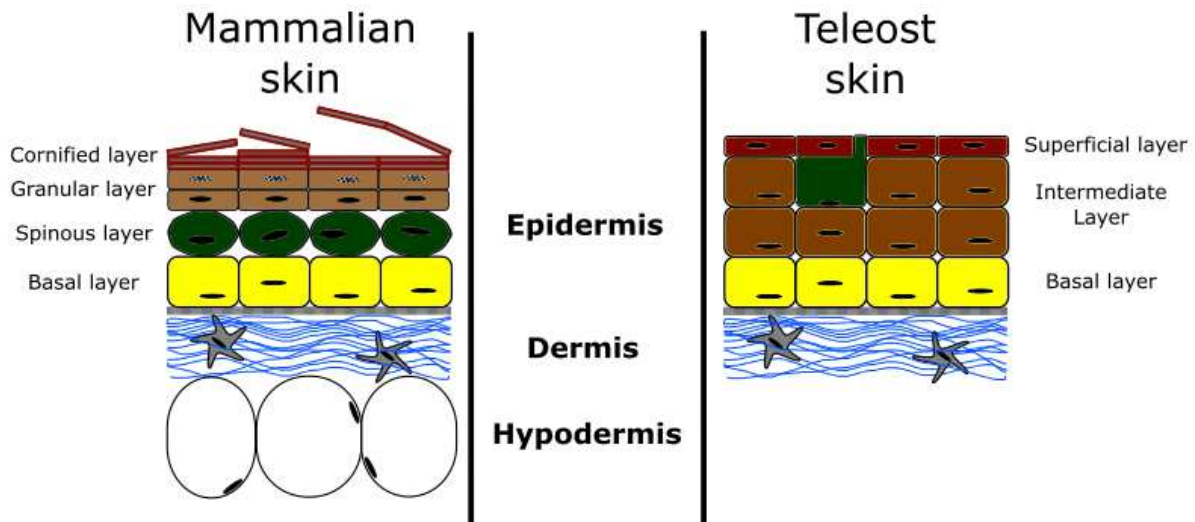
Fig. 1.1: The composition of both mammalian and teleost skin with main focus on the epidermis. From outside to inside, the skin is distinguished in epidermis, dermis and hypodermis. Mammalian epidermis is sub-divided in the proliferative basal cells (**yellow**), the spinous- (**green**), the granular- (**brown**) and the cornified layer (**red**). Cells progressively undergo terminal differentiation, manifesting in a loss of cell organelles and the nucleus, and increasing lipid and keratin deposition. In contrast to the mammalian epidermis, the different layers in the epidermis of teleosts are comprised of living cells only. Furthermore, all cells have the potential to proliferate. Epidermis and dermis are separated by the basement membrane. The dermis consists mainly of collagen fibres (**blue**) produced by fibroblasts (**grey**). The basal-most part of the mammalian skin is the hypodermis containing adipocytes (white), loose collagen, blood vessels and immune cells. Teleost skin in contrast contains scales in the dermal compartment and in most regions of the body, the epidermis and hypodermis are not in such close contact with each other as it is the case in mammals.

3.2   Cutaneous wound healing

The key function of the epidermis is the barrier to the outside world. Since injury disrupts this barrier easily and can happen several times during the life time of an organism, a fast and reliable way is needed to re-establish this barrier. In mammals, this multistep-process includes blood clotting, inflammation, re-epithelialisation, granulation tissue formation and neovascularisation followed by the tissue remodelling phase, aiming for the skin morphology prior to the wounding [20]–[24]. Wound healing in fish is highly conserved, as all of the steps are found in zebrafish as well – with the exception of blood clotting [20].

For our wound healing studies, we used two approaches to inflict injuries on the flank of adult zebrafish: Partial-thickness wounds were introduced by removal of a single scale and disrupt the epidermis (Fig. 1.2B, size of the wound is 0.5 – 0.7 mm by 1 mm). Full-thickness wounds in contrast were the result of injury by dermatology laser and resulted in a disruption of epidermis, scales, dermis, subcutaneous adipose tissue and muscle (Fig. 1.2C, size of the wound is 1.6 mm in diameter). The dynamics of wound healing were different for both wounds due to the size difference and the depth of injury. Prior to my work, it was observed that partial-thickness wounds close by cell migration of keratinocytes [25] and usually do not result in fibrosis (unpublished observation). Full-thickness wounds on the other hand closed mainly by coordinated long-range cell elongation and intercalation of keratinocytes

and caused fibrosis [20], [25]. However, all different aspects of both wound types will be explained in more detail in the following sections.
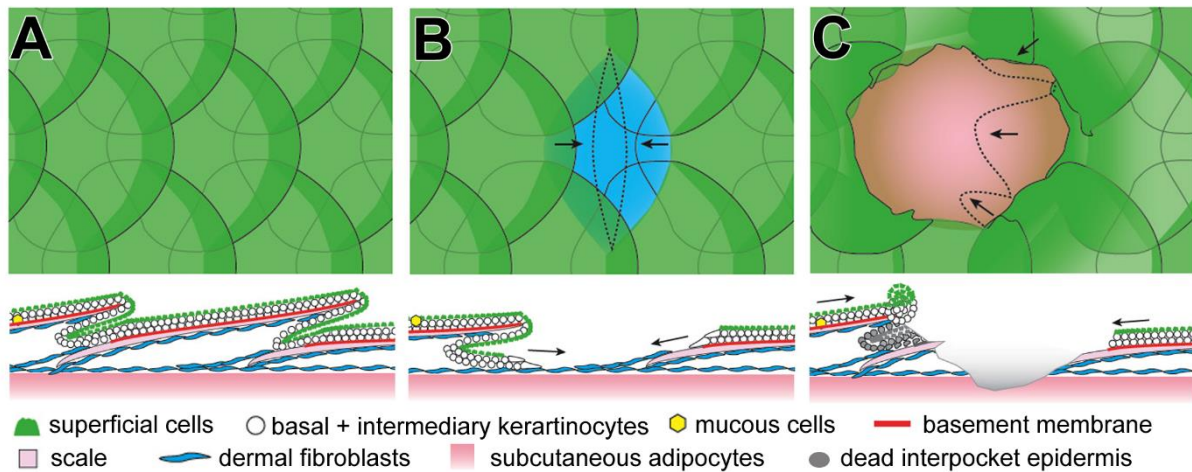
Fig. 1.2: The results of the two different wounding methods used during these studies. In **A**, the outside view of the zebrafish skin illustrates the scales with epidermis covering mainly the apical side. The transverse view below demonstrates the composition in more detail. Superficial, basal and intermediary keratinocytes sit on a basement membrane and a thin dermal compartment on top of the scale. The scale itself is anchored in dermis which sits on top of the hypodermis with the subcutaneous adipocytes. Upon scale removal (partial-thickness wounding, **B**), the epidermis is disrupted but the dermal and hypodermal compartment remains intact. In contrast, laser injury (full-thickness wounding, **C**) results in destruction of epidermis, scales, dermis, and hypodermis and can reach into the muscle. Schematic illustration by Philipp Knyphausen [25].

3.2.1   _Steps of wound healing – a comparison between fish and mammals_

Here, the focus lies on teleost wound healing with frequent comparisons to mammalian organisms to provide further insight into similarities and differences between teleosts and mammals. While the explanation and background information are given here in sequential order, the real time-line in mammals is rather difficult to dissect as many processes happen in parallel and are highly interconnected. For instance, haemostasis is described to be the first step, but provides stimuli (growth factors, cytokines) as well as migration substrate for later appearing cell types [22]. In contrast, zebrafish wound healing appears to follow a more sequential time course and interconnections appear less pronounced [20].

3.2.1.1 Re-epithelialisation of cutaneous wounds

The main goal and first step during wound healing is to seal the organism against the outside environment to avoid loss of body fluids and invasion of pathogens. In mammals, the wounds are initially closed by a blood clot, and re-epithelialisation commences later. The blood clot consists of platelets and fibrin and not only seals the wound and especially the blood vessels, but also provides a pool of growth factors and a migration substrate for leukocytes, fibroblasts and keratinocytes [24], [26]. This is already the first major difference to adult teleosts, since Richardson and co-authors showed that zebrafish wounds initially close by a rapid re-epithelialisation instead of blood clotting. Further they showed that the blockade of blood clotting by treatment with sodium warfarin did not affect wound closure rate, demonstrating that re-epithelialisation of zebrafish wounds is independent of blood clotting [20].

In general, there are three major mechanisms of epithelial closure described. The first mechanism was observed mainly in embryonic mammals, as well as larval zebrafish and *Drosophila*. In these studies, an actin-myosin cable outlines the wound and pulls the epithelium together in a circular manner, thereby closing the wound [25], [27]–[29]. This mechanism is not only connected to wound healing, but also to early development (dorsal closure of *Drosophila* embryos) and hence is one of the earliest methods an organism has in its repertoire to close gaps between epithelial sheets [28].

The second mechanism employs active cell migration and was described in several studies of adult mammalian wound closure, as well as wound closure of other organisms including larval and adult zebrafish [25], [30] and *Drosophila* larvae [29]. This mechanism includes lamellipodial outgrowth of mostly basal keratinocytes, the cyclic attachment and detachment to and from the substrate via integrins and the directed forward locomotion of the epithelial sheet with help of the actin-myosin cytoskeleton. In adult mice for instance, there is a delay of several hours after injury until active cell migration starts and is accompanied by proliferation of keratinocytes further away from the leading edge [22], [23]. Hence it is problematic to distinguish roles of growth factors on wound re-epithelialisation as they can have mitogenic effects, but at the same time inhibit cell migration or vice versa. In adult zebrafish, cell migration occurs independently from proliferation, making it easier to dissect specific roles of growth factors during the time course of wound healing [25].

The third and last mechanism is the coordinated cell elongation and intercalation seen in adult zebrafish described in a publication of our lab [25]. In full-thickness wounds, the migration substrate can be destroyed at times and since there is no provisional matrix such as a fibrin clot present in wounds of adult zebrafish, the epithelium must close the gap without relying on purse-string or migratory behaviour. The epidermal thickness of unwounded regions in the fish is approximately three to four cell layers comprised of one basal, one superficial and two to (rarely) three intermediate layers. During closure of full-thickness wounds, cells of the intermediate layers intercalate with the basal keratinocytes and flatten, leading to a decrease of layering to two cell layers. At the same time, superficial cells elongate, lose their characteristic microridges and thereby increase their surface area dramatically. These effects are propagated to further distant cells over time leading to a gradient of cell layers and thickness over the epidermis. Due to this long ranging intercalation and elongation, the epidermal tongues are pushed into the wound bed progressively

covering it without the need of pulling forces mediated by purse-string or active cell migration. A remarkable observation is that this closure mechanism seems to be prone to overshooting. This means that the thickness of the unwounded epidermis is three to four cell layers, the adjacent epidermis shrinks to two layers but the neo-epidermis can be ten or more layers thick [25].

It is important to mention that the zebrafish utilises all methods of wound closure to different proportions depending on age, size of the wound as well as condition of the migration substrate. This means, the "purse-string" closure by actin-myosin cable is not only seen in embryonic and larval stages as it is the case in mammals, but also during adulthood – if the wound is for instance only a few cell diameters in size. Further, active cell migration is observed as the predominant mode of closure in cases when cells have contact to an intact underlying migration substrate of ECM proteins, as it is the case in our scale removal model (partial-thickness wound) or on the borders of full-thickness wounds, when basal keratinocytes are in contact with scales. Lastly, we observe mostly pushing from the back by intercalation and elongation, whenever injuries are too large to be closed by purse-string and leave nothing but damaged substrate and cell debris behind as it is the case for our laser wounding model (full-thickness wound).

A major difference between teleost and mammalian wound closure is that fish do not show a combination of migratory behaviour and proliferation within the epidermis at the same time. While mammalian re-epithelialisation combines both migration and proliferation [24], these two processes are uncoupled in fish, since an increased keratinocyte proliferation happens only three days after full-thickness injury, as shown by Richardson and colleagues [25]. This opens the opportunity for dissection of these two cellular processes and their contribution to epithelial wound closure beyond the fish and allows statements about motogenic and mitogenic influences of cytokines and growth factors.

3.2.1.2 Inflammatory response and neovascularisation

Identical to mammals, in zebrafish the entire wound (epidermal, dermal and hypodermal compartment) must be cleared from pathogens and cell debris rapidly after injury. To achieve this task, specialised immune cells of the innate immune system, such as neutrophils and macrophages, migrate to the injured tissue from adjacent areas [22]. However, the immune response and recruitment in both mammals and teleosts is not limited to the vicinity of the wound but occurs system-wide, since immune cells can also arrive via the blood stream from remote tissues. They arrive passively through disrupted blood vessels [24] and are activated in response to a variety of molecular stimuli such as pathogen-associated molecular patterns (PAMPs) or damage-associated molecular patterns (DAMPs) [31]. Another attraction mechanism was discovered more recently in zebrafish larvae by Enyedi *et al.* In this study, the authors observed a recruitment of neutrophils to the wound site triggered by the influx of hypotonic medium from the outside environment [32].

In full-thickness wounds of adult zebrafish, Rebecca Richardson demonstrated the presence of leukocytes as early as four hours post wounding (4 hpw) at the borders

of the injury. By vital dye penetration assay in combination with transgenic fish labelling neutrophils (*Tg(mpx:gfp)*), she observed that neutrophils stay behind the leading edge and are not observed in the centre of the wound before closure is complete. Over the period of healing the absolute and relative number of neutrophils and macrophages varies. During the early phase of the inflammatory response (4 hpw), neutrophils are the dominant immune cell type, which shortly later (24 hpw) shifts towards macrophages [20]. This shift from neutrophils to macrophages has been described in mammals as well [33]–[35]. Overall numbers of both neutrophils and macrophages decline in zebrafish until day four post wounding [20].

The main function of leukocytes during early wound healing is the decontamination of the injury site. There are diverse methods with which neutrophils can kill microorganisms, for example by release of reactive oxygen species, cationic peptides, eicosanoids, and proteases. However, it is assumed that these substances cause collateral damage as they are not only lethal for the pathogens but also for neighbouring host cells and thereby might not be fully beneficial for wound healing [36]. Another remarkable mechanism to hunt down microorganisms is the NETosis. Neutrophils can undergo a specialised form of cell death in order to pin down and trap pathogens in extracellular traps (neutrophil extracellular traps: NETs), consisting of their own chromosomal DNA intermingled with histones and lysosomal peptides [37], [38]. However, the impact NETosis could have on wound healing is speculated to be extremely low and rather counterproductive, similar to the antimicrobial procedures [39].

In parallel to the decontamination of the site of injury, leukocytes are an important source of cytokines. They are assumed to stimulate cell migration and proliferation in mammalian wounds as well as alterations of expression profiles of several different cell types such as keratinocytes, fibroblasts and endothelial cells [24]. Re-epithelialisation for instance can be stimulated by neutrophils via Interleukin (IL)-1, IL-6 and tumour necrosis factor alpha (TNF-α) [40]. Macrophages have been shown to release epidermal growth factor (EGF), platelet-derived growth factor (PDGF), transforming growth factor (TGF)-ß, IL-1, IL-6 and TNF to stimulate the closure of the wound [40]. Further, it has been shown that especially Interleukin-1 can stimulate fibroblast and keratinocyte growth [41]–[43] and indirectly modulate the extracellular matrix by directing synthesis and degradation [44]–[46]. TNF-α has been described to act as a chemoattractant for fibroblasts [47], which indirectly influences collagen deposition and thereby fibrosis. Simultaneously, exogenous TNF application increases collagenase activity, leading to an enhanced degradation of the collagen [44].

Macrophages are observed at 2-3 days post injury during mouse wound healing. They arrive as undifferentiated monocytes via the blood stream and differentiate at the site of injury into different subsets of macrophages [21]. Classically activated, pro-inflammatory macrophages, also known as M1-macrophages, are activated by bacterial cues such as lipopolysaccharides (LPS) and interferon-γ (IFN-γ) [48]. They show phagocytic activity and express pro-inflammatory cytokines such as IL-1 and TNF-α [48], [49]. M1 macrophages – like neutrophils – can kill pathogens by increased oxidative bursts and nitric oxide production [48]. They contribute to the acute inflammation during wound healing, but also to chronic inflammation in the skin for example during psoriasis [50]. In contrast, alternatively-activated macrophages (M2 macrophages) act anti-inflammatory after stimulation by IL-4 and IL-13 by induction of angiogenesis via the release of VEGF to clear the wound of antigens

rapidly [51]. There are also indications that M2 macrophages can directly decrease inflammation by the uptake of antigens thus making them unavailable for leukocyte presentation [48]. In zebrafish, it still remains to be elucidated whether these subgroups of macrophages exist. Studies in rainbow trout demonstrated, that fish make use of inducible nitric oxide synthase (iNOS) to produce reactive N-species for host defence, which partly determines the phenotype of classically activated M1 macrophages [52]. Further, it was shown that the teleost immune system reacts to the same pro-inflammatory signals as in mice (IL-1ß and TNFα) [53], [54]. Likewise, anti-inflammatory response genes can be found in the genome of different teleosts, such as IL-4 and IL-10, but whether their function of decreasing the inflammatory response by negatively regulating *il-1* and *tnfα* expression is similar to mammals remains unknown [55]–[57].

Neovascularisation of wounds in mice takes place during the first few days after injury. Driven by growth factors like acidic and basic FGF2, VEGF, and TGF-ß, capillaries sprout into the provisional fibrin and fibronectin matrix of the blood clot. During this invasive outgrowth, aVß3 integrins mediate the interaction between the endothelial cells and the fibronectin-rich ECM of the wound. As soon as the granulation tissue (see 3.2.1.3) is formed and matures, the density of the vascular system decreases. The newly formed vascular system is thought to be necessary for gas exchange and nutrient delivery into the hypoxic wound tissue [58]. The vessel network is important for clearance of antigens as well as cell and ECM debris from the wound. Impaired neovascularisation leads to a generally impaired wound healing [22]. Interestingly, in zebrafish, neovascularisation only starts at four days post wounding, when the initial immune response is over and the granulation tissue peaks in size. During the following days, the density of capillaries and covered wound area increase and reach the maximum at the same time as the granulation tissue is resolved completely (8 dpw). During the next two days most of the capillaries disappear and the wound vasculature resembles the vessels of adjacent unwounded tissue in density and size [20]. It can be speculated from these findings that blood vessels in wounds of zebrafish are not absolutely required for the initial support of the tissue and cells, but rather for the clearance of the wound tissue as the increase of vessel density is inversely correlated with the granulation tissue. However, the exact function of wound vasculature in zebrafish wounds needs to be investigated further.

3.2.1.3 Granulation tissue formation and resolution

The new stroma that is formed after injury in the dermal compartment is called granulation tissue and consists of leukocytes, fibroblasts and blood vessels embedded in a collagen matrix [22], [23]. In mice, the chemotaxis of fibroblasts occurs approximately three to four days after the onset of keratinocyte migration and is likely initiated by the growth factor families PDGF and TGF released by leukocytes and keratinocytes directly after injury (reviewed in [23]). Despite commencing the migration later than the keratinocytes, fibroblasts are activated immediately after injury and respond to the same cytokines as the keratinocytes. Their migration is delayed due to the fact that fibroblasts have to change from a quiescent to an activated state and need to shift their integrin expression pattern from collagen-binding (unwounded dermis) to fibrin- and fibronectin-binding (wounded dermis) integrins [22]. In mice, fibroblasts are primarily, but not exclusively attracted to the

wound bed from the healthy dermis around the injury. Other possible sources are fibrocytes, which are circulating through the organism. They are derived from bone marrow progenitor cells [59], as well as multipotent cells found in the dermis which differentiate into dermal fibroblasts if required [60]. Fibroblasts rely on enzymatic proteolysis to migrate into the blood clot and its interwoven fibrin and fibronectin matrix. Upon stimulation with IL-1 and other cytokines, fibroblasts produce proteases such as gelatinases and collagenases as well as plasmin to degrade the ECM [14]. Other cell types like endothelial cells and keratinocytes utilise similar mechanisms to enable migration through the ECM of the scab [61], [62].

In zebrafish, it is unclear whether only resident fibroblasts adjacent to the wound are recruited or additional systemic recruitment takes place resulting in a mix of fibroblasts of different origin. Further it remains unknown by which signals they become migratory, proliferative and active as well as which cells secrete these stimulatory and activating signals.

Once the fibroblasts are activated in mice, they initiate the production and deposition of a provisional matrix. It consists mainly of fibronectin, vitronectin and collagen III. This provisional matrix facilitates blood vessel formation and migration of immune cells and fibroblasts through the wound. Upon reduction of inflammation, the granulation tissue is remodelled, and the ECM degradation of the provisional matrix is in balance with the deposition of new collagen I fibres [63].

In fish, the earliest time point at which a granulation tissue is detected is at two days post wounding. This tissue is clearly distinguishable from healthy skin in cross sections of adult fish. The normally thin dermal compartment of the fish is here expanded and interrupts the adipose tissue and the muscle underneath the dermis. This area is rich in cells positive for immune cell markers like *mpx* (for neutrophils and macrophages) and *lyz* (for neutrophils specifically) at this early time point. Fibroblasts increase in number from day two post injury on. These cells are characterised by the expression of *col1a2* [20], as well as their highly branched shape [64].

At day four post wounding, the granulation tissue peaks in size and shows a very high density of *col1a2* positive cells interspersed with few macrophages. Only very reduced numbers of neutrophils are detectable within the granulation tissue in comparison to day two after injury. So far it is unclear whether teleost fibroblasts lay down a provisional matrix consisting of fibronectin and vitronectin or other collagen types at all but collagen 1a2 is a very abundant ECM molecule from day two on. Interestingly, not only fibroblasts deposit a new extracellular matrix in fish wounds. Although collagen 1a2 is still predominantly produced by fibroblasts, basal keratinocytes of the neo-epidermis switch on the production as well. Expression of this gene is usually only found during early development in keratinocytes, when the dermis is mainly acellular. As soon as fibroblasts are found in the early developing dermis, *col1a2* expression is silenced again in keratinocytes [9]. This suggests that basal keratinocytes can reactivate its expression as during wound healing. It must be highlighted though, that this occurs only in a spatially restricted manner in the neo-epidermis, where the basement membrane is interrupted as well. Unwounded, wound-adjacent areas are negative for epidermal *col1a2* expression [20].

After day four post injury, the granulation tissue becomes more vascularised and is continuously decreasing in size. It remains unclear, whether fibroblasts migrate out of the wound or undergo apoptosis once they are finished with their task. Furthermore, the collagen content decreases gradually until it is back to normal levels at eight to ten days post wounding. Leukocytes return to normal levels after four days post wounding and the newly formed, dense capillary network retracts again [20].

3.2.1.4 Tissue remodelling and regeneration

In mammals and teleosts, wounding results in very different outcomes (scar tissue versus regeneration). The initial response to wounds in mammals is a seal of the body from the environment as rapidly as possible. Additionally, quick restoration of tissue stability is achieved in the form of stable fibrous tissue deposition at the expense of proper connective tissue regeneration [65]. While this is the case in adult higher vertebrates, mammalian embryos and lower vertebrates such as fish have an incredible capacity to regenerate lost and destroyed tissues. This is not only relevant for cutaneous wound healing, but also for other organs such as the brain and the heart. While a cardiac infarct or a severe brain trauma can be detrimental for mammals, zebrafish are able to remove the fibrotic tissue and restore the organ function to a high degree [66], [67]. It is not known on which genetic and molecular factors this ability to almost perfectly regenerate is based. Most of the cutaneous healing process is thought to be very similar between mouse and fish as they show activity of similar, if not the same cell populations resulting in the same collagen deposition. But in lower vertebrates, this deposition is temporary [20], [66]–[68], whereas in mammals, non-functional fibrotic tissue remains in some cases. It remains to be further investigated, which factors determine whether this fibrotic tissue is completely resolvable (as it is the case in fish) or not resolvable at all. This unresolvable and functionally limited fibrotic tissue is termed scar tissue. The problems scar tissue causes for an organism are numerous. For instance, cutaneous scars of rats after one year post wounding are only resistant to about 80% of tensile forces compared to unwounded tissue [69]. Scar tissue in brain or heart results in much more severe defects. Cardiomyocytes as well as neurons are lost permanently due to a very low regenerative capacity of those organs in contrast to skin. Further, the lost cells are permanently replaced by irreversible scar tissue – either of fibrotic nature or a reactive gliosis in the CNS [70], [71].

The zebrafish regeneration of cutaneous tissue is almost perfect. One month after injury, all tissues are restored to the original state and function, including the epidermis, scales, dermis, pigmentation, adipocytes and subcutaneous muscle [20].

3.2.2 _Genetic and molecular regulation of re-epithelialisation in fish_

To date, cutaneous wound healing studies focussing on the molecular and genetic control mechanisms in adult zebrafish are not very numerous. Despite the potential the zebrafish offers for this type of studies little is known about the influence of for

example cytokines and growth factors on different aspects of wound healing. Due to the methodical accessibility (small-molecule treatment by application into the water, *in vivo* imaging, easy genetic manipulation), zebrafish is used for studying wound healing by our group for several years. We use fish as a model organism to dissect influences of growth factors (TGF-ß, FGF) and signalling pathway components (ROCK, Dishevelled) on cellular processes during cutaneous wound closure and healing as it might give us important information on how to achieve perfect regeneration.

3.2.2.1 Towards dissection of TGF-ß induced migration effects from proliferative effects during re-epithelialisation

TGF-ß1, ß2 and ß3 are some of the earliest growth factors released in injuries. Hence, the influence of TGF-ß on wound closure by re-epithelialisation and fibrosis is investigated extensively. It is secreted in two main forms: the 'large latent complex', in which it is bound to the proteins 'latency-associated protein' and 'latent TGF-ß binding protein', and the 'small latent complex', which is stored in the blood clot and becomes bioavailable upon degradation of the clot. TGF-ß can be separated from the complex by proteolysis, low pH, irradiation and other means. Once in free form, it binds to a type III receptor which presents it to the serine-threonine kinase receptor II. This leads to recruitment and phosphorylation of the type I receptor. The type I receptor binds and phosphorylates Smad2 and Smad3 and they in turn bind Smad4. The smad-complex then translocates to the nucleus to initiate target gene transcription [72]–[74]. Studies on TGF-ß are challenging in mice, since this growth factor family has many and sometimes even opposing effects. For example, it was described that TGF-ß is beneficial for keratinocyte migration while inhibiting proliferation [75]. Surprisingly, *smad3*-deficient mice, in which the TGF-ß signalling pathway is interrupted, showed an increased rate of re-epithelialisation as well. The authors hypothesise that this is due to a decrease of apoptosis [76]. Similar effects have been reported for keratinocyte-specific *smad4*-knockout mice, which are incapable of TGF-ß and BMP dependent gene translation. In these mice, increased keratinocyte proliferation during the re-epithelialisation phase occurred which could explain the faster closure [77]. This example shows the difficulties that arise when cellular processes are tightly linked together by the same regulatory system and happen at the same time.

In fish, however, increased proliferation was only observed after re-epithelialisation. Therefore, studies in this model allow investigation of the influence of TGF-ß solely on cell migration after full- and partial-thickness wounding independently from the influences of TGF-ß on proliferation [25].

3.2.2.2 Planar cell polarity and Rho-associated kinase (ROCK) during coordinated epithelial movements

During early embryonic development, several cell populations must migrate in a coordinated manner to their destination within the embryo [78]. Cell polarity within a sheet plays an important role during these movements, since all cells need to be

oriented towards the same target and apply forces into the same direction while staying in close contact to avoid ruptures and leakage. It has been demonstrated before that the planar cell polarity (PCP) branch of the Wnt signalling pathway is of high importance during gastrulation [79], [80]. This branch was suggested to be activated by specific Wnt-ligands (zebrafish Wnt5 and Wnt11) binding to the Frizzled receptor and downstream relay by Dishevelled. The Dishevelled protein has three domains: DIX, PDZ and DEP [81]. The DIX domain is required for the canonical Wnt-signalling pathway as it binds Axin, which is an integral part of the ß-catenin destruction complex. The DIX domain is dispensable for the non-canonical pathway (PCP). The PDZ domain functions in both the canonical and non-canonical pathway and is thought to have a role in stability, localisation or tertiary structure of the Dishevelled protein [82], [83]. The DEP domain of Dishevelled is indispensable for planar cell polarity induction but not necessary for canonical (ß-catenin mediated) Wnt signalling [84]. The DEP domain of Dishevelled is suggested to be involved in G protein signalling as well as membrane localisation [80], [85].

The impact of PCP on epidermal wound repair has been reported in a study published in 2010, in which the authors showed that mouse mutants each carrying mutations in several different PCP components (*Vangl2*, *Celsr1*, *PTK7* and *Scrb1*) display an impaired wound healing that was rescued by ectopic expression of *RhoGEF19* [86]. These observations indicate that the PCP pathway and its downstream effectors are not only important for development, but also during wound healing.

Migratory capacity depends on an intact cytoskeleton and specifically the intracellular actin-myosin network. One of the factors that have been described during coordinated cell migration of convergence and extension movements is the Rho-associated kinase (ROCK) [87], [88]. It was shown that zebrafish cells expressing a dominant-negative form of Rok2 transplanted into a wild type zebrafish host exhibit a lack of elongation as well as disturbed orientation along the tissue migratory axis [87]. Since collective cell movements during gastrulation have several aspects in common with mechanisms of re-epithelialisation (sheet coherence, orientation and polarisation), Rho-associated kinase has been the centre of several *in vitro* and *ex vivo* studies on wound healing as well. The common theme is that ROCK inhibition reduces cell-cell contacts (by E-cadherin re-localisation) and thereby impacts collective sheet migration as well as trans-epithelial resistance. Further, dissociation-induced apoptosis is decreased. Additionally, orientation and polarisation of cells is impaired but adherence to the substrate is improved. However, proliferation is decreased in most cases. In summary, ROCK inhibition results in beneficial effects for wound repopulation (but not closure) by strengthening the single-cell migration aspect but simultaneously weakening the sheet cohesion and proliferation potential of cells [30], [89]–[92]. Whether the inhibition of ROCK results in beneficial effects *in vivo* has not yet been fully investigated. Especially the lack of orientation and sheet cohesion might not be beneficial for wound re-epithelialisation in an organism and rather lead to increased inflammation due to a leaky barrier and a delay of complete closure. Our studies in zebrafish allow investigation of both the PCP pathway and ROCK on epithelial closure within an *in vivo* system of a multi-layered epidermis and to solidify and complete the findings previously shown in mice.

3.2.2.3 Hypotonic stress as an early signal for barrier disruption

At present, the most common hypothesis to explain tissue injury detection is the reaction of the innate immune system to damage-associated or pathogen-associated molecular patterns (DAMPs or PAMPs). While PAMPs are the result of invading pathogens, DAMPs are described to be products of the lysis of cells and the release of intracellular components into the extracellular space. Those components, such as nucleic acids, lipids and membranes as well as organelles or intracellular proteins are detectable by the immune system [31]. In response to DAMPs or PAMPs, leukocytes switch on pro-inflammatory genes and release a cocktail of cytokines and growth factors which then results in the mobilisation of several cell types and the wound healing steps described in the previous pages. During the recent years however, it was shown by the research group of Phillip Niethammer that influx of hypotonic medium can attract immune cells in zebrafish. This rapid change in osmolarity from 270-300 mOsm of interstitial fluid to 10 mOsm of fresh water leads to an activation and Ca^{2+}-dependent re-localisation of cytosolic phospholipase a2 (cPLA2) to the nuclear membrane. There, it releases arachidonic acid metabolites, which function as a chemotactic cue for leukocytes [32]. Further, they show that, independent from the responses of leukocytes by arachidonic acid release, the non-lytic release of ATP plays a role in lamellipodia formation of basal keratinocytes [30]. Once secreted to the extracellular space, ATP is able to regulate cell migration possibly via the P2Y2 receptor by Ca^{2+} mobilisation and ERK phosphorylation [93].

This effect could be not only of interest in aquatic animals like fish and amphibians, but also in human medicine. The oral mucosa of mammals is covered by hypotonic saliva [94] and the lung epithelial cells are exposed to airways surface fluid or saliva upon injury as well, which has been implicated recently in zebrafish in increased cell motility and early carcinogenesis [95]. Due to this possible motogenic effect, it is of interest to investigate whether the described effects of hypotonic medium are limited to larval zebrafish only or if this mechanism is still active in adult fish as well.

3.2.3 _Effects of the inflammatory response on granulation tissue composition and scar formation_

The immune response of fish is a prerequisite for granulation tissue formation. If the immune response is suppressed by hydrocortisone treatment, a lack of fibroblast migration into the wound is observed [20]. Fibrosis- and scar-free healing of injuries has been reported for embryonic mice as well [96] and can be completely achieved in adult animals only upon knockout of _pu.1_, which results in an absence of macrophages and neutrophils and consequently a lack of fibrosis [35]. Since fish show scar-free healing even during adult ages [20], it is a valuable model organism to study the interaction between the immune system and collagen-producing wound fibroblasts. Due to the reduced scarring it might help to find crucial differences between mammals and teleosts leading to these different outcomes.

3.2.3.1 Is fibroblast growth factor-signalling required for fibroblast activation?

Immune suppression leads to an absence of a granulation tissue in fish [20]. However, this does not influence the occurrence and the time-frame of re-epithelialisation and neo-vascularisation. Only the stimulation of fibroblasts seems to be affected. Interestingly, abrogation of FGF signalling leads to the very same effects, although the inflammatory response happens normally [20]. In studies with mice, it was described that FGFs are highly moto- and mitogenic for endothelial cells and are necessary to drive angiogenesis [97]. Furthermore, specifically FGF9 plays an important role in hair follicle regeneration and is secreted by γδ T cells. It is perceived by wound fibroblasts, in which it triggers Wnt signalling necessary for hair follicle development [98]. Keratinocyte growth factor (KGF), which is a member of the FGF family, has been reported several years ago to be derived from dermal wound fibroblasts and to act on keratinocytes by stimulating proliferation [99], [100]. Despite the numerous studies of FGFs in wound healing, little is known whether there is an influence directly on fibroblast migration, proliferation or activation thus far. Hence, this thesis also deals with a possible connection of the immune system to wound fibroblasts via FGF signalling.

3.2.3.2 The small cysteine-rich protein Resistin-like molecule alpha (Relm-α)

Alternatively activated macrophages can be defined by expression of several marker genes. One of them, *resistin-like alpha* (*retnla*), encodes Resistin-like molecule alpha (Relm-α), also known as 'found in inflammatory zone' (FIZZ) 1. It was discovered as the first member of a novel gene family in broncho-alveolar lavage fluid from mice with induced allergic pulmonary inflammation [101] and is a small cysteine-rich protein. Since then, two additional family members were found, namely Relm-ß and Relm-γ [102], [103].

Relm-α has since been described to be involved in suppression of Th2 cytokine-dependent inflammatory responses, pointing toward an immune-regulatory function [104]. On the other hand, pro-inflammatory effects have also been described for example in colonic innate immune cells. In this study, Relm-α was found to be mainly expressed by eosinophils and intestinal epithelial cells and less in macrophages [105], while other research groups have detected expression in macrophages [104], white adipose tissue as well as in mammary tissue [102]. These – on the first look – contradictory findings for Relm-α show that its secretion is regulated very differently depending on the tissue context and can result in different outcomes.

Relm-ß was found to be expressed in colon [102] and in lung epithelial cells after induction by Th2 cytokines. Furthermore, *in vitro* data suggest that Relm-ß stimulates type I collagen and α-smooth muscle actin production in fibroblasts and thereby is associated with fibrotic lung diseases [106].

Relm-γ was identified as the last protein of the family and shown to be expressed highest in bone marrow, followed by spleen and leukocytes. Lower levels of expression were found in lung, white adipose tissue and other organs. No expression, in contrast, was detected in brain and testis [103].

To date it is unclear, which protein(s) act as receptor(S) for this secreted signal but there are indications from *in vitro* studies pointing to the toll-like receptor family [107].

More recently, a novel role for Relm-α in fibrosis was demonstrated. According to this work, alternatively activated wound macrophages start expressing and secreting Relm-α in the wounds of adult mice upon stimulation with IL-4 or IL-13 via IL-4 receptor alpha. Through yet unknown mechanisms, extracellular Relm-α is perceived by fibroblasts, which then in turn upregulate several target genes. One of those is *plod2* (coding for Lysyl hydroxylase 2), which is known to modify the crosslinking character of collagen fibrils and will be explained in more detail in the next section [108].

3.2.3.3 Lysyl-hydroxylase 2

Lysyl-hydroxylases are encoded by *plod* genes and found in several organisms, including mice, zebrafish and *C. elegans* [109], [110]. They are enzymes that are of high importance for the determination of collagen cross-linking characteristics. Depending on the isoform, the enzyme can have different target-proteins within the collagen family, but the main function is the hydroxylation of lysine residues of collagens. This modification occurs intracellularly shortly after collagen translation and has an impact on the molecular and biophysical properties. Several congenital connective tissue disorders have been linked to mutations in either of the three known isoforms in humans: mutations in *plod1* were described to cause Ehlers-Danlos syndrome type VI and Nevo syndrome, manifested in hyperflexible joints, hyperextensible skin, skin fragility and kyphoscoliosis [111], [112]. *plod2* has two splice variants (resulting in LH2a or LH2b with 21 additional amino acids) and mutations were linked to Bruck syndrome characterised by osteoporosis, joint contractures, fragile bones and short stature [15], [113]–[117]. Lastly, a mutation in *plod3* was found in patients with growth retardation, craniofacial abnormalities, scoliosis, cataracts, blistering of skin on toes and fingers, thin skin, nail abnormalities and other symptoms similar to those of patients with connective tissue disorders like epidermolysis bullosa [118], [119].

Functionally, LH2 was described to modify lysine residues in the telopeptides of both N- and C-terminus of collagens. This modification results in hydroxylysine residues that are further converted to hydroxyallysine residues by lysyl oxidase in the extracellular space. It leads to the formation of intermolecular hydroxylysylpyridinoline crosslinks between collagen fibrils. These crosslinks are usually found in bone, cartilage, tendon and ligaments [120]. Interestingly, these crosslinks, also known as dihydroxy-lysinonorleucine (DHLNL) crosslinks are mostly absent from skin and basement membrane, where lysylpyridinoline (lysinonorleucine, HLNL) crosslinks are the dominant form. However, this changes under fibrotic conditions, such as lipodermatosclerosis, where an over-hydroxylation of lysyl residues was shown [121].

As mentioned in the previous section, a link between the immune response during fibrosis and LH2 activity was established. *interleukin-4 receptor alpha* (*il4ra*)-deficient mice were shown to have a softer and more flexible granulation tissue, resulting in haemorrhages within the granulation tissue. Ultrastructural analysis revealed irregular outlines and sizes of collagen fibrils. Knipper and colleagues showed that alternatively activated macrophages in the wild type wound express and secrete

Relm-α, which is perceived by fibroblasts. They in turn activate the production of LH2 and hence export collagen fibrils that are crosslinked by DHLNL crosslinks usually found in harder tissue like bones or cartilage. The activity of this pathway was largely decreased in *il4ra* mutant mice and thus the granulation tissue was softer. These findings suggest that this pathway is crucial for the more resistant collagen matrix and scar formation after wounding in mammals [108]. Fish on the other hand, have all components of this pathway represented in their genome, except for *retnla*. Thus, investigation of this pathway might be key to finding the genetic and molecular difference between scar-free healing of lower vertebrates and scarring of higher vertebrates.

4 Aims of this thesis

The goal was to find and characterise both triggers and modulators of cutaneous wound re-epithelialisation. Hence, I aimed to target known regulators of keratinocyte migration by small molecule inhibitor treatment and determine their impact on both partial- and full-thickness wounds in zebrafish by *in vivo* imaging.

Further, the possible interplay between immune response and collagen depositing wound fibroblasts via FGF was examined by a combination of immune suppression and a transgenic approach to over-activate FGF signalling.

Moreover, the influence of Lysyl hydroxylase 2 on the character of collagen crosslinking and the persistence of collagen matrix was investigated by ectopic expression of *plod2b* in adult zebrafish.

5 Results

5.1 Adult zebrafish use active cell migration for closure of partial-thickness and long-range epidermal rearrangements for full-thickness wounds

The first observation after wounding of adult zebrafish is a rapid re-epithelialisation. Prior to my work, Rebecca Richardson and Philipp Knyphausen found two different mechanisms of adult wound closure. One mechanism employs the more rapid lamellipodial crawling of basal keratinocytes at the leading edge whereas the slower 'tissue rearrangements' are achieved by directed elongation and intercalation of keratinocytes [25].

5.1.1 TGF-ß inhibition results in delayed wound closure in partial- but not full-thickness wounds

Although the two main mechanisms of wound closure in adult zebrafish described above were delineated prior to my work, the underlying genetic pathways were not fully understood. One of the main questions was, whether the two different types of wound closure rely on two different modes of genetic and molecular regulation. Based on the data available for factors influencing cell migration *in vitro* and *in vivo*, TGF-ß was a very promising candidate to regulate re-epithelialisation of wounds in adult zebrafish.

Generally, TGF is strongly connected to a reversible 'epithelial to mesenchymal transition' (EMT) [122], lamellipodia formation [89] and a shift of integrin expression and activity [123]. It further has been described to be a key factor for cell migration during mammalian wound re-epithelialisation [24, 25]. Hence, it was intriguing to find out whether TGF-ß has an impact on adult teleost re-epithelialisation as well and might be the key regulator and activator of the migration-based wound closure in zebrafish. In order to study its function, I used small molecule inhibitors for treatment of adult fish, followed by *in vivo* time lapse imaging.

To detect and trace cellular behaviour and cell shape changes resulting from TGF-ß inhibition, I treated age-matched adult transgenic zebrafish expressing membrane-bound GFP under the control of the ubiquitous *actin beta 2* promoter independently with two different TGF-ß-receptor1 (ALK5) inhibitors (SB431542 [125] and LY364947 [126]) and subjected them to *in vivo* time lapse imaging. After pre-treatment with inhibitor- or vehicle-containing system water for four hours, the fish were anesthetised with 0.016% tricaine, embedded in low melting point agarose, intubated, wounded by scale-removal and imaged under fluorescent light. During imaging, a constant water flow containing the inhibitor and anaesthetic was provided to keep the fish anesthetised, alive and under constant influence of inhibitor or vehicle control solution for one and a half hours of imaging.

By *in vivo* imaging, a severe delay in wound closure (0.1% DMSO control 0.1485 ± 0.0364 µm/sec compared to 50 µM SB431542 0.0648 ± 0.0196 and 50 µM

LY364947 0.0665 ± 0.0122 µm/sec) and a defect in lamellipodial behaviour were observed with both small molecule inhibitors (compare Fig. 5.1A DMSO to Fig. 5.1B SB431542 and Fig. 1C LY364947, supplemental videos SV 1-3, quantifications are found in Fig. 5.12).
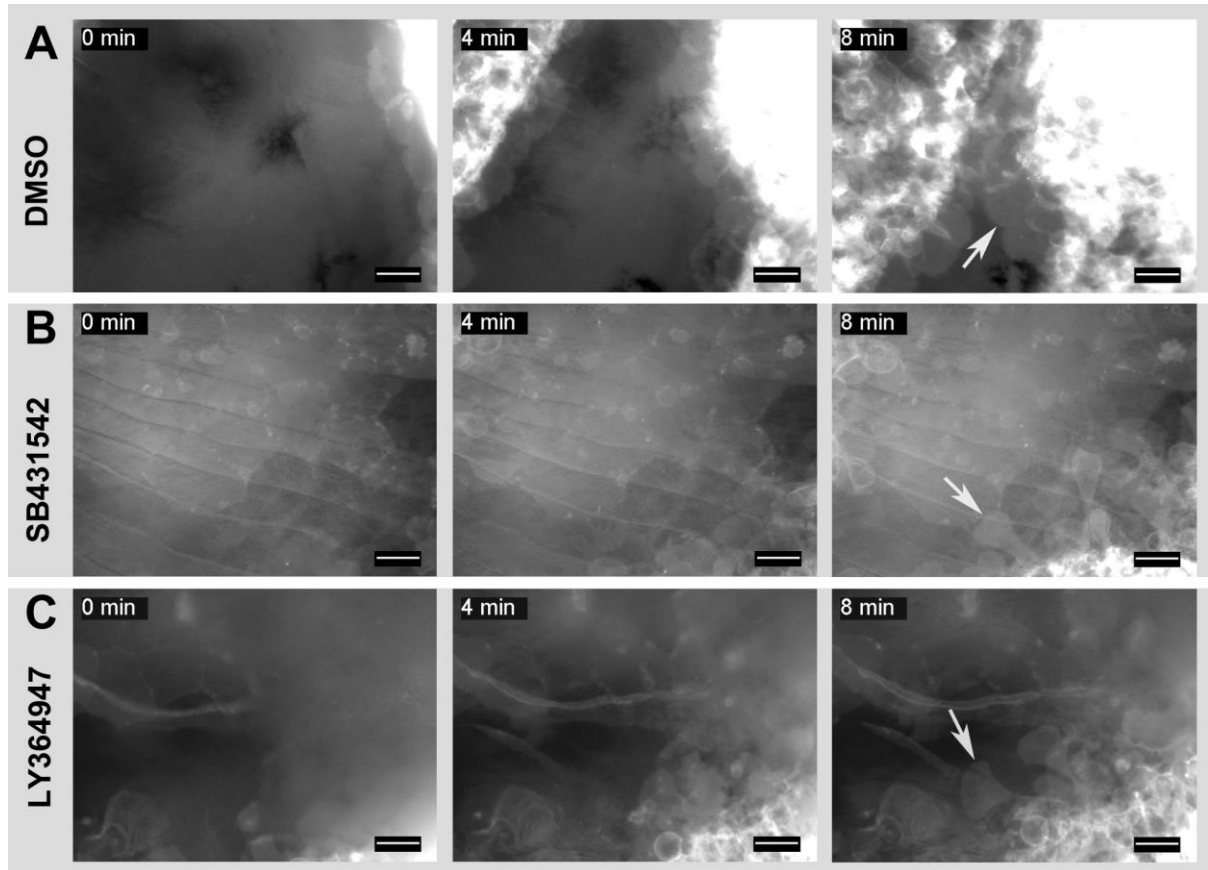
Figure 5.1: Time lapse imaging of partial-thickness wound closure. In DMSO controls (**A**), basal keratinocytes at the leading edge formed lamellipodia of approximately the same size (arrow in **A**) and closed the wound by active cell migration. In this case, the open area was nearly covered at 8 mpw. After treatment with inhibitors targeting the TGF-ß receptors ALK 4, 5 and 7 (SB431542 in **B** and LY364947 in **C**), the wounded region stayed open longer (dark background) and the basal cells formed abnormally shaped and sized protrusions (arrows in **B** and **C**). Anterior to the left, scale bars 20 µm.

While basal keratinocytes of DMSO control fish showed a homogeneous migrating front with similar lamellipodial length and area for each cell at the leading edge (Fig. 5.1A 8 min, arrow), individual lamellipodia reached out far beyond the migrating front in both TGF-ß inhibitor treated fish (Fig. 5.1B and 5.1C, arrows compared to Fig. 5.1A arrow). These individual lamellipodia stretched out to find an attachment point on the migration substrate but failed and retracted shortly afterwards (Fig. 5.2A and 5.2B). Due to this attachment failure at the migrating front, the leading edge most likely was not able to build up enough pulling force, resulting in an overall severely delayed wound closure. Since partial-thickness wounds were introduced with different sizes during *in vivo* imaging depending on the size of the removed scale, quantifications of the closed wound area were not possible. Instead I made use of single cell tracing to record migratory speed of single keratinocytes at different

locations of the leading edge (ten cells at each leading edge per fish). Indeed, after TGF-ß inhibition the migratory speed of all analysed basal keratinocytes within the epithelium was severely affected and reduced by approximately 55% after both SB431542 and LY364947 treatment when compared to DMSO controls (Fig. 5.12A). However, the migration was only reduced and not abrogated completely, meaning that the wound closed eventually.

Taken together, these findings indicate that TGF-ß inhibition does not influence the formation of lamellipodia and the cytoskeletal reorganisations necessary for migration as such, since lamellipodia were still formed. These prerequisites for EMT are unaffected. It rather appeared to influence lamellipodial attachment and cell crawling.

Full-thickness wounds were introduced by a dermatology laser and had a diameter of 1.6 mm. The wound infliction results in destroyed migration substrate and keratinocytes that contribute to closure are devoid of lamellipodia at the leading edge [25]. Given the results in partial-thickness wounds, it was intriguing to find out whether TGF-ß inhibition leads to a delay in the lamellipodia-independent closure in full-thickness wounds. The state of closure was assessed by vital dye penetration assay using methylene blue. Closed wound areas were visualised by exclusion of methylene blue while open areas were permeable.

Interestingly, in full-thickness wounds, no significant decrease of wound closure upon treatment with either TGF-ß inhibitor was observed at 10 hpw (Fig. 5.3A and 5.3B, Quantification in Fig. 5.12B, LY364947 not shown). This strengthened the previous observations of Rebecca Richardson, Thomas Ramezani and Philip Knyphausen, that closure of this wound type is largely independent of active cell migration and lamellipodial crawling. In conclusion, TGF-ß had a major impact on closure of partial-thickness, but not full-thickness wounds of adult zebrafish, by influencing cell migration on the single cell level. This influence was apparent through a failure of cell attachment to the migration substrate and a resulting reduction of overall migration speed.
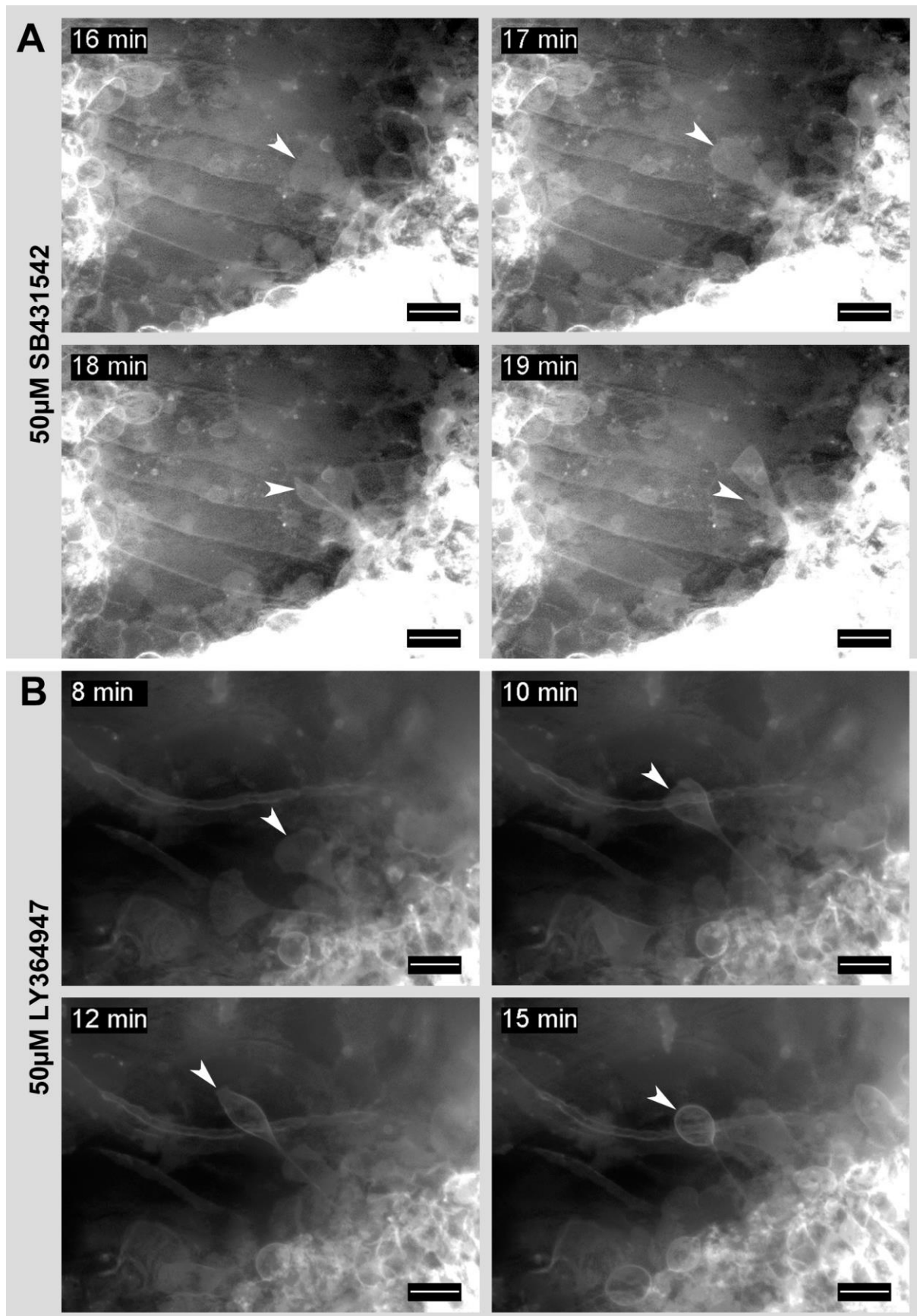
Figure 5.2: Treatment with 50 µM SB431542 (**A**) and 50 µM LY364947 (**B**) lead to a delay in wound closure and abnormally shaped and sized lamellipodia. After both treatments, lamellipodia reached out beyond the leading edge (arrowhead in **A** 16 min and **B** 8 min), tried to attach to the substrate

(arrowhead in **A** 17 min and **B** 10 min), failed to attach (arrowhead in **A** 18 min and **B** 12 min) and retracted again (arrowhead in **A** 19 min and **B** 15 min). Anterior to the left, scale bars 20 µm.
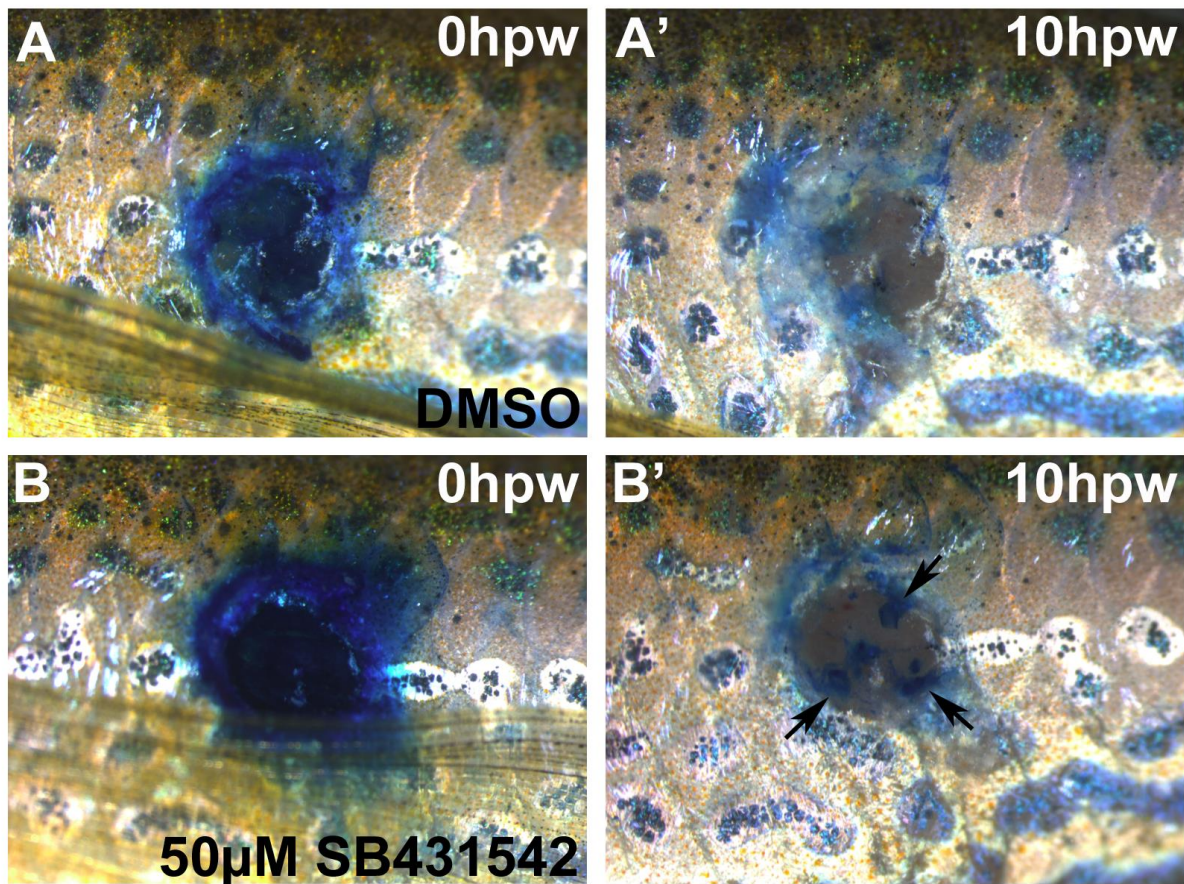
Figure 5.3: Full-thickness wounds of adult wild type fish (TLEK) treated with either 0.1 % DMSO or 50 µM SB431542 inhibitor showed no significant difference in closure at 10 hpw. Pictures **A** and **B** show the methylene blue-stained wound directly after injury. The blue area demonstrates the open wound tissue lacking the epidermal barrier resulting in a penetration of methylene blue. Pictures **A'** and **B'** show the same animal 10 hours later. All spots where the wound is covered by neo-epidermis are impermeable for methylene blue and thereby lack the staining. After evaluation of six fish treated with DMSO and six fish treated with SB431542, no statistical difference in closed wound area was found (**Fig. 5.12B**), despite a small tendency towards more open wound area in SB431542 treated fish (as seen by small blue areas, arrows in **B'**). Anterior to the left.

5.1.2 <u>Binding of Integrins to ECM-components is required for re-epithelialisation of partial-thickness wounds</u>

TGF-ß can mediate a shift in integrin expression and activity [123] and cell attachment is mediated by extracellular integrin receptors (reviewed in [127]). To investigate if a complete failure of cell attachment during re-epithelialisation would result in a similar phenotype, I treated age-matched adult *Tg(actb2:hras-egfp)vu119* fish with DMSO as control, or 1 mM GRGDS peptides for 4 hours prior to wounding. GRGDS peptides compete for binding of integrins to fibronectins [128], vitronectins [129], laminins [130], collagens [131], thrombospondin [132] and osteopontin [133]. After pre-treatment, fish were anesthetised, embedded in low-melting point agarose, intubated, wounded by scale-removal and imaged under fluorescent light.

Although the responses varied in their severity, the most strongly affected case did not show epithelial migration at the posterior leading edge for 25-30 minutes (Fig. 5.4B, SV5), compared to an immediate migration within 5 minutes in DMSO controls. Complete wound closure was achieved in approximately one hour in the most severe case (Fig. 5.4B, SV5), again in contrast to a maximum of 30 minutes in DMSO control fish (Fig. 5.4A). It was observed during *in vivo* imaging that lamellipodia were formed but did not lead to a sheet migration of keratinocytes in treated fish. The lamellipodia were highly active, searching for attachment, but failed to build up pulling forces that are required for closure of partial-thickness wounds. The overall migration speed across all treated fish was severely reduced (0.1% DMSO control 0.1485 ± 0.0364 µm/sec compared to 1 mM GRGDS 0.0785 ± 0.0225 µm/sec) of control migratory speed (Fig. 5.12A), resembling TGF-ß inhibition.

Due to the destroyed migration substrate after laser injury and the results obtained with the TGF-ß inhibitor SB431542 I did not expect an influence of integrin-based cell migration. Hence, I did not test the GRGDS treatment on full-thickness wounds.
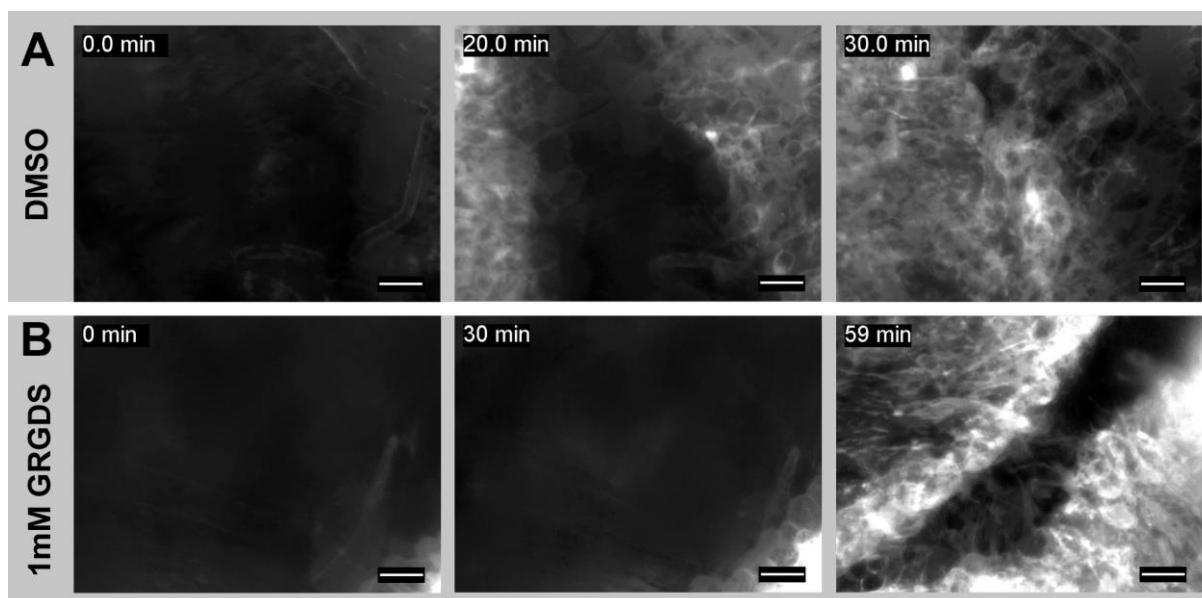

Figure 5.4: Adult wild type fish with partial-thickness wounds were treated with 0.1 % DMSO or 1 mM GRGDS peptides for competitive blockade of integrin-ECM interactions. DMSO control fish showed complete closure of their wounds within 30 minutes in all cases (**A**). In comparison, 1 mM GRGDS

lead to lamellipodia formation with comparable size and shape, yet some of these lamellipodia were elongated and stretched over the leading edge. They seemed to be incapable of attaching to the extracellular matrix. The leading edges were not moving until at least 10 minutes post wounding in all examined fish. Consequently, overall wound closure was severely delayed (**Fig. 5.12A**) and, in this example, was completed after one hour only (**B**). Anterior to the left, scale bars 20 µm.

5.1.3 *Full-thickness wound closure is delayed after suppression of ROCK and JNK activity*

As it became evident by the previous experiments, partial-thickness wounds are primarily closed by lamellipodial crawling of basal keratinocytes, most likely executed by TGF-ß induced alterations in integrin-ECM binding characteristics. Full-thickness wounds behaved differently and were not influenced by TGF-ß inhibition. Thomas Ramezani observed lamellipodia only when keratinocytes were in contact with scales, which happened mainly at the borders of wounds (see supplemental figure 2B and 2C in Richardson *et al.* 2016 [25],). While the epidermal sheet was moving into the wound bed, lamellipodia disappeared and at most filopodia were observed. Coincidentally, cell elongation of superficial keratinocytes became evident adjacent to the wound (Fig. 5.11A and 5.11B). This cell elongation was propagated over time to further distant superficial keratinocytes and lead to a collective orientation of the epithelial cells towards the wound. Concomitantly with directed elongation, superficial keratinocytes lost their characteristic microridges, thus increasing their surface area. Furthermore, undifferentiated keratinocytes of the intermediate epidermal layer started to intercalate with basal cells, leading to a reduction of epidermal layering from approximately four layers down to only two layers [25]. Taken together, these two described processes contributed to the 'cellular replacement reservoir' which was used for wound closure of bigger wounds. This reservoir was additionally increased by recruitment of keratinocytes sitting between the scales in structures known as epidermal pockets (Fig. 5.5A'' arrowhead). The epidermis wraps around scale tips and is present on both the apical and basal side of the scale. In epidermal fluorescently labelled transgenic fish, the fluorescent signal is thereby stronger in the tips than in the base (Fig. 5.5A'' compare arrowhead to arrow). During later stages of re-epithelialisation, these epidermal pockets disappeared mostly due to the long-range recruitment of epidermal cells (Fig. 5.5A' arrow, Fig. 5.5A'' arrow). Indeed, experiments by Philipp Knyphausen with scale-less fish carrying a mutation in the *ectodysplasin receptor* gene (*edar^{t3R367W}* [134]) show that this component has a major impact, as re-epithelialisation is delayed in comparison with fish that have scales. Further, re-epithelialisation of full-thickness wounds in *edar* mutants occurs in a more concentric fashion and epidermal cells enter the wound not predominantly from the posterior but both from the anterior and posterior side [25]. In support of these conclusions implicating a role for scale epidermal cells in rapid wound closure, I showed that wounds in naturally scale-free areas, such as the forehead, closed more slowly and in a more concentric fashion than wounds on the flank, resembling the *edar* mutant (Fig. 5.5B and 5.5B').
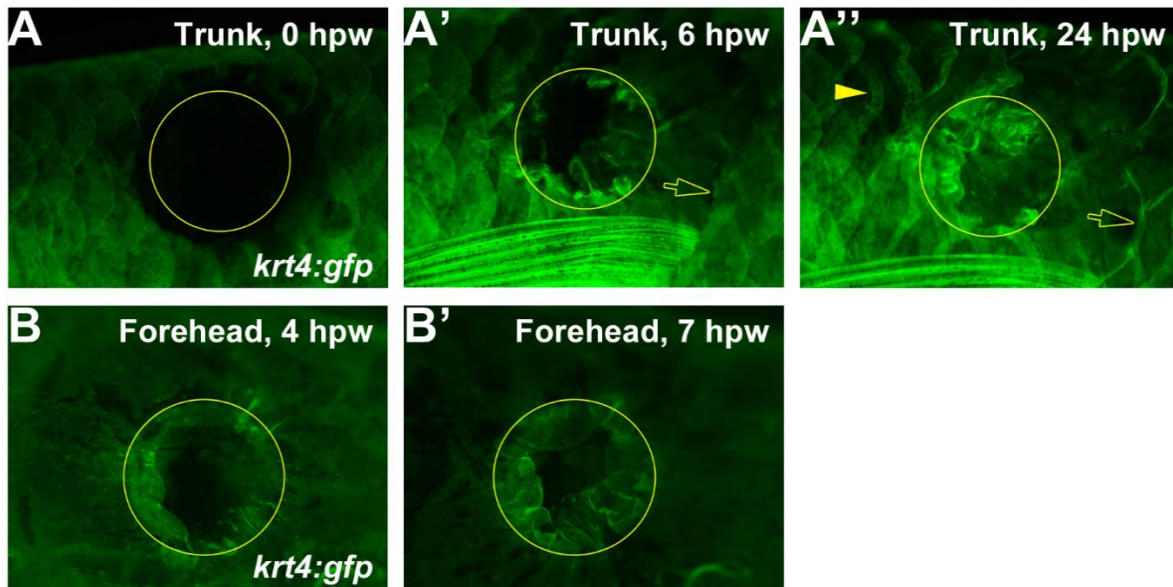
Figure 5.5: Adult fish (anterior to the left) carrying the *gfp* gene under control of the *krt4* promoter showed a fluorescent signal in the superficial keratinocytes only. After full-thickness wounding (yellow circles), the process of wound closure was monitored *in vivo*. Picture **A** shows the wound immediately after laser injury and demonstrates that all superficial keratinocytes were destroyed (**A**, inside vs. outside of yellow circle). After 6 hours, wound-adjacent keratinocytes started to elongate and intercalate and push the neighbouring epidermis into the wound (**5A'**). The posterior half of the wound was closed faster than the anterior half (**A', A''**), probably due to the absence of larger obstacles like the edges of scales. **A''** shows an example of a scale pocket which was recruited to close the wound. As the keratinocytes were moving into the wound, the double-layer of gfp positive cells disappears between 6 hpw (**A'**, arrow) and 24 hpw (**A''**, arrow). In scale-free areas like the forehead, the wounds close more concentric without bias for the anterior or posterior side and are slightly delayed (**B** and **B'**). Anterior to the left.

All these observations of full-thickness wound closure shared the common theme of coordinated, major cytoskeletal rearrangements across the whole epithelium, suggesting the planar cell polarity (PCP) pathway as the underlying regulator [135].

The planar cell polarity pathway is a branch of the Wnt signalling cascade and is responsible for cellular polarisation within an epithelial sheet. Its activation is regulated at the level of Dishevelled (Dsh). Downstream of Dsh, the small GTPase Rho is activated, which interacts with and activates ROCK. This kinase subsequently interacts either with the cytoskeleton directly by phosphorylation of myosin light chain (MLC) or myosin phosphatases, or inhibits actin depolymerisation via LIM kinase [136]. In addition, a crosstalk takes place between ROCK and JNK, which influences polarity within epithelia by altering actin distribution and depolymerisation [137][138].

Upon treatment with ROCK inhibitor Y-27632, a 30% decrease of migratory speed in comparison to DMSO treated control fish was observed (Fig. 5.12A), leading to a significant delay in partial-thickness wound re-epithelialisation. In contrast to TGF-ß or integrin inhibition, lamellipodial morphology was not affected and the leading edge appeared homogeneous (Fig. 5.6A and Fig. 5.6B, SV05 and SV06). Moreover, Rebecca Richardson found that full-thickness wounds remained open for a longer period upon ROCK inhibition with 50 µM Y-27632, which was reproduced during my work with both 50 µM Y-27632 (Fig. 5.6E and 5.6F) and 50 µM ROCKOUT [139] inhibitors (Fig. 5.6G and 5.6H). A possible explanation for the delay of full-thickness

wound closure is that the previously described directed cell elongation was impaired in ROCK inhibitor-treated fish in comparison to control fish. And indeed, staining cells with phalloidin to visualise actin revealed that keratinocytes were pointed into random directions in inhibitor-treated fish. Less than 30% of wound-adjacent keratinocytes were oriented directly towards the wound (less than 10° deviation, Fig. 5.11C and 5.12C) in comparison to 90% of superficial keratinocytes of DMSO control fish. Epithelial cells did not elongate as much, manifesting in a circularity of approximately 0.61 after treatment with Y-27632. This value lies in between the value of circularity of unwounded fish with nearly circular cells (circularity 0.77) and DMSO control fish (circularity 0.39; Fig. 5.11C, quantifications are found in Fig. 5.12D).

Cross-sections of the wound and adjacent regions revealed that unwounded epidermis consisted of four cell layers (Fig. 5.7A – 5.7A''') while epidermis adjacent to wounds consistently showed flattened cells (compare Fig. 5.7A and Fig. 5.7B, yellow line), decreased layer numbers (Fig. 5.7B') and intercalation of intermediate and basal keratinocytes (Fig. 5.7B'', arrow). After ROCK inhibition this cell flattening (compare Fig. 5.7B and 5.7C, line), the decrease in layer number (Fig. 5.7C') and the intercalation of intermediate and basal keratinocytes was less pronounced (Fig. 5.7C'', arrow), resulting in a reduction of radial intercalation. As Rho-associated kinase can affect the cytoskeleton independent of the planar cell polarity pathway, these findings do not necessarily imply a participation of Wnt signalling and planar cell polarity, but revealed the dependency on long-range, coordinated cytoskeletal rearrangements within the epithelial sheet.
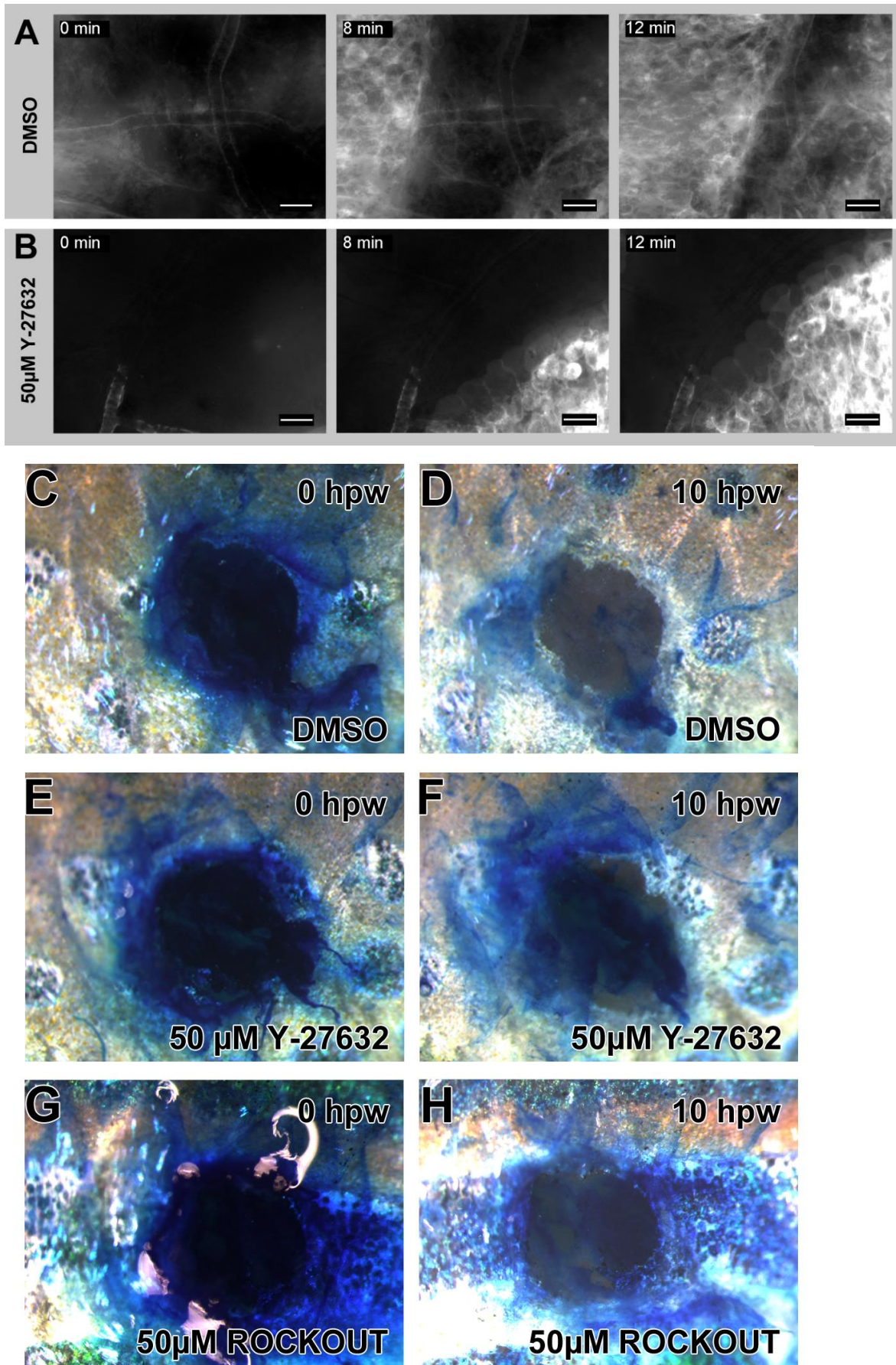
Figure 5.6: Partial-thickness wounds treated with 0.1% DMSO as control (**A**) and 50 µM ROCK inhibitor Y-27632 (**B**). The latter showed lower migratory speeds without obvious lamellipodial defects

or abnormalities as it was observed after TGF-ß or Integrin inhibition (**Fig. 5.12A**). The leading edge depicted in **B** showed an even distribution of lamellipodial size and shape as seen in DMSO controls. Nevertheless, the wounds closed comparably slower. Full-thickness wounds stained for non epithelialised regions with methylene blue penetration assay revealed severe defects during full-thickness wound closure. Wounds of identical size and depth (**C**, **E**, **G**) were largely still open at 10 hpw after two separate ROCK inhibition treatments (**F**, **H, Fig. 5.12B**) in contrast to the DMSO control fish (**D**). Anterior to the left, scale bars in **A** and **B**: 20 µm.
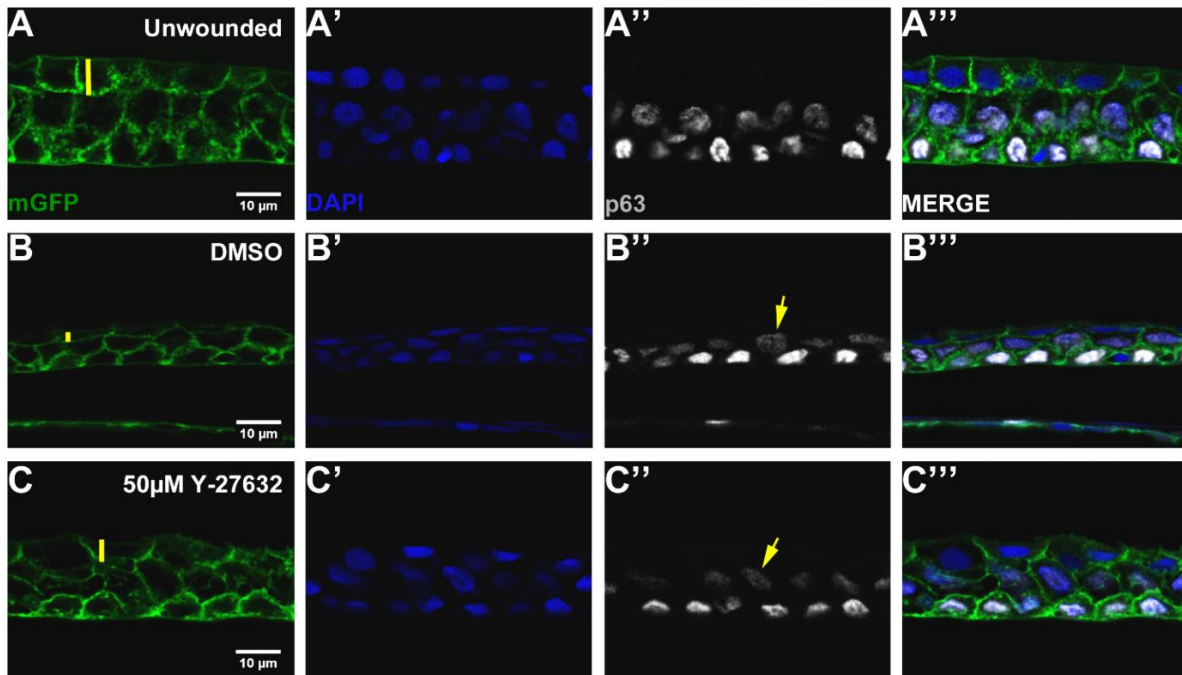
Figure 5.7: Cross-sections of adult *Tg(actb2:gfp)^{zp5}* epidermis at 1.5 mm distance posterior to the wound at 4 hours post wounding. Membrane bound GFP aided visualisation of cell shape in response to wounding. As demonstrated in **A**, the cells had a square shape – which is not visible anymore at this distance after 4 hpw (**B**). Especially the superficial cells elongate and reduce their lateral membrane compartment (compare **A** and **B**, yellow lines). After treatment with 50 µM Y-27632 this reduction is not as prominent anymore (**C**). Cell layer reduction from four layers in unwounded (**A'**) to three in 4 hpw epidermis (**B'**) appears less obvious upon ROCK inhibition (**C'**). Intercalation of p63 positive intermediate and basal cells after wounding (**A''**, **B''**) does not seem to occur after chemical interference (compare **B''** and **C''**, arrows) as two p63 positive cell layers are clearly on top of each other. Anterior (and wound) to the left, scale bars: 10 µm.

To strengthen the evidence for a role of planar cell polarity in wound closure of adult zebrafish and to block an additional important component of the planar cell polarity pathway regulating epithelial sheet polarity, I targeted JNK by use of the JNK-specific inhibitor SP600125. Comparable to ROCK inhibition, wound closure of partial-thickness wounds was affected by approximately 30% as shown by *in vivo* imaging and migratory speed assessment (Fig. 5.8A and 5.8B, SV07, Fig. 5.12A). Furthermore, closure of full-thickness wounds was delayed by approximately 20-30% as well (Fig. 5.8C, 5.8D and 5.8E, 5.8F, Fig. 5.12B). Moreover, directionality and elongation of superficial cells were compromised in fish treated with JNK inhibitor (Fig. 5.11D), although to a lesser extent compared to ROCK inhibition (Fig. 5.11C). SP600125 treated animals displayed proper wound orientation (less than 10°

deviation) of only 60% of superficial keratinocytes in comparison to 90% in DMSO control fish (Fig. 5.12C). The circularity of 0.50 in comparison to 0.39 of DMSO control fish further demonstrated statistically less elongated cells after JNK inhibition (Fig. 5.12D).
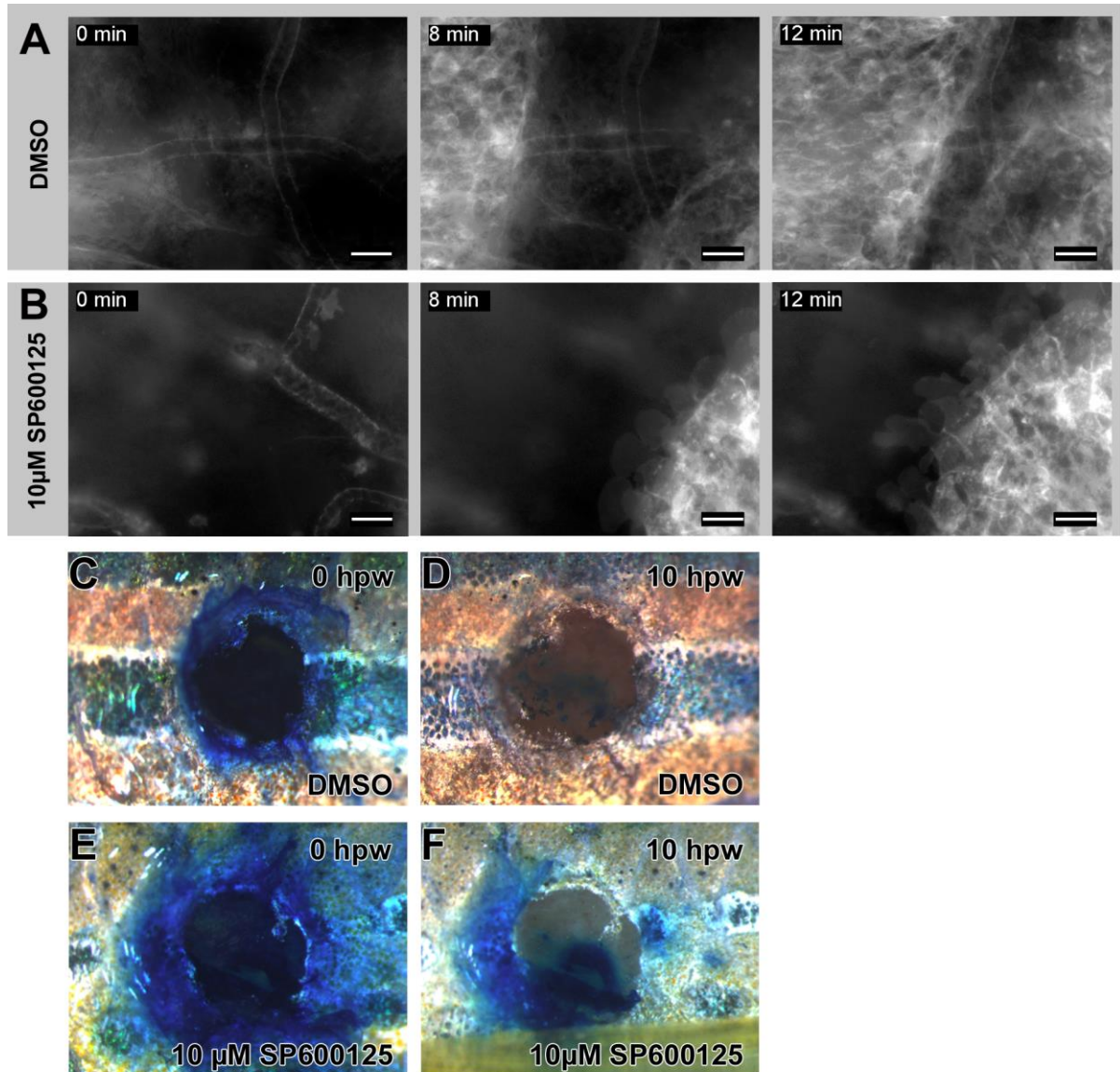
Figure 5.8: Inhibition of jun N-terminal kinase (JNK) by SP600125 lead to a significant delay of partial-thickness closure compared to control animals (**A** and **B**). This observation was comparable to ROCK inhibitor treated fish. In line with Y-27632 treatment, JNK inhibitor treatment lead to a major delay of wound closure of full-thickness wounds as well. Laser wounds were open to 60 % by 10 hours post injury (**E**, **F**), while control wounds were closed completely by the same time (**C**, **D**). Anterior to the left, scale bars in **A** and **B**: 20 µm.

Finally, the planar cell polarity regulator Dishevelled (Dsh) was targeted by a genetic approach. The DEP domain of Dsh binds and activates downstream pathway components resulting in activation of the JNK signalling cascade for instance [140]. My goal was to overexpress exclusively the DEP domain (amino acids 337-736) of *Xenopus laevis* Dishevelled by heat shock to compete with endogenous Dsh for binding and to thereby block downstream component activation due to the lack of other domains. RNA injections of this construct were described to lead to inhibition of the PCP pathway and abrogation of cell elongation, without inhibiting the canonical Wnt signalling during *Xenopus* development [80].

After tol2 recombinase mediated transgenesis and germline transmission I saw stable expression of the construct upon heat shock in adult fish (Fig. 5.9A and 5.9B) as well as defects during gastrulation similar to described PCP mutants like *silberblick* [79] manifesting in a shorter body axis (Fig. 5.9C and 5.9D), compact somites (arrowheads in Fig. 5.9C and 5.9D) and fused eyes (Fig. 5.9E and 5.9F). *In situ* hybridisation analysis with the somite marker *myogenic differentiation 1* (*myod*) demonstrated the outcome of dysfunctional convergence-extension movements during early development (Fig. 5.9G and 5.9H). Both examples in Figure 5.9G and 5.9H developed 12 pairs of somites at 30 hpf. Nevertheless, the body axis was markedly reduced. This observation was explained by the fact that the inter-somitic spacing was decreased and the somites were more closely packed (Fig. 5.9H) than in heat shocked wild type controls (Fig. 5.9G). Further, the length of single somites was nearly double compared to wild type controls (compare length of somite 5 marked by arrowhead in Fig. 5.9G and 5.9H).

I heat shocked the fish one hour before wounding and examined the closure after ten hours by methylene blue penetration assay. Re-epithelialisation of full-thickness laser wounds with ectopic DEP domain expression was not significantly delayed (Fig. 5.10B compared to Fig. 5.10D) in contrast to Y-27632 or SP600125 treatment (Fig. 5.12B). This was even though cell orientation (33% of cells below 10° deviation, Fig. 5.12C) as well as cell elongation (circularity of 0.51 in comparison to 0.39 in DMSO controls, Fig. 5.12D) were affected to a degree comparable to ROCK and JNK inhibition.
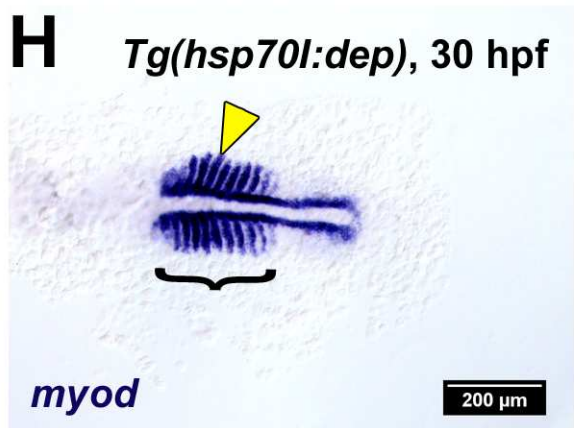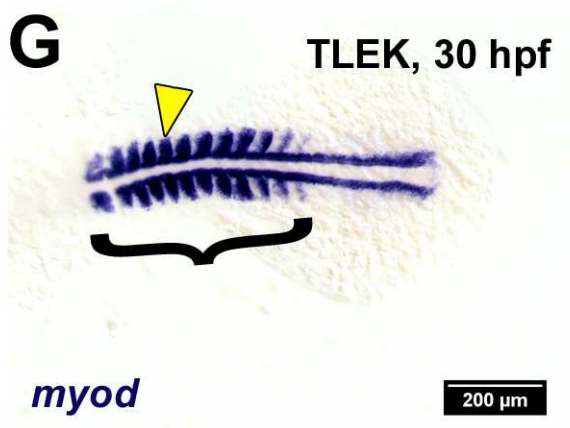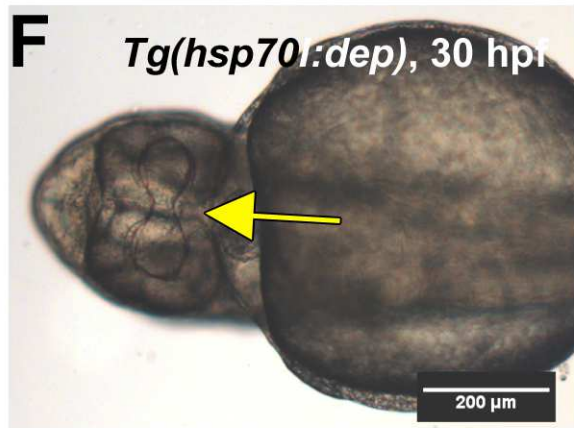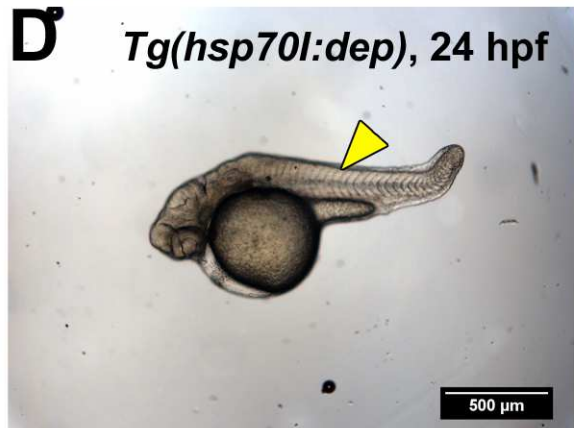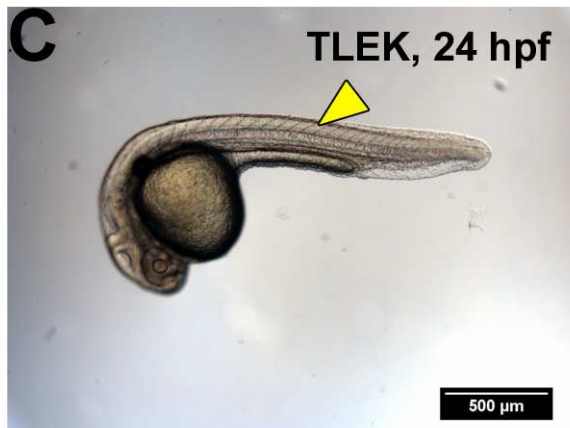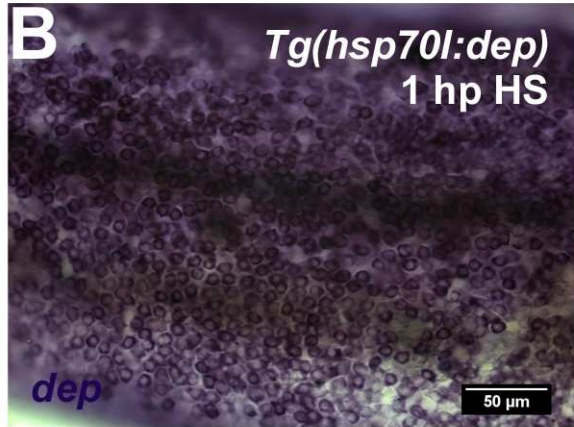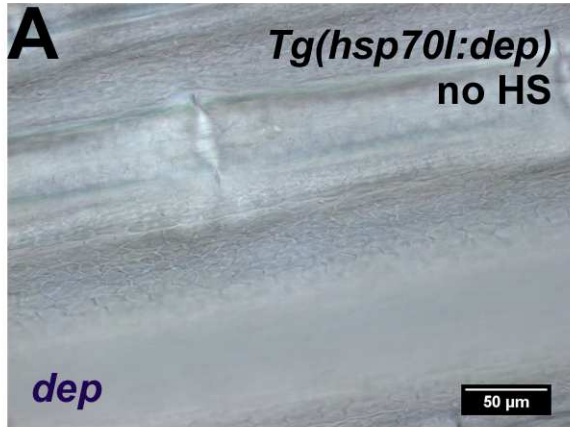
Figure 5.9: Analysis of the *Tg(hsp70I:dep)^fr37* transgenic line during adult and larval stages. Tailfins of anesthetised adult transgenic fish were collected after 1 hour post heat shock and subjected to *in situ* hybridisation to demonstrate expression of the transgene encoding the Dishevelled DEP domain (**A**, **B**). Indeed, 1 hour post heat shock, all keratinocytes of the fin were positively stained for the antisense probe (which was specific for the *Xenopus laevis* DEP domain of *dishevelled*, **B**) and non-heat shocked fish (as well as heat shocked wild type fish) lacked this staining completely (**A**). Overall morphology was examined 14 hours post heat shock. In comparison to heat shocked wild types (**C**) the body axis was markedly reduced, especially apparent in the tail region and the yolk extension (**D**). The posterior portion of the tail was bent towards dorsal, the somites were more compact than in wild type controls (arrowheads **C** and **D**), the head was severely malformed, and the eyes were located more anterior. The ventral view demonstrated that wild type eyes were located more lateral and were clearly separated (**E**), while heat shocked transgenic fish displayed a fusion of the eyes on the anterior side (**F**). After in situ hybridisation against *myod*, the phenotype in body axis elongation was clearly visible (**G** and **H**, brackets outline the length of the body axis containing 12 somites in both cases). The spacing of somites of heat shocked transgenics seemed closer than that of wild types and further, the single somites appeared thinner and longer in comparison to heat shocked wild types (**G**, **H**).
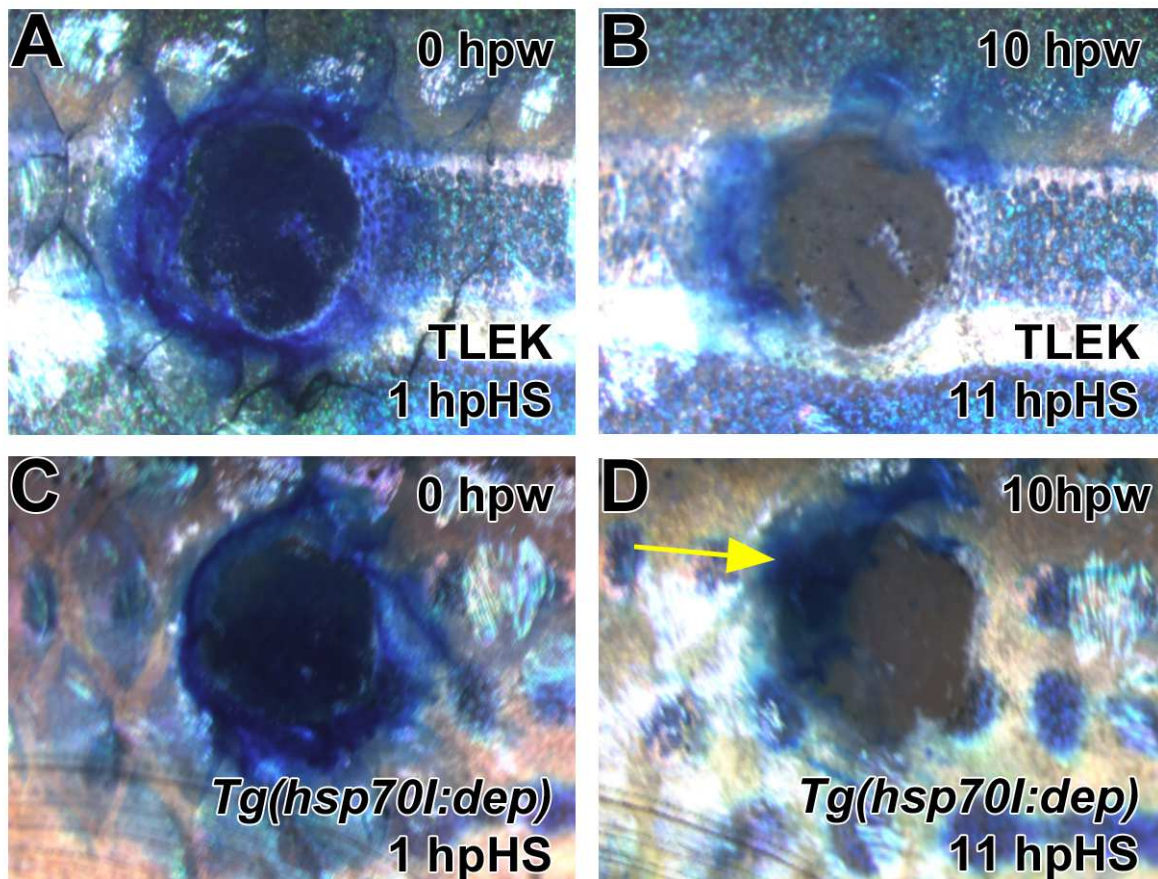
Figure 5.10: Full-thickness wounds of heat shocked wild type and *Tg(hsp70I:dep)^fr37* transgenic adults were stained with methylene blue immediately after wounding (**A**, **C**) and 10 hours after wounding (**B**, **D**) to detect regions devoid of epidermis. While wild type fish displayed complete closure at 10 hpw (**B**), the transgenic fish showed slightly delayed closure in majority of cases (**D**, arrow). Quantifications and statistical analysis however, showed a non-significant tendency to delayed wound closure of the transgenic fish.
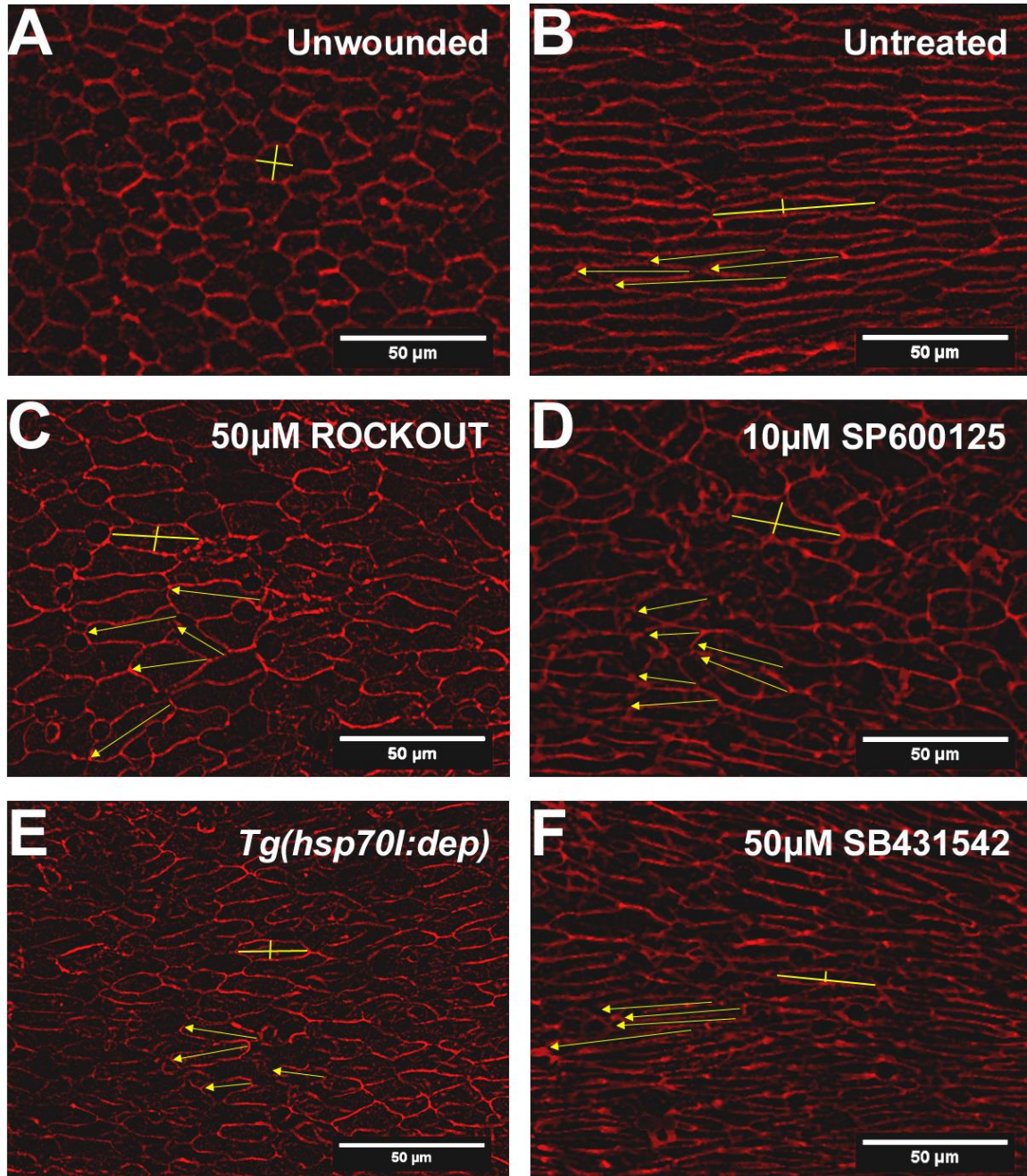
Figure 5.11: Wound-adjacent regions (wound to the left) of adult fish with different inhibitor treatments or genetic background stained with phalloidin at 10 hours post wounding. In unwounded regions, superficial keratinocytes were not oriented or elongated into a specific direction (**A**, comparison of cell axes represented by the yellow lines). After wounding, adjacent superficial cells elongated over time (**B**, yellow line for longitudinal axis increased, transverse axis decreased) into the direction of the wound (**B**, arrows). After treatment with ROCKOUT (and Y-27632), SP600125 and activation of the transgene *hsp70I:dep* to interfere with different planar cell polarity pathway components, cell elongation was hampered (longitudinal axes in **C**, **D** and **E**). Additionally, orientation of cells was severely disrupted (arrows in **C**, **D** and **E**). After block of TGF-ß signalling however, cell elongation (**F**, yellow lines) into direction of the wound (**F**, arrows) occurred without obvious defects.
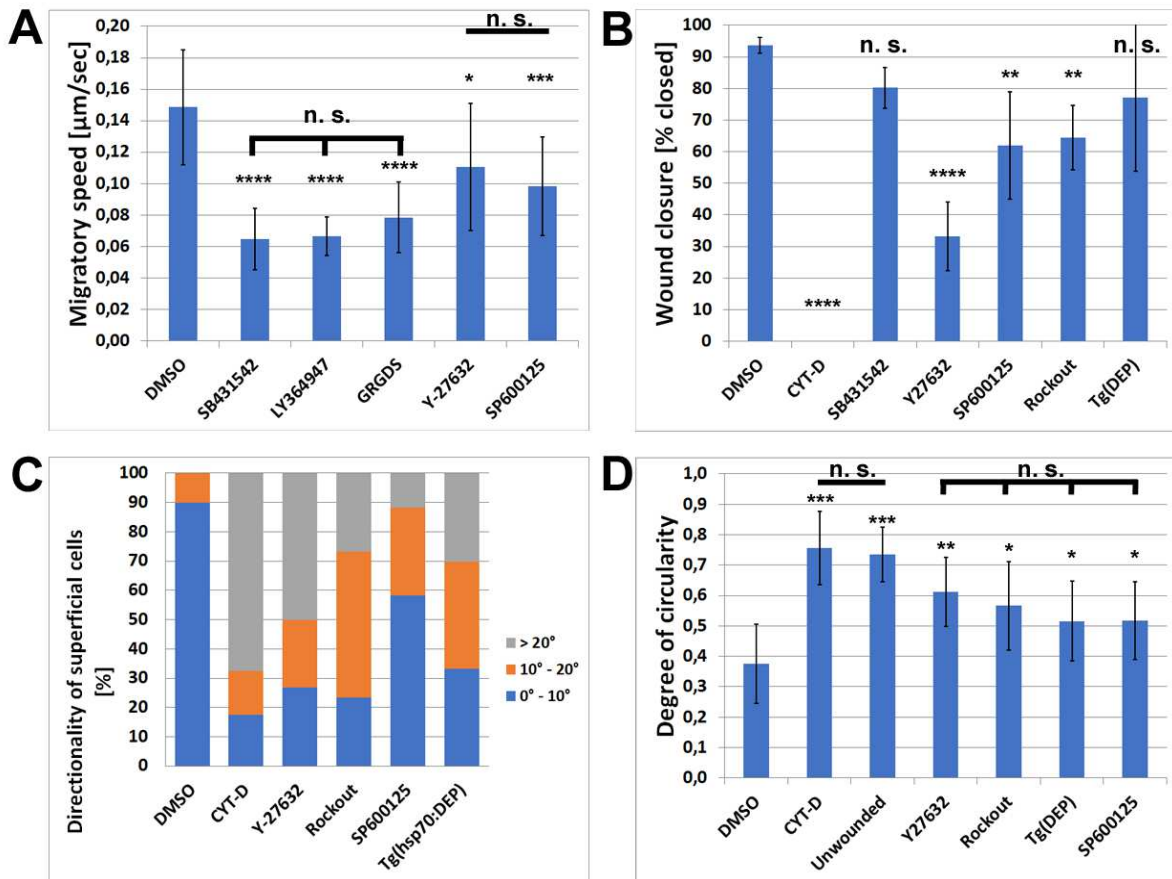
Figure 5.12: Quantification of all previous experiments. (**A**) The migratory speed of basal keratinocytes in partial-thickness wounds was decreased to approximately 50% (compared to 0.1 % DMSO control n=10) after the treatment with SB431542 (n=14) and LY364947 (n=4) to block TGF-ß signalling, as well as after treatment with GRGDS (n=10). The decrease was subtler at 30% reduction of speed after treatment with ROCK inhibitor Y-27632 (n=10) and JNK inhibitor SP600125 (n=16), yet still significant. (**B**) Wound closure of full-thickness wounds was affected at 10 hours post wounding after different treatments. As positive control, cytochalasin D data was included here in these graphs. After treatment with 2 µM cytochalasin D all kind of cell movement was completely blocked due to the block of actin polymerisation. TGF-ß inhibition (SB431542) had no effect on closure, but Y-27632, SP600125 and ROCKOUT delayed the closure by 20-60%. The transgene *Tg(hsp70I:dep)*[fr37] however showed a non-significant decrease in wound closure rates. On cellular level, two parameters were connected to the delay in wound closure. The directionality towards the wound (**C**) and the elongation of superficial cells (**D**). Cytochalasin D inhibited directed cell elongation almost completely and resulted in circularity values comparable to unwounded conditions (0.72). Treatment of fish with Y-27632 and ROCKOUT resulted in a higher percentage of cells with deviation above 10° of the cell longitudinal axis from the axis towards the wound (approximately 72% and 76%). Keratinocytes were further approximately 20% less elongated than DMSO. Similar results were obtained with JNK inhibitor SP600125 and after heat shock of *Tg(hsp70I:dep)*[fr37] fish. ANOVA with Dunnett's post hoc test; n.s.: not significant; *: $p<0.05$; **: $p<0.01$; ***: $p<0.005$; ****: $p<0.001$.

5.1.4 *Hypotonic medium influx triggers wound closure*

All above mentioned signalling pathways and components influence the process of closure by either promoting lamellipodial crawling (partial-thickness) or coordinated cell elongation and intercalation (full-thickness), but little is known about the initial cues that mediate the information of a disrupted epithelium. Since the epidermal barrier is of such crucial importance for survival of the organism, the cues must be immediate and rapidly transmitted. In mammals, cell rupturing and blood vessel leakage lead to an activation of cellular stress signals. Among them is the regulation of mitogen-activated protein kinases p44/42 and p38 [141] as well as EGFR and ERK1/2 phosphorylation [142], stimulating homeostatic repair mechanisms like cell proliferation and cell shape changes. Furthermore, the activation of platelets combined with formation of a fibrin network leads to blood clotting to stop blood loss and to provisionally seal the organism. Additionally, platelets are a source of several moto- and mitogenic growth factors such as EGF, PDGF, IGF and TGF-ß which contribute to the rapid start of re-epithelialisation, inflammation and tissue repair [22]. In fish, blood clotting does not occur to the same extent and is not required for wound closure at all [20]. Moreover, re-epithelialisation starts immediately which could mean that the initial cues might be of a chemical and / or physical nature, rather than growth factor induced signalling cascades and transcription and translation of downstream effectors.

In line with this hypothesis, it was published that zebrafish immune response as well as wound closure depends on the influx of hypotonic medium into the organism [32][30]. Although these studies were concerned with larval zebrafish, neutrophil recruitment and lamellipodia formation are central observations during adult wound closure as well.

To examine the effect of the influx of hypotonic medium on the initiation of wound closure, I made use of *in vivo* imaging of partial-thickness wounds with exposure of the animals to either hypotonic medium or isotonic medium. Indeed, the leading edges showed a severe delay of migration initiation in the presence of isotonic medium (Fig. 5.13, SV08 and SV09 and quantifications shown in Fig. 5.15A). On average it took 8.75 ± 0.9574 minutes until the first lamellipodia were observed in hypotonic medium, while protrusions were first detected after 23.2857 ± 8.7505 minutes under isotonic conditions. Migratory speed of keratinocytes during the main closure phase was also delayed from 0.1214 ± 0.0386 µm/sec in hypotonic to 0.0640 ± 0.0267 µm/sec in isotonic medium (quantifications are found in Fig. 5.15B). In summary, treatment with isotonic medium led to a severely delayed closure of partial-thickness wounds (hypotonic medium: 0.1214 ± 0.0386 µm/sec compared to 0.0640 ± 0.0267 µm/sec).

However, despite the later commencing and slower cell migration there were no indications for a lamellipodial defect resembling the TGF-ß inhibition phenotype. There were no single lamellipodia reaching out over the migratory front leading to an asynchronous migration and no retraction of lamellipodia could be observed pointing toward a problem with attachment as it was the case with TGF-ß inhibition.

In line with the notion that full-thickness wounds do not rely as much on lamellipodial crawling, laser-wounded adult fish did not show a delay of wound closure with 250 mM Mannitol treatment. In both hypotonic and isotonic conditions, wounds were closed to approximately 70% after 8 hours (Fig. 5.14A and 5.14B, Fig. 5.15B).
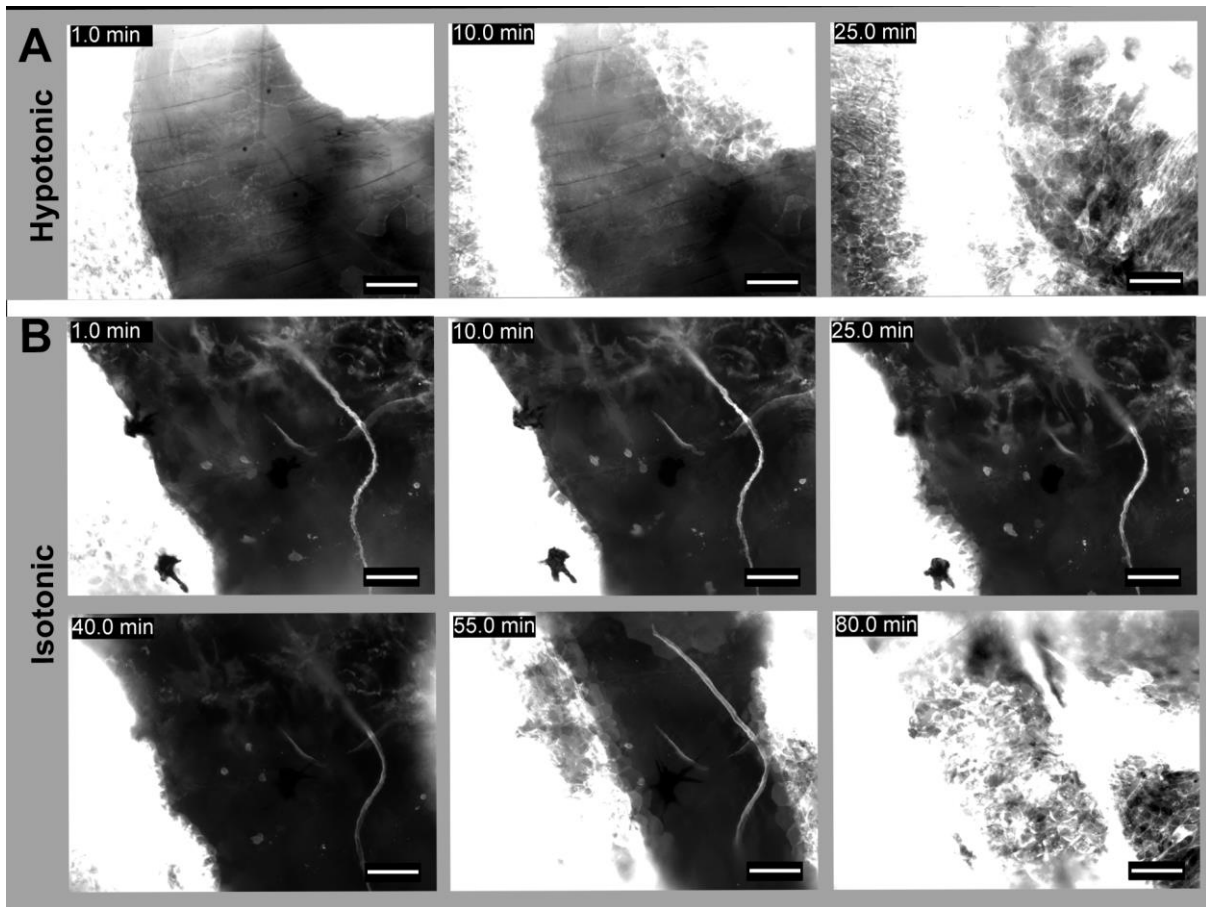
Figure 5.13: Partial-thickness wounds were introduced and imaged with different tonicity of the outside medium. While fish incubated and wounded in hypotonic medium (system water) show immediate formation of lamellipodia and a closure by 25 minutes (**A**), incubation in isotonic medium (system water containing 250 mM mannitol) lead to a delay of migration-start (**B**, 25 min) and a great delay in closure (**B**, 80 min). However, there were no obvious signs of a cell attachment defect in all cases. Anterior to the left, scale bar 50 μm.
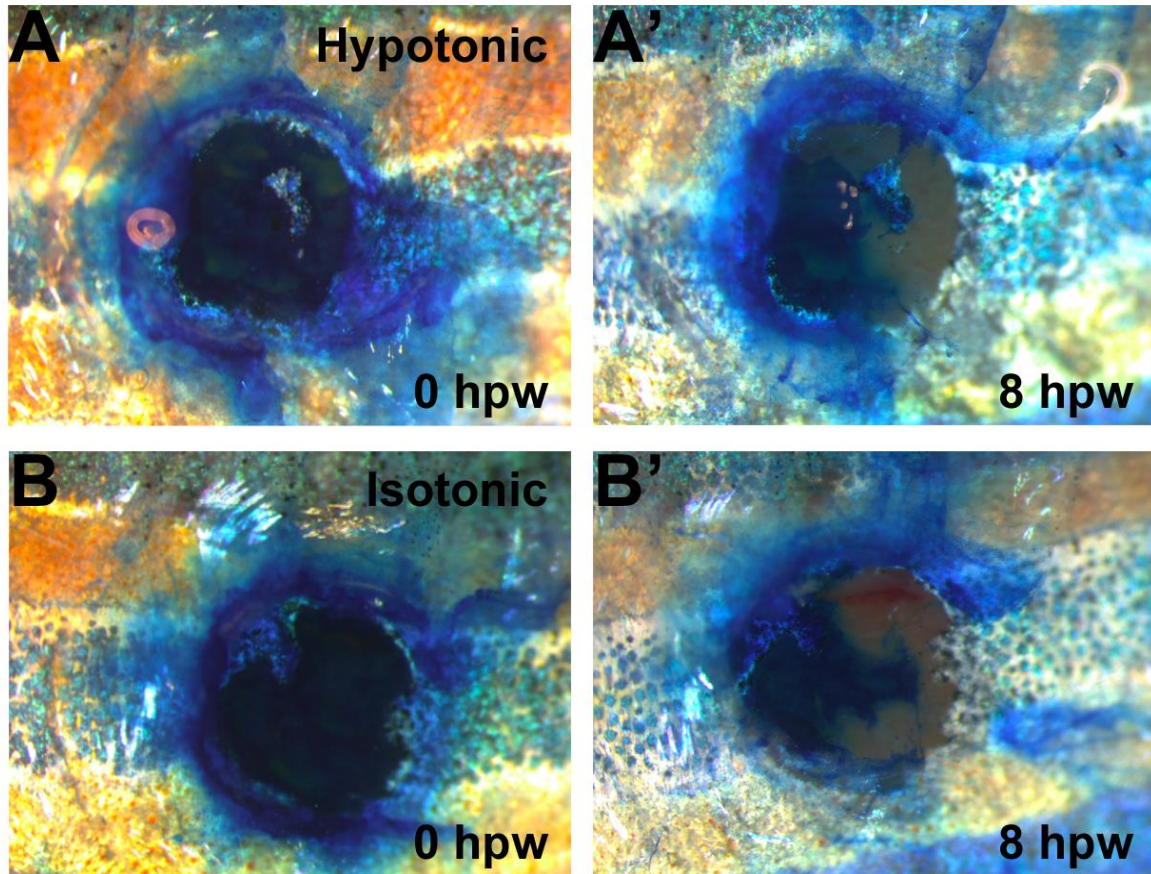
Figure 5.14: Full-thickness wounds in hypotonic medium (system water) closed an area of 70% of the initial wound surface by 8 hours post wounding (**A**, **A'**). The same extent of closure was visible with isotonic medium (system water with 250 mM mannitol) by 8 hours post wounding (**B**, **B'**). Anterior to the left.
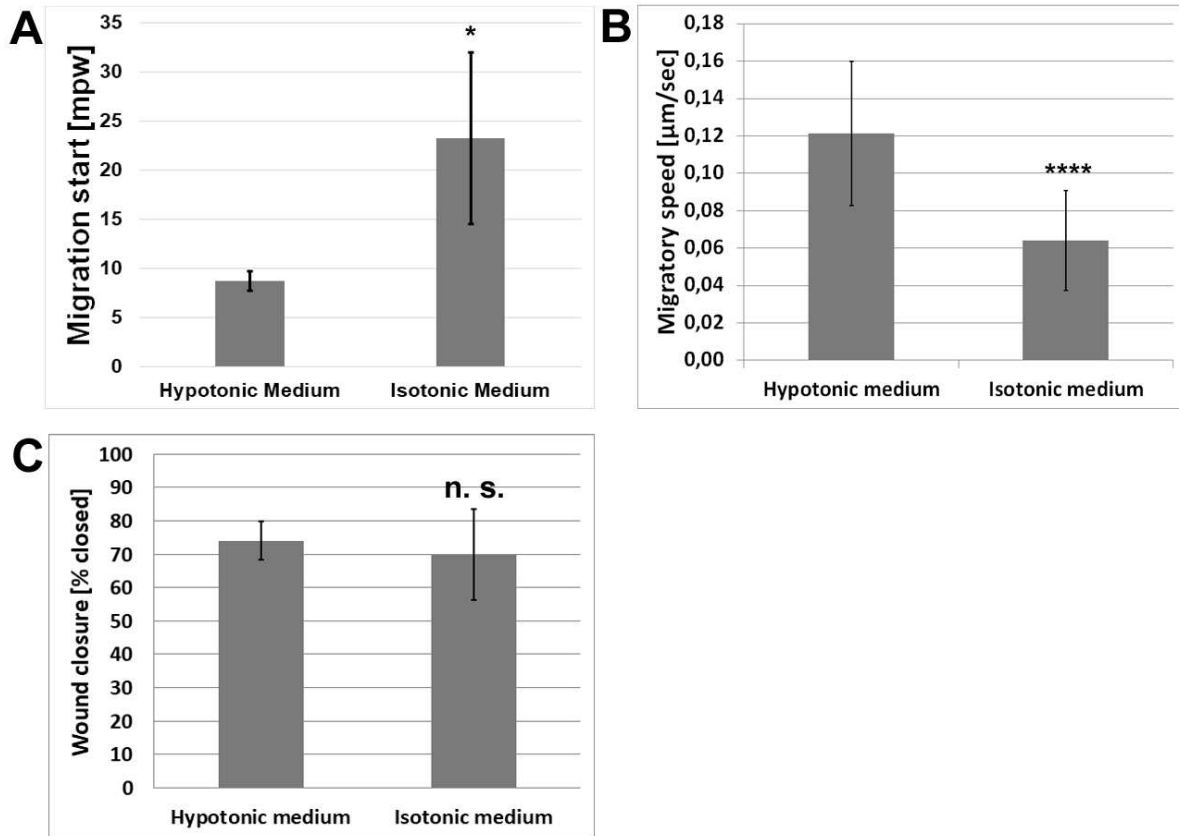
Figure 5.15: The initiation of cell migration during partial-thickness wound was delayed by on average 15 minutes upon incubation in isotonic medium (250 mM mannitol) compared to hypotonic fish water (**A**, hypotonic n=8 fish, isotonic n=7 fish). Additionally, basal keratinocyte migration was reduced from 0.12 µm/sec to an average 0.06 µm/sec (**B,** hypotonic n=7 fish, isotonic n=8 fish). The re-epithelialisation of the initial wound area of full-thickness wounds was not affected by isotonic medium treatment (**C,** hypotonic n=3 fish, isotonic n=3 fish). n.s.: not significant, *: $p<0.05$ ****: $p<0.001$, Statistical significance was calculated by unpaired two-tailed Student t-test.

5.1.5 *Hypotonic stress acts possibly via FAK and / or PI3K*

Changes in the osmolarity can be sensed by cells in different ways. Firstly, osmotic stress can lead to cell swelling and death, resulting in a release of tissue damage signals which can attract immune cells and lead to further signalling [18], [49]. Secondly, cell swelling can lead to activation of mechanosensitive ion channels and calcium influx into the cells, which triggers migration independently of cell death [143], [144]. Thirdly, osmotic stress can be sensed by heparan-sulfate proteoglycans which interact with cells by modulating for example focal adhesion kinase activity, leading to an activation of downstream signalling cascades and to cytoskeleton- and cell shape changes [145]. Lastly, G-protein coupled purinergic receptors, like P2X and P2Y can be activated upon recognition of extracellular nucleotides like ATP. This in turn triggers calcium influx and activation of downstream pathways such as mTOR for example [30], [32], [146].

Since cell swelling is a common theme upon hypotonic stress and the linked cell death and release of damage signals was described well in other models, I tested the second mechanism by *in vivo* imaging. One family of mechanosensitive channels that was described in the context of calcium influx and directed cell migration is the transient receptor potential vanilloid (TRPV). A study showed that TRPV1 in particular is responsible for localised calcium influx thereby determining the direction of cell migration [147]. This study furthermore describes the migratory behaviour of cells in culture after inhibition with specific small molecules. One of them was capsazepine, a specific TRPV1 antagonist, leading to a significant reduction of calcium influx and thereby decreased cell motility. In my adult transgenic fish however, I could neither observe a reduction in migratory speed nor a lamellipodia specific phenotype upon capsazepine treatment (Fig. 15.6A-5.16B, SV10 and SV11).
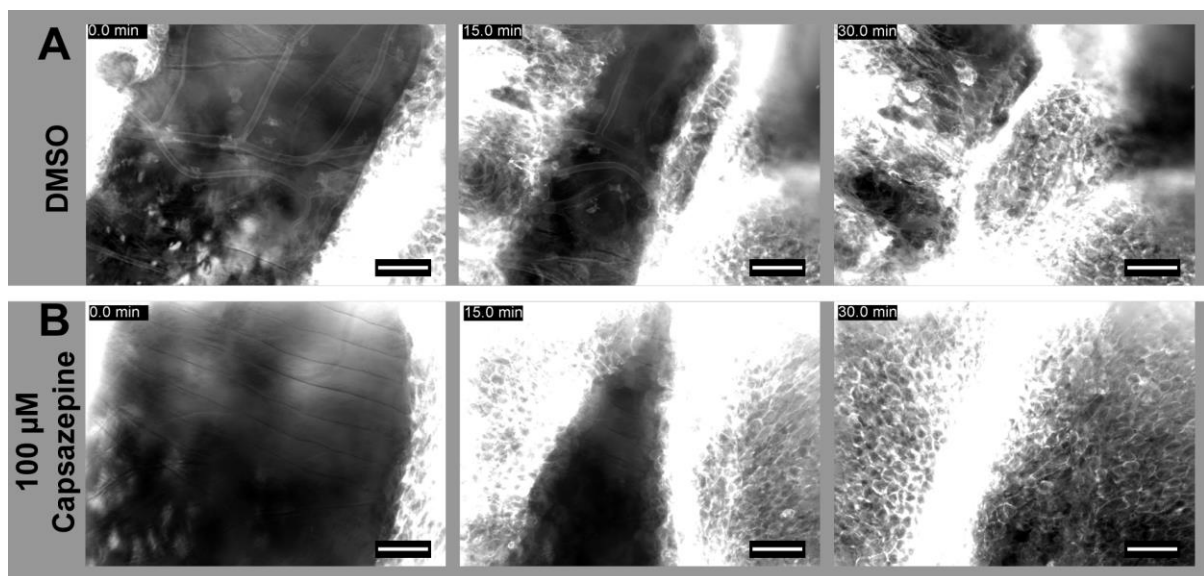
Figure 5.16: Capsazepine targets TRPV-type mechanosensitive ion-channels. No significant delay was detected upon treatment with 100 µM capsazepine (**B**) in comparison to 0.1% DMSO controls (**A**). Both partial-thickness wounds closed within 30 minutes and displayed normal lamellipodial behaviour. Anterior to the left, scale bar 50 µm.

Since blocking TRPV1 alone did not result in a reduction of migratory speed, a broader approach was used to test if mechanosensitive ion channels in general play a role during epithelial closure in our model. Gadolinium (Gd^{3+}), a lanthanide with a similar size as Ca^{2+} and Na^+, has been shown to act as a general inhibitor of stretch-activated ion channels in *Xenopus* oocytes [148]. To investigate if other mechanosensitive ion channels such as piezo1 or other TRPV-family members could be responsible for the required Ca^{2+} influx and migration, I tested Gadolinium in different concentrations ranging from 5 µM to 100 µM in combination with time lapse imaging of age-matched *Tg(actb2:hras-egfp)vu119* zebrafish. None of the concentrations tested showed a significant delay of closure (Fig. 5.17 B, 5.17C, SV12-SV14) compared to control fish (Fig. 5.17A). However, a tendency towards slower migration of basal keratinocytes was visible (Fig. 5.17, Fig. 5.21).
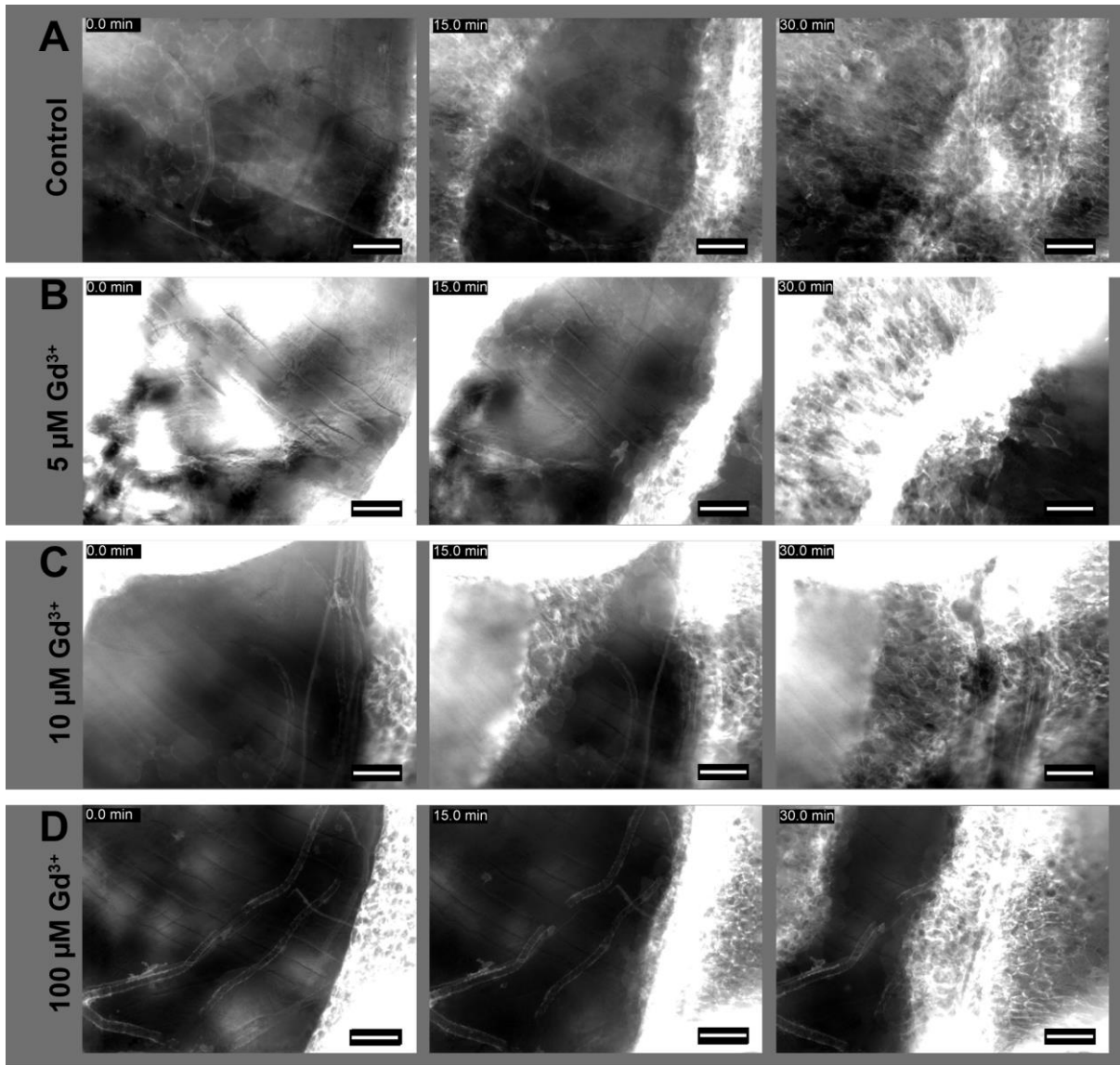
Figure 5.17: Partial-thickness wounds of adult zebrafish were treated with different concentrations of Gadolinium (Gd^{3+}, **B-D**) and compared to untreated controls (**A**). With increasing concentration, the wound re-epithelialisation was increasingly delayed and the migratory speed shows a tendency to be slower in treated fish (**C** and **D**, at 30 minutes post wounding there are still open areas). Anterior to the left, scale bar 50 µm.

To test the influence of heparan-sulfate proteoglycans on wound closure via focal adhesion kinase (FAK), transgenic adult zebrafish (*Tg(actb2:hras-egfp)vu119*) *o*f the same age were treated with FAK inhibitor PF573228 4 hours prior to partial-thickness wounding. I observed a slight (non-significant) decrease of migration speed by approximately 15% along the leading edges in FAK inhibitor-treated fish (Fig. 5.18A-C, Fig. 5.21), although the lamellipodia formation and maintenance seemed unaffected. Possible downstream effectors of FAK in the context of wound closure are not fully investigated and remain unknown. So far, proper inhibitor controls were not possible yet due to the lack of downstream read-outs available for immunohistochemistry, western blot or *in situ* hybridisation. However, it has been described that FAK can activate phospho-inositol-3 kinase (PI3K), connecting it to cell survival and migration via AKT and mTOR [149]. Independent of hypotonic stress, mTOR was described in *Drosophila melanogaster* larvae to be required for

closure of epithelial wounds, where a combination of purse-string and lamellipodial crawling are utilised [29].
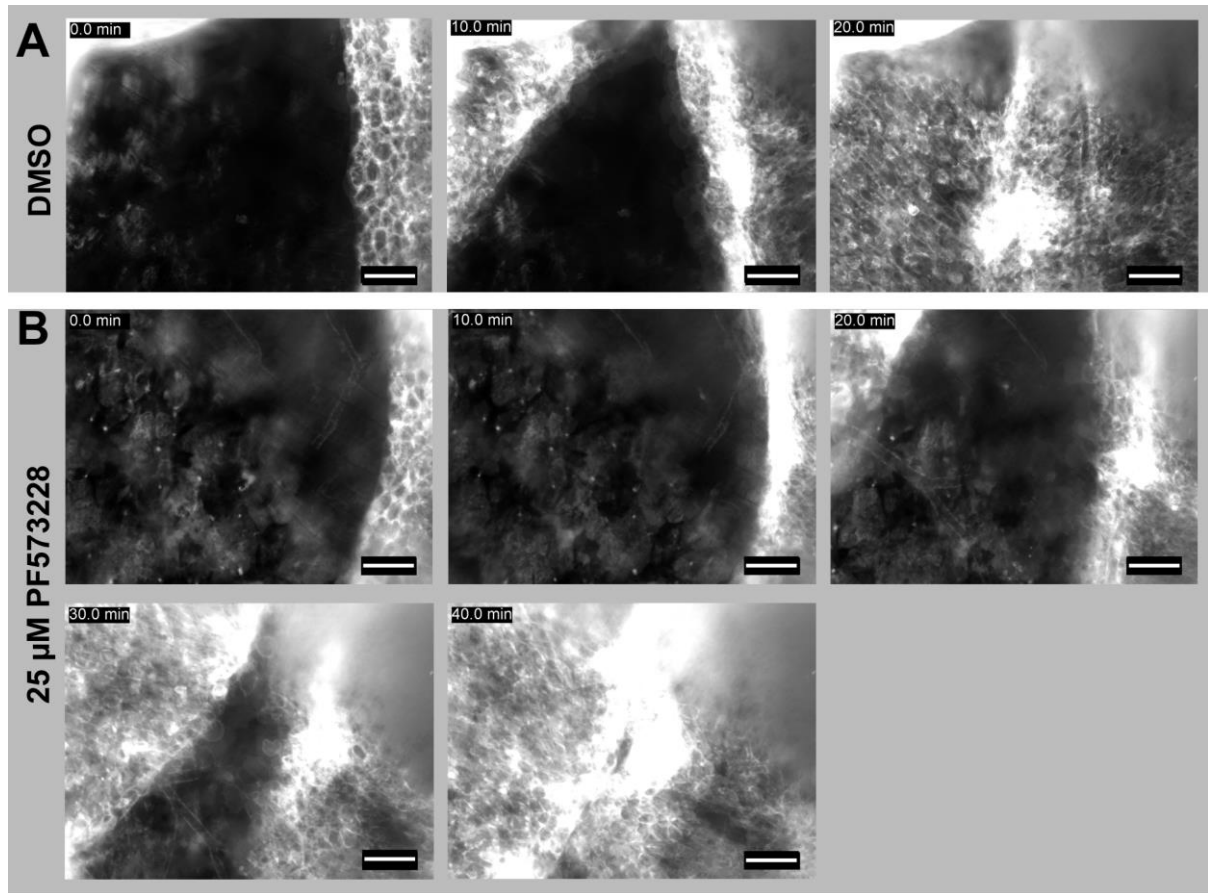
Figure 5.18: Adult *Tg(actb2:hras-egfp)vu119* wounded by scale-removal and treated with focal adhesion kinase inhibitor PF573228 were imaged and analysed for closure and migratory speed. The DMSO control fish shown here as an example exhibited complete re-epithelialisation by 20 minutes post wounding (**A**), while fish treated with the inhibitor showed closure only by 40 minutes post wounding (**B**). However, the wound appeared to be larger in this specific case and quantification of migratory speed showed no significant difference (**Fig. 5.21A**). Anterior to the left, scale bar 50 µm.

To determine if PI3K signalling was involved in wound closure and could integrate the hypotonic stress signals to cellular responses, adult zebrafish were subjected to partial-thickness wounding and sacrificed 30 minutes post wounding. As a readout for PI3K activity, phospho-AKT antibody staining was performed on whole mount partial-thickness wounded adult fish. Interestingly, I observed a signal exclusively in cells immediately at the leading edge with hypotonic medium. The signal was visible in a continuous line of one to two cells deep outlining the wound (Fig. 5.19A-A''). Cells further distant to the wound edge were negative for pAKT at 30 minutes post wounding. This pAKT signal at the wound edge was reduced in fish treated with isotonic medium (Fig. 5.19B-B'') as well as in animals incubated in PI3K inhibitor PIK-90 (Fig. 5.19C-C'').
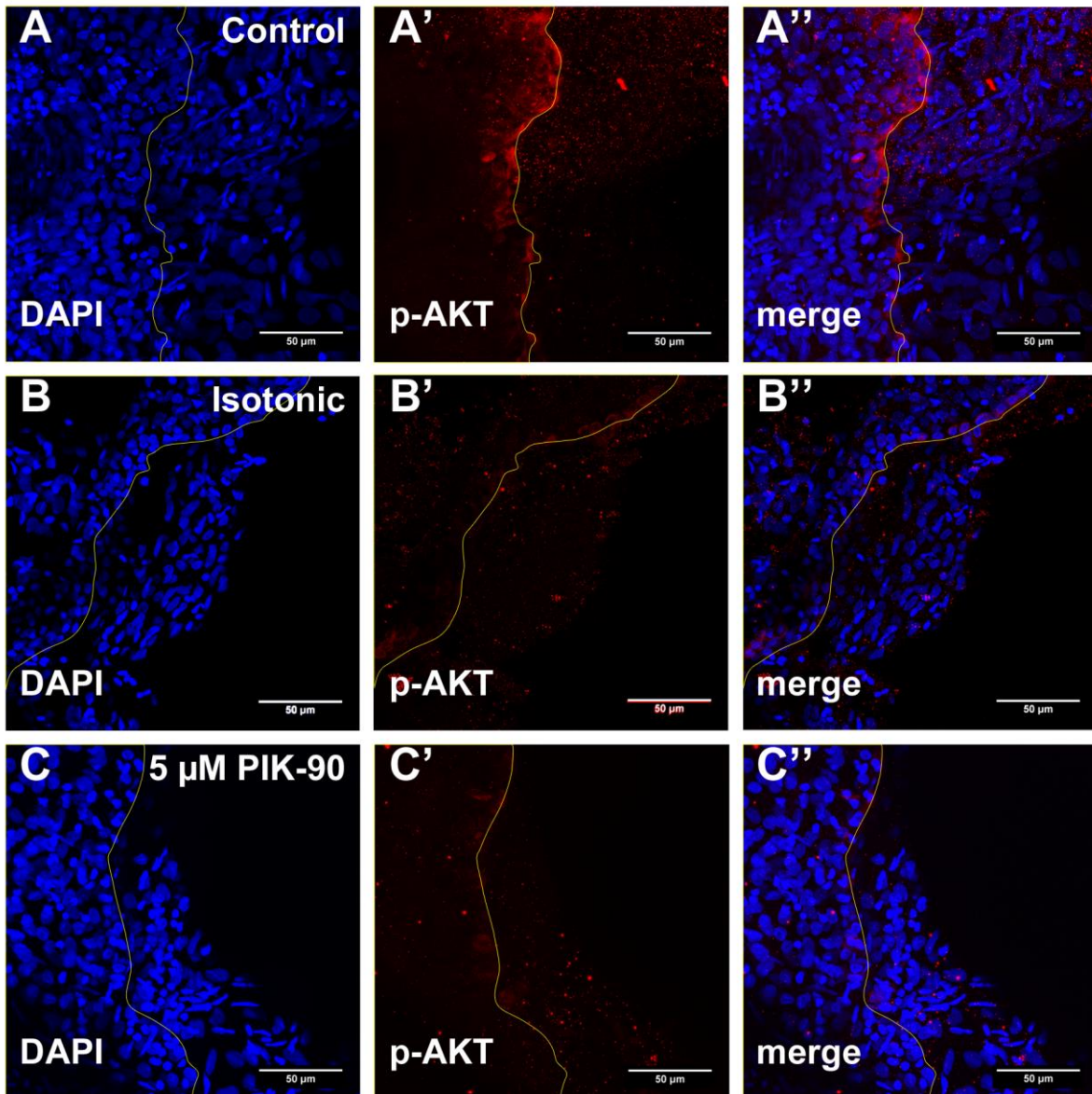
Figure 5.19: Partial-thickness wounds were stained by immunohistochemistry against pAKT. Adult wild type fish were sacrificed and fixed 30 minutes post wounding. The first row of basal keratinocytes at both leading edges was positive for pAKT. In closer view of the leading edges, it appears that mostly one line of cells is positive (**A-A''**). With incubation in isotonic medium, the strong pAKT signal in both leading edges is dampened (**B-B''**). Similar observations were made after PI3K inhibition (**C-C''**). Anterior to the left.

To further strengthen the hypothesis that PI3K and AKT influence wound re-epithelialisation, the previously mentioned PI3K inhibitor PIK-90 was used for *in vivo* imaging of adult zebrafish. Age-matched *Tg(actb2:hras-egfp)vu119* transgenic fish were treated with 5 µM PIK-90 4 hours prior to wounding and imaging. Basal keratinocytes of treated fish moved along the substrate with a significantly lower speed after treatment with PIK-90 in comparison with DMSO control fish (Fig. 5.20A, 5.20B, Fig. 5.21). However, in contrast to treatments with isotonic medium, a lamellipodial defect was observed in PIK-90 treated fish, manifesting in extensive lamellipodial outreach and moderately affected attachment to the substrate (Fig. 5.20C). Hence, the remaining question is why inhibition of the PI3K signalling

pathway could show additional defects, if it is only relaying the external hypotonic stress to intracellular changes. To date it is unknown what causes this additional lamellipodial defect and how the connection between hypotonic stress as an input and PI3K mediated wound-closure could be composed.

There are numerous signalling branches downstream of PI3K and AKT which could be activated. One of the most studied routes results in an activation of mTORC1. As mentioned above, this complex has recently been described to be involved in epithelial wound closure of *Drosophila* [29]. In this study, Kakanj and colleagues showed that inhibition of mTORC1 by rapamycin delays wound closure severely, and that expression of a constitutively active ribosomal protein S6 kinase can rescue the rapamycin-induced effect. To test whether the observed activation of PI3K and phosphorylation of AKT in adult zebrafish wounds results in activation of mTORC1, I inhibited mTORC1 activity using rapamycin. Adult fish (*Tg(actb2:hras-egfp)vu119*) were pre-treated for four days with 200 nM rapamycin or 0.1% DMSO (with daily exchange of the medium). On day four of treatment, the fish were anesthetised and subjected to *in vivo* imaging after partial-thickness wounding. Although the efficient decrease of mTORC1 activation was proven by western blot with approximately 80-85% lower levels of phospho-ribosomal protein S6 (pRPS6, Fig. 5.21B and 5.21C), re-epithelialisation of partial-thickness wounds was not significantly delayed (Fig. 5.20D, 5.20E and 5.21A). On a cellular level, no extensive elongation or retraction of lamellipodia was observed, leading to the conclusion that PI3K and pAKT mediated effects are presumably not linked to mTORC1 but follow a so far unknown route.
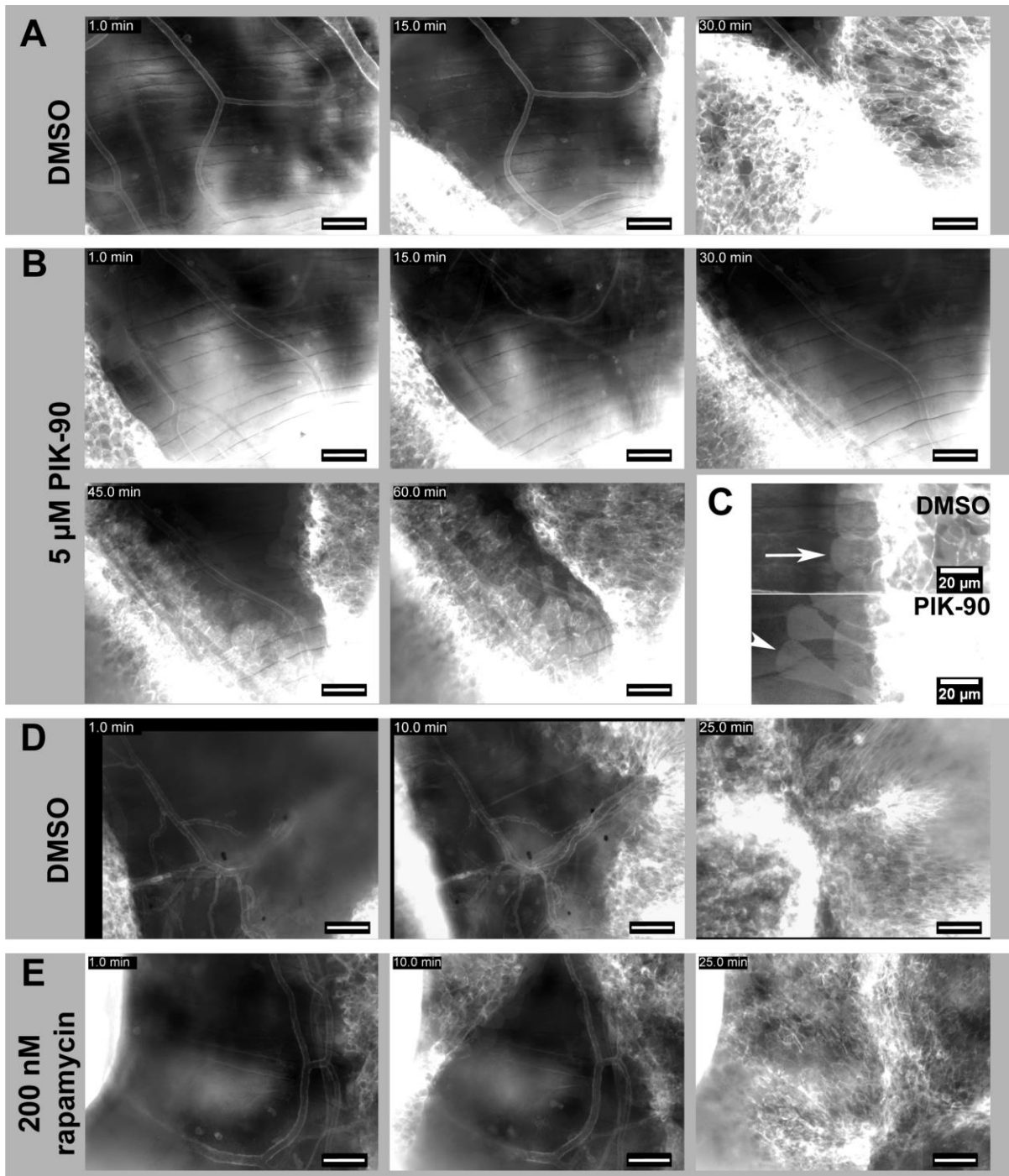
Figure 5.20: Scale removal wounds with DMSO treatment resulted in almost complete closure after 30 minutes (**A**). In contrast, PIK-90-mediated inhibition of PI3K lead to severe delay of closure (**B**) and a decrease of migratory speed by approximately 50% (**Fig. 5.21**). In contrast to DMSO controls (as well as isotonic medium treatment, capsazepine, Gd^{3+}, PF573228 and rapamycin), there were obvious lamellipodial differences upon PI3K inhibition. While DMSO controls had protrusions of similar size and shape along the leading edges, 5 µM PIK-90 lead to elongation of lamellipodia over the leading edge (**C**) which had not been seen under other circumstances apart from TGF-ß and integrin inhibition. Downstream inhibition of TORC1 by rapamycin did not result in any obvious defect during wound healing (**E**) since wounds closed within the usual timeframe of 20-30 minutes post wounding of the respective control fish (**D**). Anterior to the left, scale bar 50 µm if not stated elsewise.
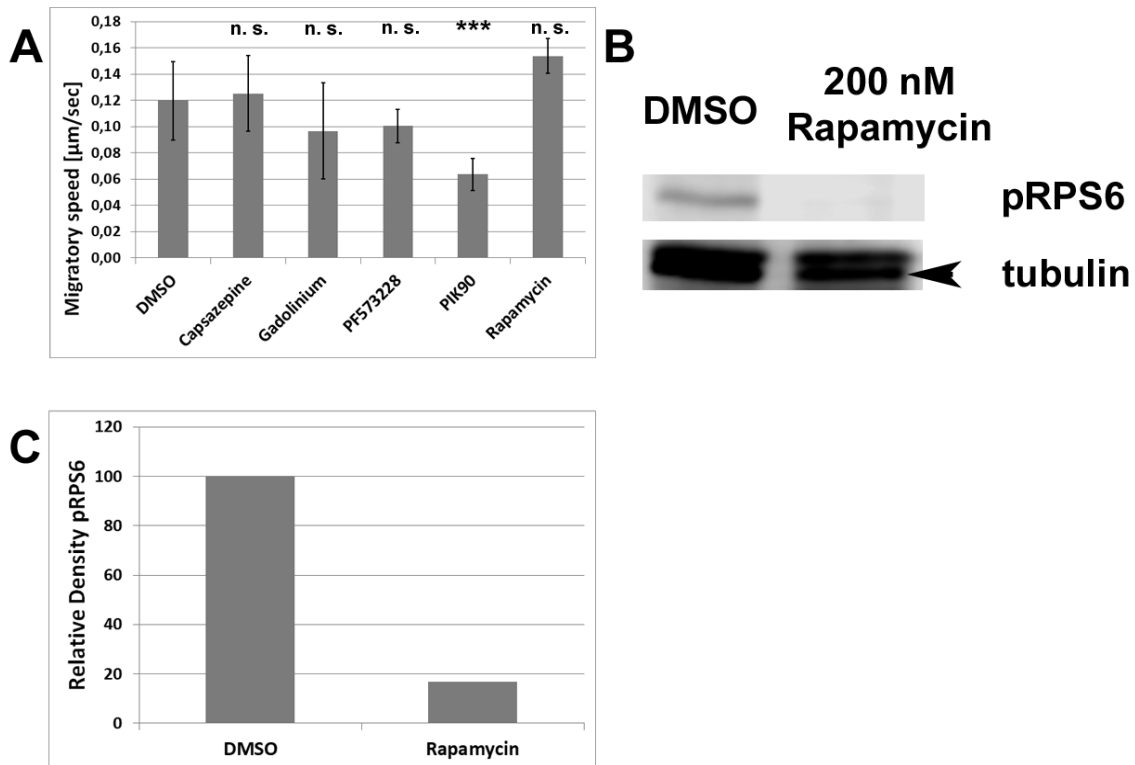
Figure 5.21: Migration speed of keratinocytes was assessed after different treatments with combined DMSO control fish (n=10) (**A**). Capsazepine (n=4) did not show any decrease, while both 100 µM Gadolinium (n=3) and FAK inhibitor PF573228 (n=3) showed a non-significant decrease of migration speed by approximately 15% on average. The only treatment resulting in a significant decrease was the PI3K inhibitor PIK-90 (n=6). Rapamycin (n=3) on the other hand showed a non-significant tendency to increased migration speed. After imaging, fins of the rapamycin treated fish were pooled, lysed and used for western blotting against TORC1 target pRPS6 as control for the successful inhibition. Picture (**B**) shows the bands of the DMSO controls (left column) and the rapamycin treated fish (right column). The upper band is representing the pRPS6 levels and for normalisation, (lower) bands for tubulin were used. The graph in (**C**) shows the normalised result of rapamycin treatment, which was a decreased activity of TORC1 down to 15-20% of normal levels.

5.2 Granulation tissue formation relies on both immune response and FGF signalling

5.2.1 *Granulation tissue formation and resolution – the time course of tissue remodelling*

Rebecca Richardson and colleagues published in 2013 the time course of wound healing in zebrafish. Concomitantly with wound re-epithelialisation, immune cells such as neutrophils and macrophages migrate into the injured tissue and clear it of cellular debris, destroyed ECM components and pathogens [20]. To extend the knowledge about wound repair, I repeated this time course and included BrdU incorporation, thereby enabling conclusions about proliferation within the wound and especially the granulation tissue.

With haematoxylin and eosin staining of longitudinal sections it became apparent that laser injury resulted in the disruption of scales (Fig. 5.22A, arrowhead) and epidermis as well as adipose tissue in the hypodermis (Fig. 5.22A, asterisk). At two days post wounding, the neo-epidermis was thickened in comparison to adjacent unwounded skin (Fig. 5.22A, inlay). The wounded area under the neo-epidermis was largely musculature and only a few nuclei were visible (Fig. 5.22A, inlay). At day four post wounding, the neo-epidermis was still thickened (Fig. 5.22B, inlay) and the granulation tissue was fully formed and very prominent by massive cellular infiltrations (Fig. 5.22B, arrow). As shown by Richardson and colleagues, these cells are mainly *col1a2* positive fibroblasts. Indeed, Collagen1 antibody staining showed an accumulation of collagen fibrils in the granulation tissue as well [20]. Day four after injury was the time point when the granulation tissue was at its peak size. Afterwards, as seen in Fig. 5.22C, the granulation tissue appeared less dense and cellular (Fig. 5.22C, inlay), while the thickened epidermis was still undergoing reorganisation (Fig. 5.22C, inlay). Below the thickened neo-epidermis there were merely traces of the granulation tissue left at eight days after injury (Fig. 5.22D, inlay). At ten days after tissue disruption, the first signs of scale regeneration became visible (Fig. 5.22E, inlay). Further in all five examined animals, this was the latest time point at which granulation tissue was resolved completely. At 15 dpw, adipocytes as well as melanocytes were detectable while migrating into the original locations in hypodermis and dermis respectively (Fig. 5.22F, inlay). Almost complete regeneration was achieved at 25 dpw, when the epidermis was back to normal layer numbers, scales were nearly back to normal dimensions (Fig. 5.22G, green arrowhead) and dermal and hypodermal compartments were completely restructured (Fig. 5.22G; melanocytes: yellow arrowhead, adipocytes: red arrowhead).
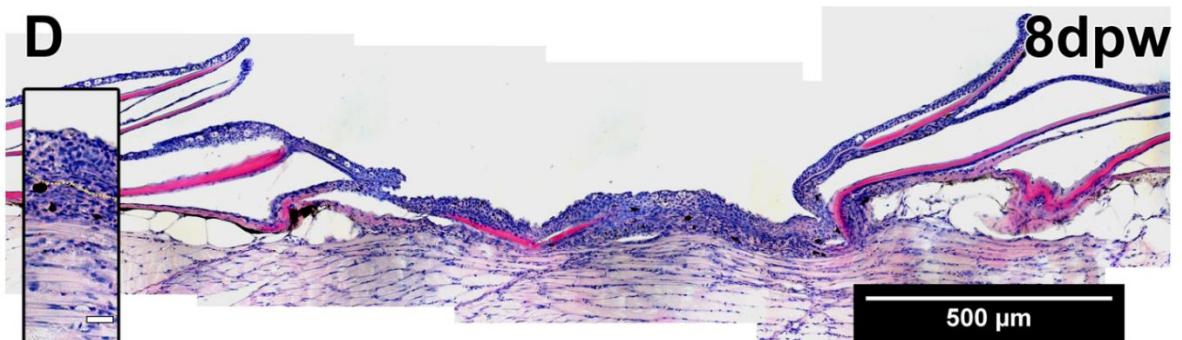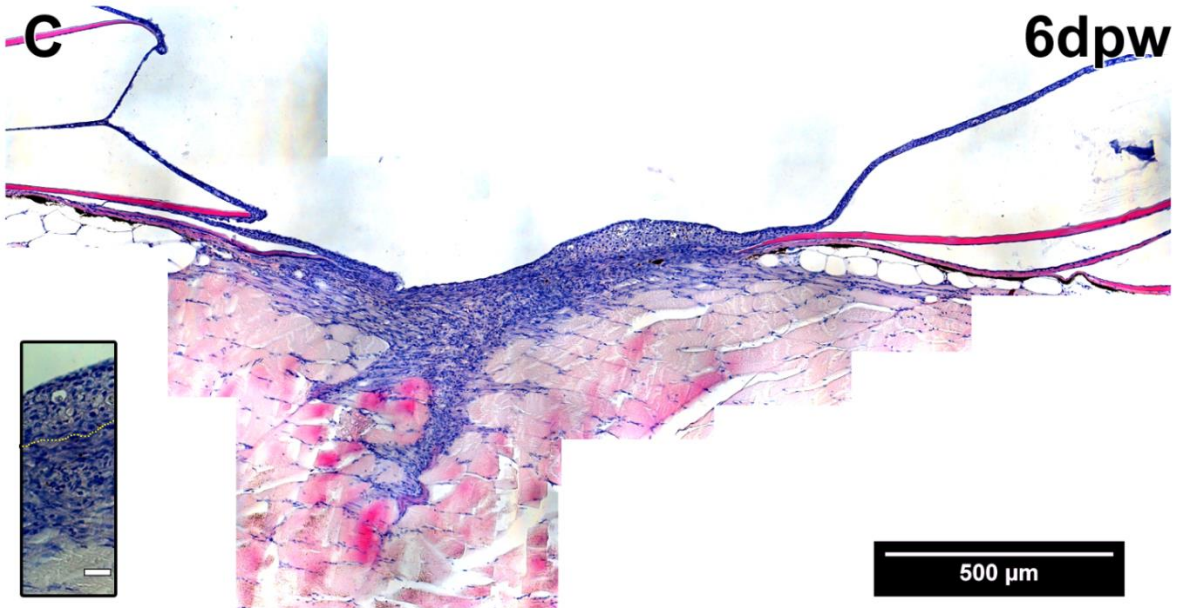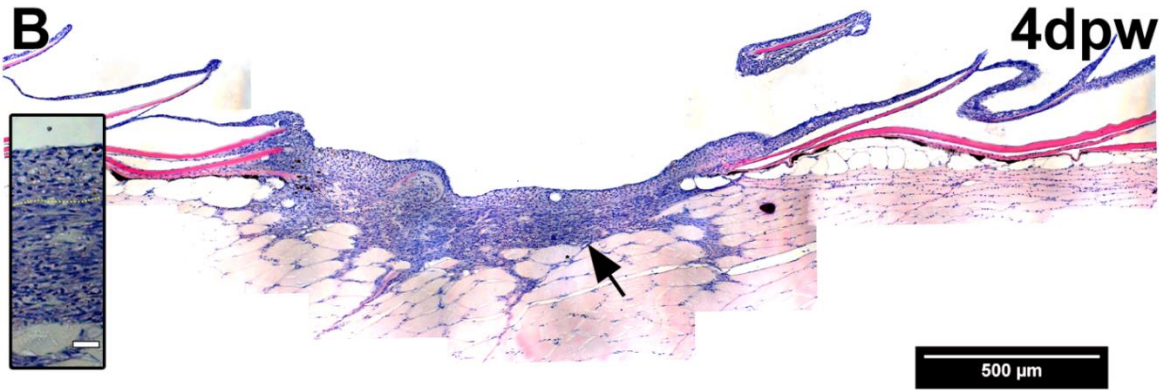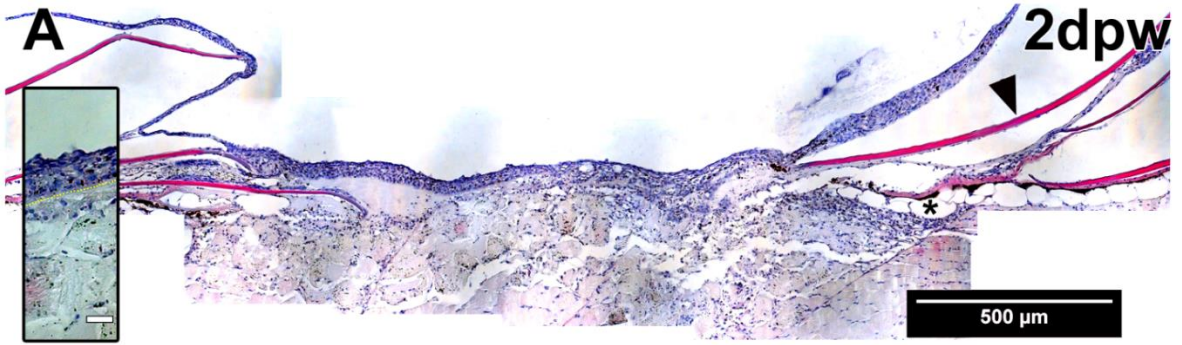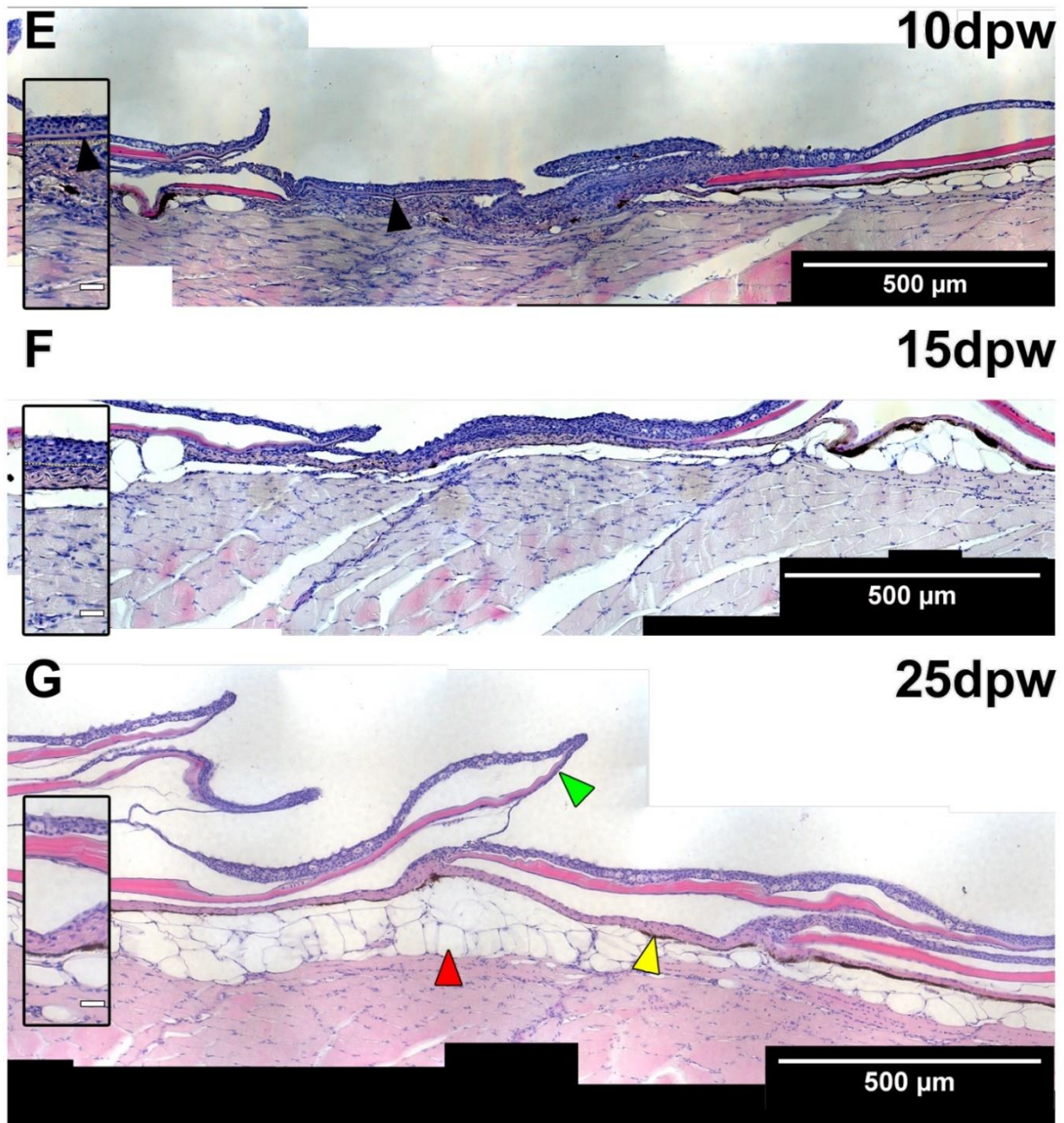
Figure 5.22: Long term analysis of granulation tissue formation and resolution in adult zebrafish. (**A**) At 2 dpw, the wound is covered by neo-epidermis with an increased number of keratinocyte-layers in comparison to adjacent regions. The scales (arrowhead) as well as sub-epidermal structures such as dermis with melanocytes and adipose tissue are disrupted (asterisk shows intact adipocyte and melanocyte above). (**B**) A high amount of nuclear haematoxylin staining is visible below the epidermis at 4 dpw. This area contains leukocytes, fibroblasts and collagens and is called granulation tissue. (**C**) At 6 dpw, the granulation tissue is shrinking in size and cells presumably start to migrate out of the wounded region or undergo cell death. (**D**) The granulation tissue is very small around day 8 post wounding and the first signs of melanocytes are visible below the epidermis. (**E**) The first signs of scale regeneration can be seen at latest between 8 and 10 dpw (inlet, arrowhead). The granulation tissue is nearly completely resolved. (**F**) The epidermis is still thickened but the granulation tissue is almost completely resolved at 15 dpw. Some cells are visible between the muscle which suggests a migration of leukocytes and / or fibroblasts out of the wounded area. (**G**) At 25 dpw, the wounded tissue is almost completely regenerated. Epidermis and scales are wavy but intact (green arrowhead) melanocytes within the dermis (yellow arrowhead), as well as adipose tissue (red arrowhead) are visible and no accumulation of cells or ECM is visible in the sub-epidermal space. Anterior to the left.

It was intriguing to determine if fibroblasts that arrived in the destroyed area were proliferating extensively to constitute the densely populated granulation tissue visible at day four post wounding. For this purpose, BrdU incorporation was utilised to track cell proliferation over a time window of ten hours. At two and four days after injury, when the granulation tissue size was increasing (Fig. 5.23A, 5.23B, 5.23F), the proportion of proliferative cells was at 40% on average (Fig. 5.23G). As mentioned above, the granulation tissue area declined at six days post wounding and later time points (Fig. 5.23C – 5.23E, Fig. 5.23F). Concomitantly, the proportion of mitotic cells decreased to below 20% where it stayed until the complete regression of the granulation tissue at ten days post injury (Fig. 5.23G). In summary, these data suggest that proliferation rates change during the repair of full-thickness wounds. The formation of the granulation tissue (two to four days post wounding) is accompanied by increased proliferation rates, which decline again as the granulation tissue is degraded and declines in size.
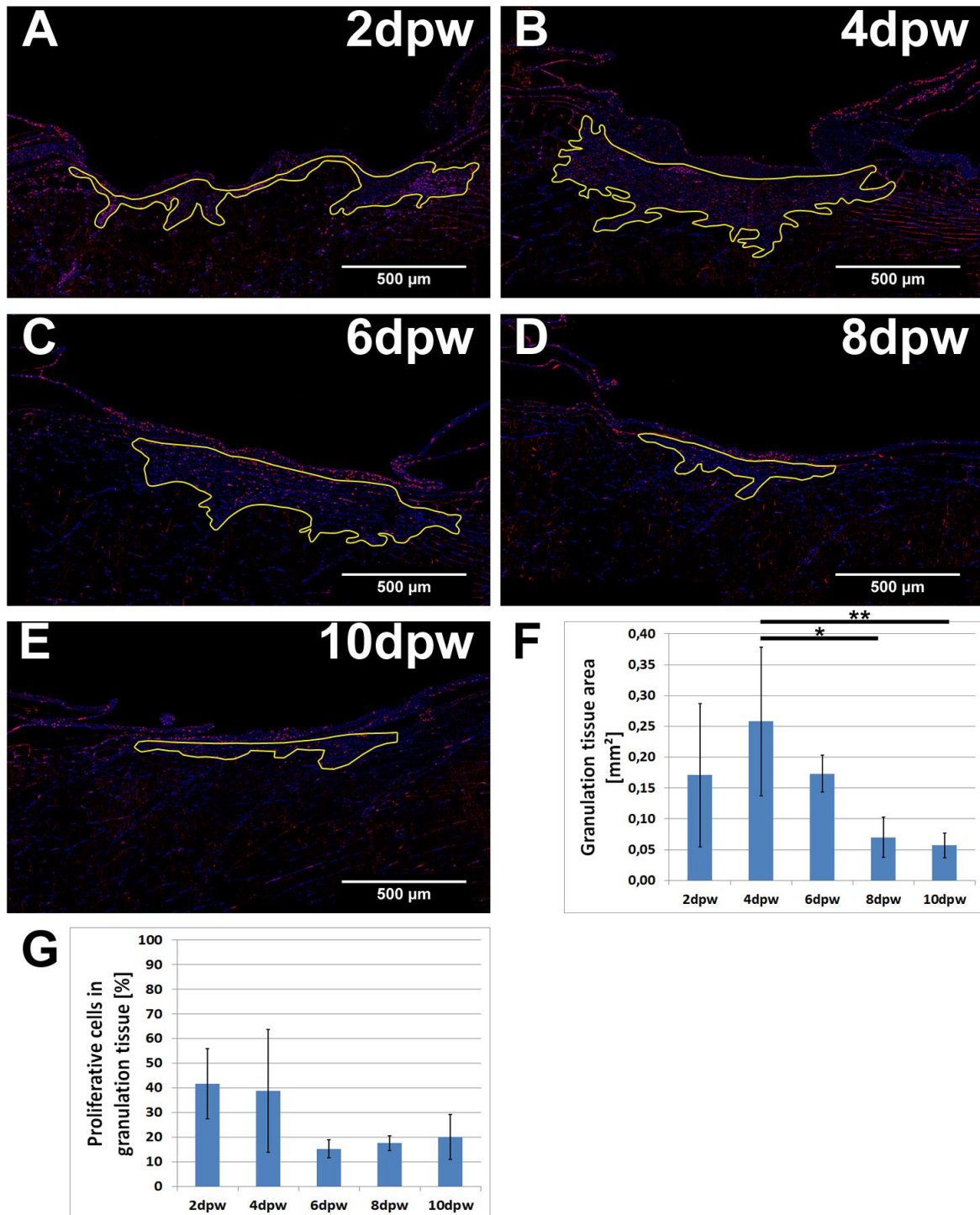
Figure 5.23: BrdU incorporation for 10 hours before each time point was used for proliferation analysis in the granulation tissue. (**A**) At 2 dpw, the granulation tissue is in the process of formation. Within the yellow encircled area, the density of cells is increased in comparison to surrounding muscle regions. Within this area of the presumptive granulation tissue (**F**, n=5) the number of BrdU positive, thereby proliferative cells is on average 40 % (**G**, n=5). (**B**) While the area of the granulation tissue appears increased at 4 dpw (**F**, n=5), the BrdU positive to BrdU negative ratio stays at approximately 40% (**G**, n=5). (**C**) Around day 6 post wounding, the granulation tissue retracts again and decreases in size (**F**, n=4). This could be linked to less proliferation in the sub-epidermal space, since the ratio sinks to approximately 15% (**G**, n=4). (**D**) At 8 dpw the granulation tissue size is significantly smaller compared to the peak in size at 4 dpw (**B**, **F**, n=5). The proliferation levels stay below 20% during this time point as well (**G**, n=5). (**E**) The granulation tissue is nearly completely resolved and only 0.05 mm² in size (**F**, n=5). During this time, the ratio of proliferative and non-proliferative cells stays at about 20% (**G**, n=5).

Anterior to the left; *: p<0.05, **: p<0.01 with one-way ANOVA followed by Bonferroni post-hoc analysis.

5.2.2 _Inflammation and FGF signalling are both required for a functional granulation tissue_

It was shown by Richardson and colleagues, that the correct formation of a granulation tissue depends heavily on both the immune response and fibroblast growth factor (FGF) signalling, since both treatment with immune suppressing hydrocortisone and overexpression of a dominant negative variant of FGF-receptor 1 (dnFGFr1) lead to a lack of a granulation tissue [20]. However, it is unknown how the immune system and FGF signalling can lead to very similar, if not identical, phenotypes and whether they are connected. If they are connected, it would be intriguing to find the cell type responsible for the release of the FGF which stimulates fibroblasts. Further, it is undiscovered yet whether a motogenic or mitogenic effect of FGF (or both) on fibroblasts is required for formation of a granulation tissue or a complete lack of it upon inhibition of FGF signalling pathways. To get first indications for a connection between the immune response and FGF signalling I made use of a combination of chemical immune suppression (hydrocortisone) and transgenic over-activation of FGF signalling (_Tg(hsp70I:ca-fgfr1)pd3_). Wild type and transgenic fish were heat-shocked daily for one hour and kept in system water containing either 0.2% DMSO or 275 µM hydrocortisone. Wild type animals treated with vehicle DMSO formed a granulation tissue of 0.25 mm² by day four post injury (Fig. 5.24A, Fig. 5.25C). This size was in line with previously analysed granulation tissue areas (Fig. 5.23F). Upon treatment with hydrocortisone, wild type fish lacked the granulation tissue almost completely (Fig. 5.24B, Fig. 5.25C). DMSO treated fish with constitutively active FGF receptor 1 signalling showed granulation tissue areas which were comparable to DMSO treated wild type fish (Fig. 5.24C, Fig. 5.25C). But in contrast to immune-suppressed wild type fish, _hsp70I:ca-fgfr1_ fish treated with hydrocortisone do form a granulation tissue (Fig. 5.24D, Fig. 5.25C).

A **WT, 0.2% DMSO**

B **WT, 275 µM HC**

C *hsp70:caFGFr1*, 0.2% DMSO

D *hsp70:caFGFr1*, 275 µM HC
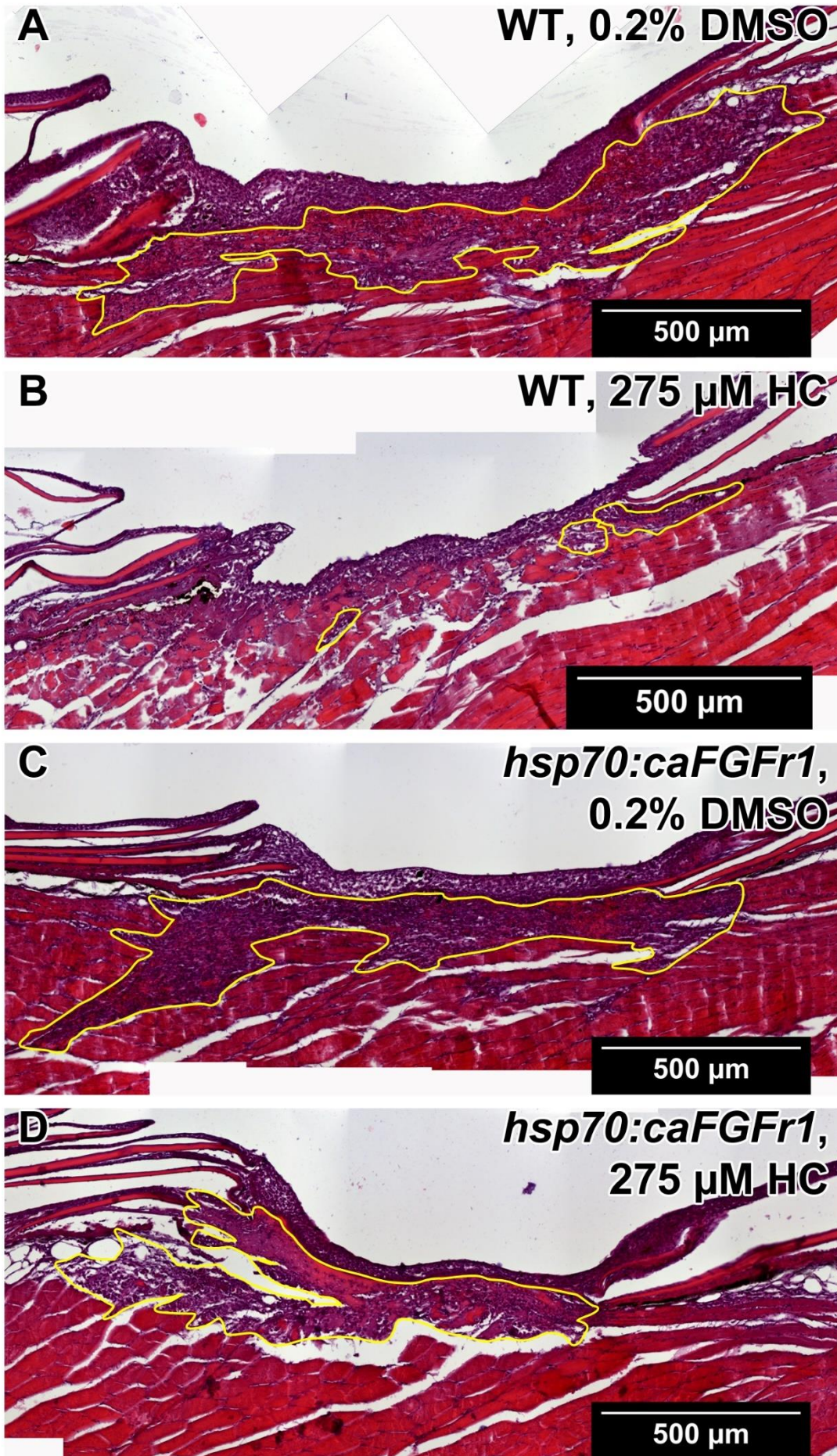
Figure 5.24: Adult fish of wild type or (*Tg(hsp70I:ca-fgfr1)^pd3^*) strain were treated with either DMSO or 275 µM hydrocortisone and subjected to daily heat shock and sacrificed at day 4 post wounding. While granulation tissue formation can be inhibited almost completely by treatment with hydrocortisone (compare **A** and **B**) the expression of a constitutively active FGF receptor can overcome the immune suppression by hydrocortisone almost completely (**C** and **D**). In contrast to immune suppressed wild type fish (B), constitutively active FGF receptor fish display a granulation tissue in the sub-epidermal region by day 4 post wounding (D) which is approximately 20% smaller than without immune suppression (quantifications in **Fig. 5.25C**). Anterior to the left.

One hypothesis was that macrophages are responsible for secreting FGFs and thus stimulating fibroblasts. Although it has never been proven in zebrafish, colony stimulating factor has been shown to be expressed and required by macrophages in mice [150], [151]. I wounded adult *csf1ra* mutant fish (*pfeffer, pfe^tm236b^*), which lack osteoclasts and xanthophores and potentially also lack macrophages [152]–[154]. Adult wild type and mutant fish of similar age were wounded, and both groups were kept separately in tanks with a constant supply of system water. At four days post wounding, all fish were sacrificed and fixed, then embedded in paraffin and sectioned. To determine the size of the granulation tissue, the sections were stained with haematoxylin and eosin, imaged and evaluated with FIJI to measure the granulation tissue area. In the representative images in Fig. 5.25A and 5.25B, the granulation tissue of age matched wild type controls (Fig. 5.25A) was approximately the same size as *pfe* mutants. After quantification of all examined fish, there was no statistically significant difference between granulation tissue area of wild type and mutant fish (Fig. 5.25D).
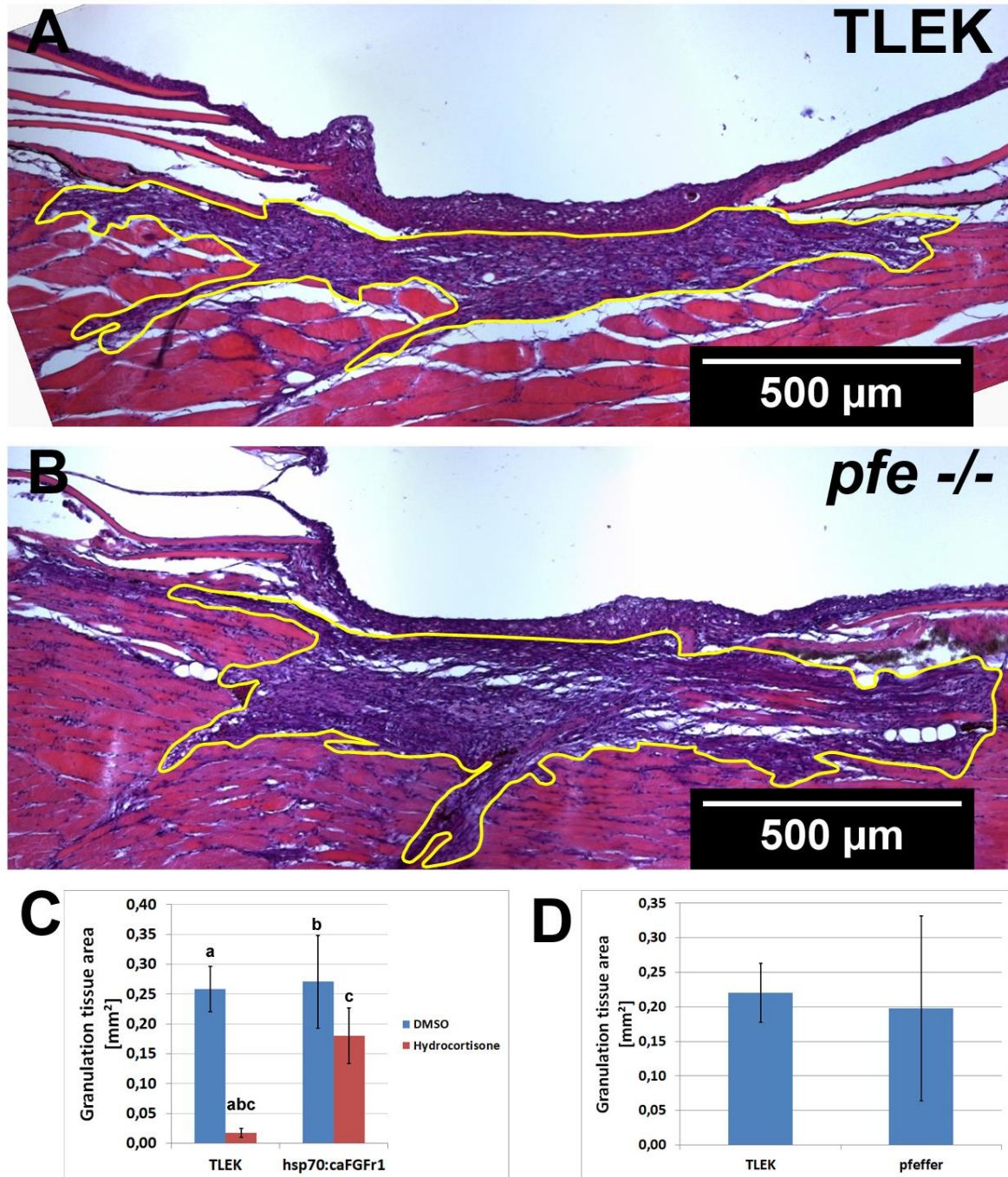
Figure 5.25: Fish of either wild type or *csfr1a* mutant genotype were wounded by dermatology laser and sacrificed on day 4 post wounding. Wild type fish showed a granulation tissue area in the wound centre of 0.22 mm² on average (**A**, **D**), which is in line with previous experiments. Upon loss of *csfr1a* and thereby most likely the monocytes and macrophages, the granulation tissue shows a similar area (**B**, **D**). The graph in **C** shows the evaluation of granulation tissue area after treatment with either DMSO as a control or hydrocortisone to suppress the immune response. DMSO controls of heat shocked wild type (n=3) and *hsp70l:ca-fgfr1* fish (n=3) showed similarly sized granulation tissue areas at approximately 0.25 mm², while the hydrocortisone treatment resulted in an inhibition of granulation tissue formation only in wild type fish (n=3) but not *hsp70l:ca-fgfr1* fish (n=3). Anterior to the left. Statistic evaluation of data for **C** was performed using ANOVA followed by Bonferroni post-hoc test. Three fish were used each for TLEK DMSO, TLEK hydrocortisone, caFGFr1 DMSO, caFGFr1 hydrocortisone, granulation tissue area was measured on two sections per fish. If not stated otherwise statistical evaluation proved no significant difference. a: $p<0.005$, b: $p<0.005$, c: $p<0.05$.

5.3 Differences in granulation tissue composition between mouse and fish as key to scar formation

5.3.1 *Granulation tissue of zebrafish does not result in a scar due to lack of Lysyl-hydroxylase 2 activity?*

In contrast to mammals, zebrafish do not form scars [20]. As mentioned in the introduction, land-living vertebrates show a scar-free healing only during embryonal development and lose the ability to regenerate tissues almost perfectly shortly before birth. Hence, the question that came up was how the difference in phenotype between embryonic stages and post-birth is regulated genetically and on a molecular level. There are several parallels between embryonic mammals and adult teleosts such as the humid environment, immune responsive mechanisms and simpler skin structure. Thus, adult zebrafish could be used as a model system for scar-free healing. To compare teleost data to mammalian data, our lab collaborated with Prof. Dr. med. Sabine Eming, who published the influence of macrophage signalling on fibroblasts to alter the characteristics of post-injury collagen networks. They found that macrophages, activated by IL-4 and IL-13, secrete Resistin-like alpha molecule (Relm-α), which in turn stimulates expression of several genes in wound fibroblasts. One of these genes is *plod2* encoding Lysyl hydroxylase 2 (LH2), which modifies lysine residues of collagen fibres prior to export, resulting in dihydroxy-lysinonorleucin (DHLNL) crosslinks. This type of extracellular collagen crosslinks is usually found in hard tissues like bone and cartilage. In mice lacking IL-4 receptor α, as well as Relm-α deficient mice, collagen fibrils in the granulation tissue are of irregular shape and size and show decreased amounts of DHLNL crosslinks in comparison to wild type mice [108]. Upon extensive search in the genome browser ensembl (ensembl.org/Danio_rerio) and zebrafish specific database ZFIN (zfin.org) it was intriguing to find all factors involved in DHLNL crosslinking present in the genome, except for Relm-α, which drives expression of *plod2* in mammalian wound associated fibroblasts. Furthermore, Tamara Migge showed by *in situ* hybridisation that there was no expression of *plod2* in zebrafish full-thickness wounds 5 dpw despite *col1* being expressed extensively (Fig. 5.26A and 5.26B). This led to the conclusion that collagen most likely is expressed and deposited in zebrafish wounds but not crosslinked by DHLNL crosslinks as it is the case in mice. In collaboration with Prof. Dr. med. Jürgen Brinckmann at Lübeck University, biochemical properties of mouse as well as carp granulation tissue were examined. While mice show a shift of collagen crosslinking type towards DHLNL, carp granulation tissue contains at each investigated time point almost exclusively hydroxy-lysinonorleucine (HLNL) crosslinks (Fig. 5.26C). Finally, ultrastructural analysis of zebrafish granulation tissue at 4 dpw revealed collagen fibril structure resembling in shape and size IL4Rα (and Relm-α) deficient mice (Fig. 5.26D-F).
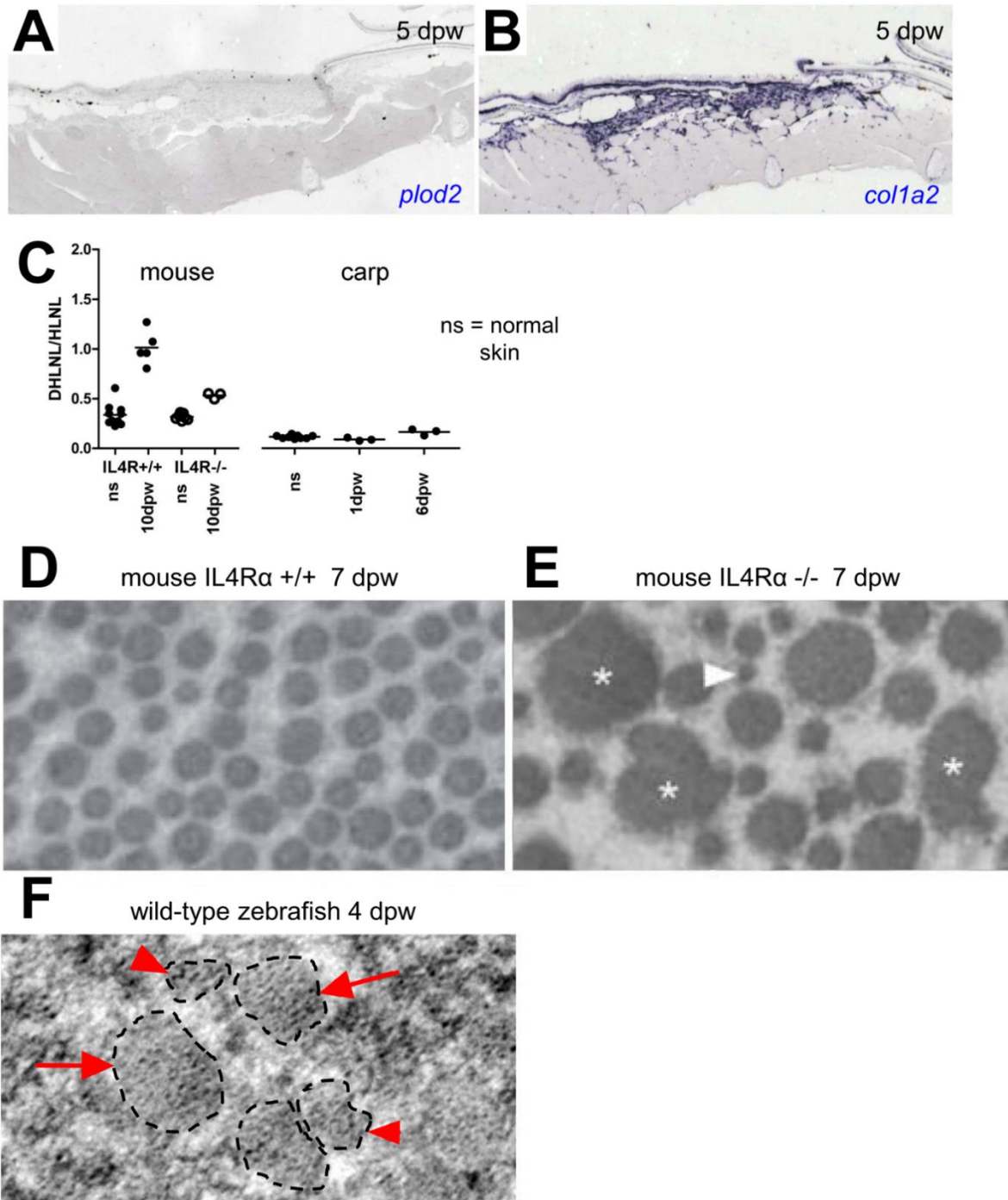
Figure 5.26: Observations resulting from collaborations with Jürgen Brinckmann, Sabine Eming and Wilhelm Bloch. Adult zebrafish do not show expression of *plod2b* within full-thickness wounds at day 5 post wounding (**A**), although *collagen1a2* is highly expressed during that time (**B**, Tamara Migge). (**C**) In mice, the ratio of DHLNL to HLNL crosslinks in normal skin (ns) is on average at 0.4. Ten days after wounding the ratio increases to approximately 1. Mouse mutants for IL4R show a less pronounced increase of the DHLNL part after wounding. Carp shows a low portion of DHLNL crosslinks in normal skin and the ratio further does not increase at 1 dpw or 6 dpw (courtesy of Sabine Eming, and Jürgen Brinckmann [108] and unpublished results). Wild type mice show an even distribution of collagen fibril size, and regular outlines of single collagen fibrils in TEM micrographs of the granulation tissue at 7 dpw (**D**). IL4R mutants in contrast display irregularly shaped (**E**, asterisks) and irregularly sized collagen fibrils (**E**, compare asterisk and arrowhead). The granulation tissue of adult zebrafish at 4 dpw shows a high abundance of proteoglycans and the collagen fibrils are – like the il4r mouse mutant – irregularly shaped (**F**, dotted outline) and sized (**F**, arrowheads: small diameter fibrils compared to arrows: larger diameter, Wilhelm Bloch).

5.3.2 *Transgenic approach to mimic mammalian wound healing*

To explore the hypothesis that the IL4 - Relm-α - LH2 pathway is the major difference between mammals and teleosts that is causative for decreased scarring in fish, I aimed to generate a transgenic line ectopically expressing *plod2b* by Gateway recombination and tol2 mediated integration.

The transgene that was injected into one cell stage zebrafish embryos contained the hsp70I promoter for heat shock inducible expression of the *plod2b* gene. Injected fish were sorted for GFP (G0), raised to adulthood and crossed to each other to screen for successful integration into the genome and germline transmission. GFP-positive progeny (F1) was partly used for expression-analysis of the transgene and also raised to adulthood.

In the meantime, adult transiently expressing fish of the G0 generation were used for wounding experiments and collagen content was assessed with a collagen1 antibody. The chosen example for a transiently expressing fish (Fig. 5.28) is the 'best case' scenario. The fish was heat shocked daily for one hour and sacrificed on day seven post wounding. While the wild type control had only few collagen fibrils in the remaining granulation tissue (Fig. 5.27A, arrow), the transiently expressing fish showed more abundant fluorescent staining of collagen (Fig. 5.27B, arrow). However, this represents the exception as nearly all other GFP positive transiently expressing fish resembled the wild type condition.
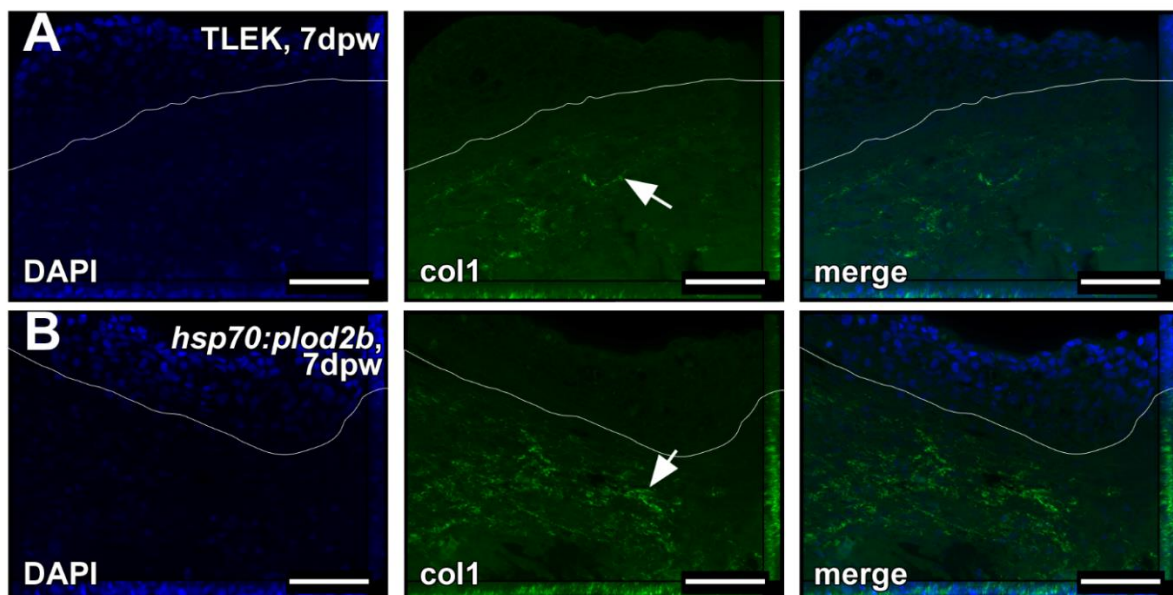
Figure 5.27: Immunohistochemistry with an antibody against col1 demonstrates collagen fibrils in the granulation tissue (below white line) of adult heat shocked wildtype fish at 7 dpw (**A**, arrow). In transiently expressing fish of the injected generation, the abundance of Collagen1 fibrils was higher in several cases (**B**, arrow). However, this could not be shown for fish of later generations with stable genomic integration of the construct (Bachelor thesis, Katharina Bieker). Anterior to the left, scale bar 50 µm.

The F1 embryos for transgene analysis were heat shocked at day two post fertilisation for one hour at 40°C and analysed for transgene expression by *in situ* hybridisation with GFP-negative siblings as reference. GFP-negative siblings (Fig. 5.28A), as well as non-heat shocked transgenics (Fig. 5.28B) showed no expression of the transgene. Additional information from the *in situ* analysis of non-heat shocked transgenes is that the integrated transgene did not give any background signal (Fig. 5.28B) even though the integrated (transgenic) *plod2b* coding sequence was identical to the mRNA sequence. Upon heat shock of GFP-positive fish a strong signal was obtained from the *plod2b* antisense probe (Fig. 5.28C, arrow). However, this signal was not uniformly found in all cells of the organism as it would have been expected with the *hsp70l* promoter. Once transgenic fish of the F1 generation were adult, they were heat shocked for one hour and tail fins were amputated one hour after the end of the heat shock. The tail fins were examined for transgene expression by *in situ* hybridisation with the *plod2b* antisense probe. As a positive control, the *col1a2* probe was used. While *col1a2* was expressed very densely without gaps (Fig. 5.28E), the transgene expression was patchy and seemed not present in some areas (Fig. 5.28F). Nevertheless, these fish (alongside wild type siblings) were wounded by laser injury, heat shocked daily and sacrificed at day seven post wounding. After histological staining, there was no obvious difference of the granulation tissue area at 7 dpw in transgenic (Fig. 5.28G) compared to wild type fish (Fig. 5.28G). Later generations of this transgenic line lost the signal of transgene expression even further despite the positive transgenesis marker (heart-specific GFP, data not shown).
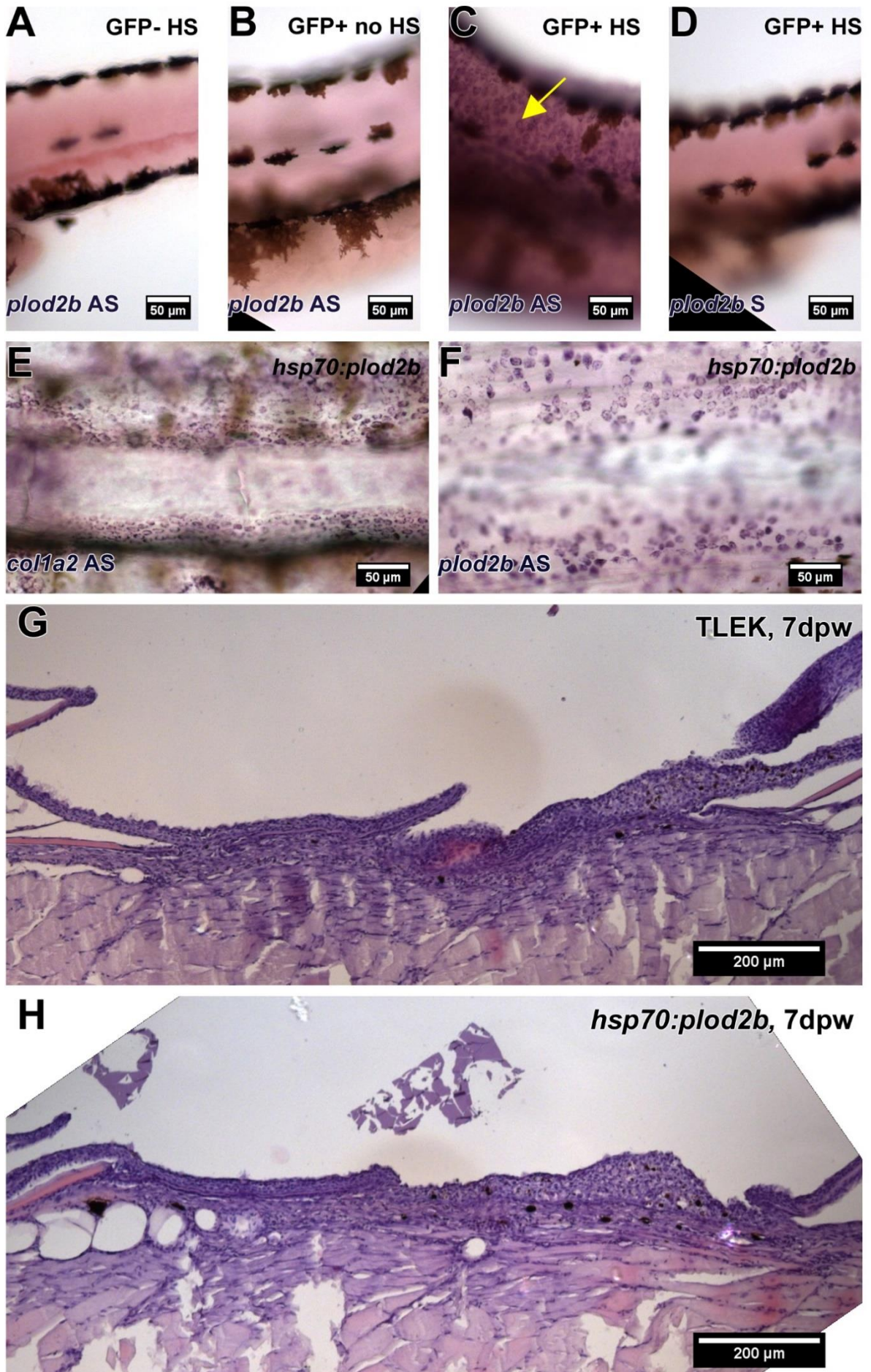
Figure 5.28: Functional analysis of the *hsp70I:plod2b* transgenic line. Offspring of injected and identified carriers were heat shocked 1 hour prior to fixation on day 2 post fertilisation. GFP negative siblings did not show any expression of plod2b after heat shock (**A**), as well as GFP positive carriers of the transgene without heat shock (**B**). GFP positive carriers with heat shock however, displayed a strong staining with the *plod2b* antisense (AS) probe, demonstrating stable and strong expression of the construct after heat shock in almost ubiquitous fashion (**C**). As a control for probe specificity, the sense (S) probe hybridisation of heat shocked carriers did not result in staining (**D**). Adult transgenic fish were heat shocked for 1 hour and tail fins were amputated 1 hour after the end of the heat shock. In situ hybridisation with *collagen 1a2* antisense probe resulted in a strong perinuclear staining in unspecified cells of the tail fin (**E**). In comparison, the plod2b transgene however appeared to be not as ubiquitously and strongly expressed (**F**). From wounding experiments with adult heat shocked fish, it was evident that the granulation tissue resolution was occurring in transgenic animals (**G**) to the same degree as in wild type fish (**H**). Anterior to the left.

5.3.3 Injection of Relm-α into adult zebrafish wounds is not suited for analysis of granulation tissue size

As a more direct approach, I obtained recombinant mouse Relm-α protein from Prof. Dr. Raimund Wagener and performed daily injection of 1 µg Relm-α into full-thickness wounds of adult wild type zebrafish. As a control, I injected PBS into wounds of siblings. Although it was unclear which protein acts as a receptor for Relm-α and whether it is represented in the zebrafish genome, initial analysis of recombinant Relm-α-injected fish showed increased granulation tissue area at day seven post wounding (Fig 5.29A – 5.29C). However, PBS injected fish showed abnormal granulation tissue area at 7 dpw, which was most likely the result of repeated injection into the wound and thereby caused micro-injuries with the capillary. For example, while one muscle compartment was injured and displayed fibrosis (Fig. 5.29A yellow outlined area), the adjacent muscle compartment was fully intact (Fig. 5.29A, arrowhead). Due to these artificial and constant injuries and the observed prolonged fibrosis, these experiments were not pursued any further.
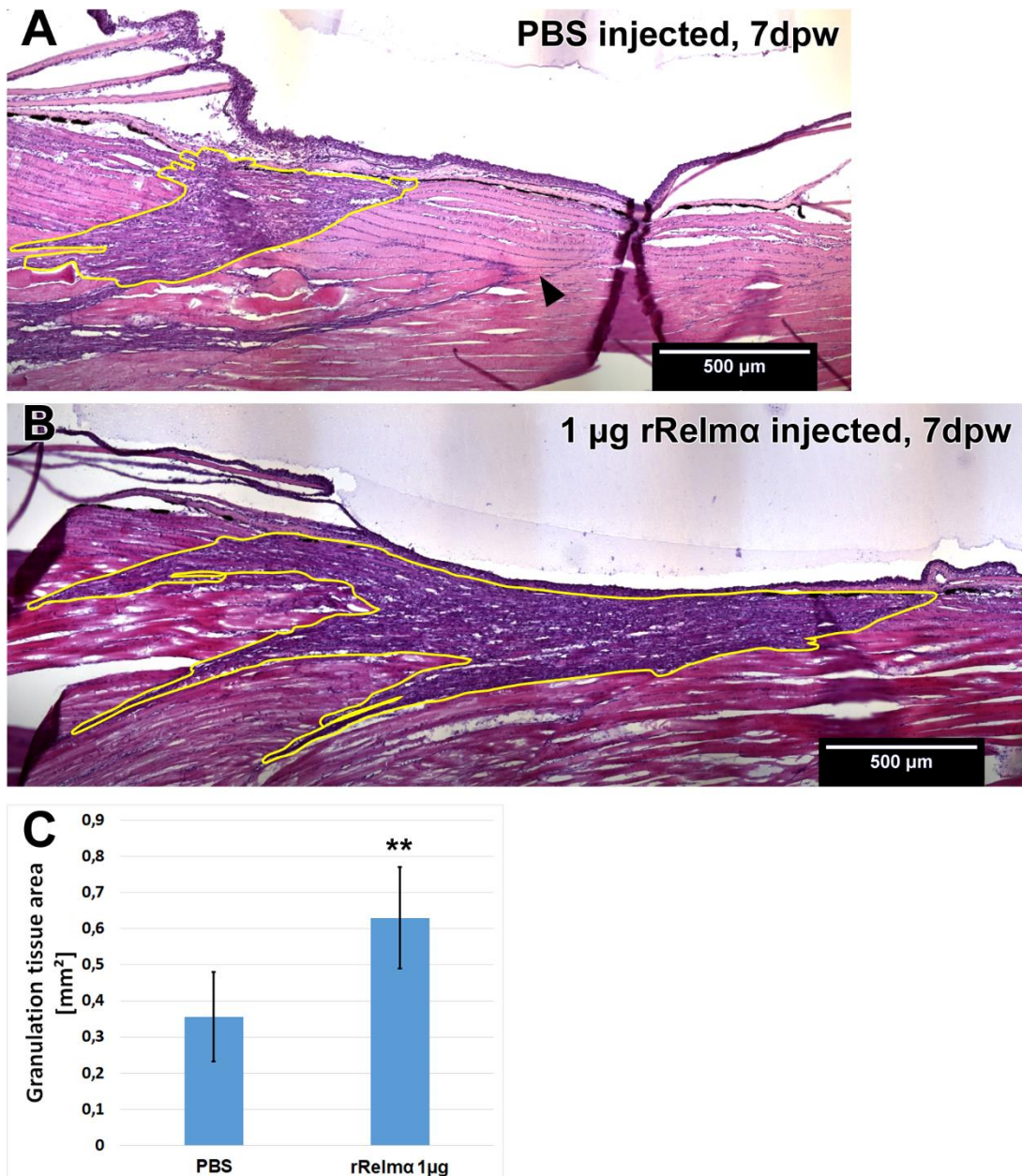
Figure 5.29: Two adult fish were injected with either PBS (**A**) or recombinant mouse Relm-α (**B**) for 5 continuous days after wounding. On day 7 post wounding, the granulation tissue of PBS injected fish was on average 0.3 mm² in area of wound centre sections (**C**) which was contradictory to previous granulation tissue measurements (**Fig. 5.23F**). It seems as if only one muscle compartment was affected by fibrosis (yellow outline), while the other muscle compartment was unaffected (arrowhead). Since PBS or rRelm-α was injected into the wound, this observation serves as an example for microinjuries. In wild type fish injected with recombinant Relm-α protein, the granulation tissue area was even significantly bigger at around 0.6 mm² (**B**, **C**: n=3 sections of 2 fish per condition, Student t-test, p<0.01). Anterior to the left.

6 Discussion

6.1 <u>Re-epithelialisation is driven by cell migration as well as intercalation and elongation</u>

According to the observations made *in vitro* and *in vivo* in mammalian wound healing models, TGF-ß influences both cell migration (positively) and proliferation (negatively) of keratinocytes [76], [155]–[157]. Hence, it has been thus far difficult to determine whether this pathway has either beneficial or adverse effects on wound healing *in vivo*. Further, the identity and function of downstream mediators of the two different outcomes remain unclear. The difficulties are reflected in seemingly contradictory results of published studies. TGF-ß signalling as part of the initial growth factor cocktail released upon injury increases the migration speed and thereby accelerates the closure of wounds both *in vitro* and *in vivo* [155], [156]. Surprisingly though, the knockout of *tgfb1* or its downstream effector *smad3*, accelerates wound closure *in vivo* as well [76], [157].

This contradictory observation can be explained by the influence proliferation has on wound healing in mammals. In mice, migration and proliferation occur in parallel and contribute to the closure [24], [158]. Previous studies in the Hammerschmidt lab however demonstrated that proliferation is not an immediate driving force of wound closure in adult zebrafish and is not increased until day 3 post wounding, when the wound is already completely covered by multiple cell layers called neo-epidermis [25]. The reasons for this remain unclear. One explanation for this might be that the adult zebrafish epidermis has a large reservoir of undifferentiated 'basal keratinocyte-like' epithelial cells present in the intermediate layer, which can be recruited to close and cover the injury and thus the closure is independent from proliferation. These intermediate cells are positive for the basal keratinocyte marker p63 and have the potential to proliferate. Thus, the zebrafish epidermis does not have to draw the required replacement cells for re-epithelialisation from specialised stem cell pools with limited numbers as it is the case in mice. It can replace lost basal keratinocytes directly with intermediate cells which then presumably take over basal keratinocyte function. Moreover, in mammals, the wounds are closed provisionally by a scab which is formed rapidly, therefore the time pressure for re-epithelialisation is not as high anymore and can take several days. Zebrafish don't show signs of blood clot formation to close the wounds and rely heavily on a rapid re-epithelialisation [20], [25]. Studies of adult amphibian wound healing are rare, but initial research in axolotl revealed that blood clotting appears to be uncommon in other aquatic animals as well. Excision skin wounds in adult axolotl are also not accompanied by extensive bleeding and scab formation as it is the case in mammals [159]. Taken together, this indicates that the time pressure for re-epithelialisation is higher in aquatic animals and thus needs to occur faster.

This major difference in initial closure and the independence from proliferation allowed us to dissect the positive influence of the TGF-ß signalling-induced motogenic branch from the negative influence on the mitogenic branch in the *in vivo* system zebrafish. Especially zebrafish partial-thickness wounds rely heavily on active cell migration (Fig. 5.1, 5.2, 5.12). Upon chemical block of TGF-ß receptors ALK1, 5 and 8, the migration speed was decreased by approximately 55%. This reduction demonstrates that TGF-ß is required for the rapid closure of partial-thickness of

zebrafish by promoting cell migration. Nevertheless, TGF-ß inhibition with two different inhibitors did not block wound closure entirely. This either means, TGF-ß is not alone regulating the migration during re-epithelialisation or that long-range cell elongation functions in the background. And indeed, closure speed of partial-thickness wounds under TGF-ß signalling inhibition closes with approximately the same speed as full-thickness wounds. But given that cell elongation and tissue rearrangement occurs as backup mechanism, TGF-ß inhibition still causes a massive effect. This might mean that either TGF-ß signalling is the most important and dominant modulator for partial-thickness wound closure, or that other signalling pathways (such as FGF7 [160] or EGF [161]) terminate in the same downstream targets to promote cell migration. However, it remains to be elucidated to which extent other pathways influence cell migration and wound closure in zebrafish.

The inhibition of TGF-ß signalling did not affect initial aspects of cell migration such as lamellipodial formation and outgrowth despite the striking impact it has on epithelial to mesenchymal transition induction [162]. This indicates that at least in this model, TGF-ß signalling acts as a migration modulator by activating specific factors necessary during migration but is dispensable for the initiation of cell migration. Since migration relies on several inputs and modulators, it appears challenging to reveal the specific mode of action for TGF-ß signalling. Due to the abundance of downstream targets of TGF-ß reported from other models it seems inefficient to target all of them over time by chemical or genetic inhibition.

Nevertheless, a previously described outcome of elevated TGF-ß signalling in response to injury is a shift in integrin expression and localisation in keratinocytes (reviewed in [163]). Here, the application of RGD peptides that compete for the binding of integrins to components of the extracellular matrix during migration led to a severe delay of wound closure and a morphologically similar phenotype as TGF-ß signal inhibition (Fig. 5.4). Lamellipodia were formed and the cells showed an EMT-like phenotype manifested in increased motility. Despite that, the leading edges did not move towards each other with the speed observed in untreated controls but showed a decrease of approximately 48%.

In fact, both the chemical block of TGF-ß-signalling and integrin-ECM interaction led to the conclusion that the cells do not find enough grip on the migration substrate to move and close the wound efficiently. The lamellipodia were formed, making it unlikely that the cytoskeleton itself was affected by either treatment, but the protrusions quickly retracted again after the failure to establish stable contact to the migration substrate. Afterwards, lamellipodia reached out into other directions and 'searched' for other possible contact points.

Although direct evidence for a TGF-ß mediated integrin-shift after injury has not yet been presented for fish, integrin interference using RGD peptides clearly demonstrated the importance of integrin-dependent migration during wound closure. Although the connection between TGF-ß and integrins remains speculative, it is intriguing that the observations of both TGF-ß and integrin interference overlap in several aspects. In future experiments, proof for a change in integrin expression and / or re-localisation on cellular level needs to be provided. However, in zebrafish, in contrast to mice, the mobilisation of the epidermis occurs within a very short time frame and is finished within 30 minutes, making it unlikely that the epidermis has enough time to inactivate one population of integrins, shut down their expression and initiate the expression, translation and transport of other types of integrin-

heterodimers. It is more likely that a possible rapid shift of integrins in this case occurs independent from gene expression. This implies that the 'migratory' integrins are stored inside vesicles for emergency and used upon demand or are re-localised within the cell to mediate protrusive behaviour and attachment of lamellipodia by focal adhesion formation. Thus far there is no implication for the storage of integrins, but it has been investigated to which part integrin trafficking and recycling can regulate cell migration on a cellular level [164], [165]. It was shown that for example PDGF stimulated rapid recycling of αvß3 integrin to the plasma membrane in a rab GTPase-dependent manner [166]. Further it was demonstrated that growth factor signalling can regulate the externalisation of integrins via the PI3K – AKT – GSK-3 axis [167]. To summarise, both (expression-dependent and independent) cases have to be investigated by use of methods such as *in situ* hybridisation and immunohistochemistry.

A different mechanism for epithelial mobilisation after injury, which I observed during my studies involved the organised epithelial rearrangement driven by Rho-associated kinase (ROCK) and the planar cell polarity pathway. This keratinocyte reorganisation occurred in long range over the epidermis adjacent to the wound. Intermediate cells of the zebrafish epidermis have basal-like characteristics in the form of proliferative potential. Thereby, these undifferentiated keratinocytes represent the ideal replacement for basal cells. To relocate to the basal-most layer however, they have to move horizontally within the epidermis. This involves coordinated parallel elongation of keratinocytes and radial intercalation. Tissue rearrangements that employ coordinated elongation and radial intercalation of cells are very frequently observed during early development of different animals [28]. Very often during these developmental tissue movements, the planar cell polarity branch of the Wnt signalling pathway plays an important role. I found by chemical and genetical experiments that ROCK, JNK and Dishevelled play a role also during epidermal repair of adult zebrafish. All of these approaches showed pronounced defects in cell elongation, directionality and radial intercalation, ultimately resulting in a decrease of closure rates of full-thickness wounds (Fig. 5.6, 5.8, 5.10 and 5.12).

Interestingly, the effects on the closure of partial-thickness wounds were less pronounced, but still present (Fig. 5.12). This can be explained by the fact that active cell migration, tissue rearrangements and to some extent most likely also purse-string are all active at the same time and it is likely that the fastest way of closure is dominant. This means specifically active cell migration is the first mechanism to be used (with an average speed of approximately 500 µm/hour, Fig. 5.12 and [168]). Only if it is not possible to use cell migration due to the absence of the proper migration substrate, the slower wound closure by coordinated cell elongation and radial intercalation is observed predominantly (at a speed of around 250 µm/hour, full-thickness wound *in vivo* imaging Philipp Knyphausen, [25]). However, this does not mean the other pathways or closing mechanisms are inactivated in consequence. During *in vivo* imaging of partial-thickness wounds it was visible that cells behind the leading edge were elongated as well (data not shown). The direct cause of the elongation during partial-thickness closure could be the tension across the tissue, building up by the migrating leading-edge cells. However, the results achieved by ROCK inhibitions and PCP pathway downregulation strongly suggest that elongation and intercalation act in the background as a replacement in case migration fails. Intriguingly, the speeds at which partial-thickness wounds close upon failure of

migration (TGF-ß inhibitor and RGD peptide treatments) are matching those of full-thickness wounds. Likewise, in scanning electron microscope studies it was demonstrated by Thomas Ramezani and Rebecca Richardson that active cell migration is occurring as long as the cells can attach to the substrate, and the mechanism of closure changes towards elongation and intercalation only as this contact to the substrate is lost [25]. Taken together, it seems as if the impact of the different pathways that control migration or intercalation depends on the status of the wound, but all are active at the same time and used according to closure speed when applicable.

6.2   Hypotonic medium influx is a trigger and modulator for re-epithelialisation

Several cues can be sensed by different cell populations that mediate a leak in the epidermal barrier. While the most dominant cue for mammals are PAMPs and DAMPs, it might be very different for aquatic vertebrates like fish. It was shown in earlier studies that both neutrophils and keratinocytes of larval zebrafish react to the influx of hypotonic medium. It even seems as if the zebrafish 'injury perception system' is conditioned to hypotonic medium influx since both neutrophil recruitment and keratinocyte protrusions are delayed upon exposure to isotonic outside medium [30], [32]. I found that in adult scale removal wounds the formation of the lamellipodia was delayed in isotonic medium (Fig. 5.15A) pointing to a role of hypotonic medium influx for the initiation of keratinocyte migration. Full thickness wounds, which do not rely heavily on lamellipodial crawling, do not show any effect in response to isotonic medium treatment (Fig. 5.14 and 5.15C).

In contrast to the lack of lamellipodial attachment upon TGF-ß inhibition or RGD treatment, no obvious defect in lamellipodial structure or behaviour was observed in isotonic medium (Fig. 5.13). Neither overextension beyond the leading edge, nor a loss of contact and retraction was observed in all cases, but the overall migration speed was reduced by 47% (Fig. 5.15B).

The general motility of the cells could be decreased due to the inactivity of 'motors'. For instance, the actin cytoskeleton polymerisation and depolymerisation or myosin phosphorylation could be disturbed, leading to a reduction in forward movement capability of each cell. Implications for this are found in the literature, as for example actin cytoskeleton reorganisation depends on the activity of Rho-associated kinase and jun N-terminal kinase [137], [138], [169], [170] which both respond to hypotonic stress [171], [172]. In contrast to TGF-ß and integrins, which most likely affect extracellular integrin-ECM binding, this would mean that a change in tonicity affects intracellular processes. This hypothesis can be examined by high-resolution *in vivo* imaging of a transgenic line expressing a *lifeact* construct [173], [174] under control of a basal keratinocyte-specific promoter like *krt19* or *p63*. A possible defect in actin polymerisation and depolymerisation should become evident with this approach.

In isotonic medium, the cells might not receive the main cue that the barrier is broken, which under normal conditions is provided by the change in tonicity. Consequences of this could be that the re-epithelialising keratinocytes show a cytoskeleton composition that resembles unwounded epidermis. For instance, the

keratin intermediary filaments could be still in a stationary condition while the actin-myosin network tries to migrate. This hypothesis could be resolved by ultrastructural analysis of partial thickness wounds shortly after injury.

6.3 <u>Mechanosensitive ion channels, FAK and other receptors for hypotonicity</u>

Few mechanisms of tonicity-perception of keratinocytes have been reported so far. One cue for a barrier disruption and the subsequent exposure to hypotonic medium could be the activation of volume regulated anion channels and a concomitant calcium influx, which is necessary for directed cell migration in other systems [147]. Activation of the channels is caused by cell swelling and subsequent Ca^{2+} influx [147]. Blockade of Ca^{2+} influx by capsazepine (Fig. 5.16) and Gd^{3+} (Fig. 5.17) however, did not affect wound closure (Fig. 5.21). The initiation of re-epithelialisation occurred within normal time frames and both lamellipodial outgrowth and migratory speed were not influenced (SV11-15). It must be noted however, that for both capsazepine and Gd^{3+} there are no appropriate positive controls to test their efficacy in our model. Although the concentrations used were ten-fold higher than those in *ex vivo* studies, *Xenopus* oocytes and zebrafish larvae [147], [148], [175], [176] it is not clear whether the chemical interference was sufficient to block calcium channels. To test the influence of calcium influx in future it might be intriguing to use calcium live imaging [177], [178]. Using this tool, possible calcium sparks in the leading edge basal keratinocytes should be visible under normal conditions but absent upon treatment with isotonic medium, capsazepine or Gd^{3+}, respectively as it is the case *in vitro* [147].

The other mechanism of tonicity perception employs heparan-sulfate proteoglycans and focal adhesion kinase [145]. The treatment with an inhibitor of focal adhesion kinase resulted in a non-significant tendency toward a slower migration, but no delay of migration start was observed. Due to the lack of a downstream readout as positive control except for absence of focal adhesions [179] there is no conclusion as to whether or not the inhibitor works in our model. Nevertheless, in case both ion channels and focal adhesion kinase are dispensable for the hypotonic sensation other possible receptors for hypotonicity have to be identified. In renal epithelial cells, it is known that receptor tyrosine kinases stimulate the sodium uptake upon hypotonic stress [171] and EGF and PDGF inhibitors showed inhibitory effects on Na^+ uptake. The next steps in investigating the tonicity perception in the context of wound closure would thereby be to elaborate and definitively exclude ion channels and focal adhesion kinase, and to screen for other possible perception mechanisms for hypotonicity and signalling cascades starting with EGF and PDGF.

6.4 <u>Hypotonicity stimulates AKT phosphorylation</u>

Downstream effectors of TOR influence the closure of larval *Drosophila* wounds [29] and a response of TOR to osmotic stress also was demonstrated [180], suggesting an involvement of this pathway as intracellular regulator of cellular behaviour in response to hypotonic stress as well. In my studies, I chose the phosphorylation of AKT as a readout for cascade activation upstream of TOR complex 1 [95]. The time

point 30 minutes after scale removal was chosen to investigate signalling during the main migration phase. Phosphorylated AKT was found in the first row of keratinocytes. Strikingly, AKT phosphorylation was strongly reduced upon treatment with either isotonic medium or the PI3K inhibitor PIK-90. With this information it can be concluded that hypotonic stress influences AKT activation and most likely acts via PI3K.

From these results it could be hypothesised, that both PI3K and AKT activation lead to increased TOR complex 1 (TORC1) activity to regulate biological processes such as protein synthesis or cell survival (both necessary for an intact leading edge and cell migration). And indeed, PI3K inhibition by PIK-90 led to a decrease in migratory speed, as was the case for isotonic medium treatment. However, PIK-90 treated wounds additionally exhibited lamellipodial dysfunction. In time lapse movies of partial-thickness wound closure after PIK-90 treatment it was evident that lamellipodia reached out over the homogenous leading edge, searching for attachment points on the ECM (Fig. 5.20). Further downstream in the signalling axis PI3K/AKT/TOR, inhibition of TOR complex function by rapamycin did not affect keratinocyte migration speed. It has to be kept in mind though that TOR complex 1 is only one of a variety of downstream targets of AKT. Taken together, all these observations mean that PI3K function influences migratory speed, AKT is activated by hypotonicity and TORC1 does not participate in closure of partial thickness wounds.

PI3K and AKT were shown to act on integrins via GSK-3 (section 6.1, [167]). This poses one possible mechanism that fits to the observations made with immunohistochemistry and chemical inhibition. The published regulation of integrin trafficking also explains the additional lamellipodial defect, I observed with PIK90. The total PI3K inhibition might have caused the integrin trafficking defect which was for yet unknown reasons not present in in isotonic medium. It can be speculated that hypotonic medium is likely to follow the route via PI3K and AKT (and possibly also via GSK-3). But then, upstream of integrin trafficking, there are other signalling cascades with partly compensatory function and this is the explanation why the PIK-90 phenotype is more pronounce. Moreover, PI3K has been linked to cell migration due to its function in PDGF and EGF induced formation of cell protrusions [181], [182]. Additionally, PI3K determines the leading edge and maintains the cell polarity in migrating leukocytes for instance [183]. This shows that there are multiple ways for PI3K to directly and indirectly influence cell migration. AKT itself can regulate cell migration by several different means aside from influencing integrin recycling and re-locating. To mention the most important mechanisms, phosphorylated AKT is co-localised with actin bundles and regulates their formation and actin phosphorylation [184]. Proteins which are bound by AKT, such as Girdin are necessary for remodelling of the actin cytoskeleton and thus contributing to cell migration [185].

To connect all these results, it is further necessary to inhibit AKT activity and test whether a reduction in migratory speed can be achieved. If this is the case, it strengthens the hypothesis, which should be further supported by rescue experiments with PI3K inhibition and a constitutively-active version of AKT. If this combined treatment resulted in no significant migratory speed reduction, this would be strong evidence that PI3K acts through AKT in this specific case. Further it would require a combination of isotonic medium treatment (migratory speed decrease) and an over-activity of either PI3K or AKT (normal or even increased migratory speed) to see which effect would be dominant. With this epistasis analysis it could then be

shown that hypotonic stress acts via PI3K and AKT but not TOR (Fig. 5.20E and Fig. 5.21) to promote cell migration.

In fact, there are several publications utilising a constitutively active version of PI3K for non-skin related research [186], [187]. Among them, Hu et al. generated a fusion of the catalytic subunit of PI3K p110 and the inter-Src homology region 2 (iSH2) of the p85 subunit. Between the two fragments, they integrated a hinge region ("glycine-kinker") to facilitate the interaction of the two proteins and this fusion protein functioned as a constitutively active version of PI3K. They showed this by thin-layer chromatography of produced phosphatidyl-inositol-3 phosphates (PIPs) as a result of PI-3 kinase activity [188]. Since they were able to express their constitutively active construct in *Xenopus* oocytes with a subsequent increase of Raf-1 activity, it could be possible to express the construct ectopically (by heat-shock) in zebrafish as well.

Constitutively active AKT is available and has been used as well [189]–[192]. For this protein, there is a zebrafish transgenic line that expresses a myristoylated version of the human AKT1 that lacks the pleckstrin homology domain [193]. Myristoylated AKT associates with the membrane where it is constitutively phosphorylated and thereby activated [189].

Once this epistasis is delineated clearly, the remaining questions are on one hand, how the hypotonic stress is perceived and on the other hand, how the migratory behaviour of keratinocytes is achieved if not by TOR complex activity.

6.5 Concluding remarks and thoughts about cell migration in the context of re-epithelialisation

The main reasoning behind the examination of hypotonic stress in the context of cell migration was the rather biophysical or biomechanical character of cell stimulation. It seems logical that an immediate cell response is only possible if the necessary prerequisites are present and stored ready-to-use in the cell itself and the initiator is supplied. Hypotonic stress for instance leads to calcium influx [194], [195], which is necessary to enable actin-myosin interaction in muscles and migrating cells [196], [197]. Both integrin re-localisation and calcium influx happen very quickly and utilise cytoskeletal components already present in the cell. Hence, both mechanisms to regulate cell migration are optimal molecular mechanisms to initiate and mediate the immediate re-epithelialisation in this partial-thickness model. The activation of AKT (and TGF-ß) can not only cause the immediate initiation of cell migration but simultaneously cause a long-term reaction to the injury (e.g. increased survival, increased biosynthesis of structural proteins, increased proliferation etc.) to enhance long-term healing.

It remains unclear whether the time between injury and the first signs of keratinocyte migration in our model is enough to mediate the transition of a stationary cell to a migratory cell by a shift in expression. It might make sense that during mammalian wound closure the activation of pathways and a shift in expression patterns can be utilised to induce migration, but this mechanism seems unlikely in the case of the fast closing fish wound. In general, the question whether a few minutes are enough to change cellular behaviour from one to the other extreme by a shift of transcription,

translation, processing and transport is intriguing and needs to be investigated in future.

6.6 Fibroblast recruitment relies on FGF signals most likely originating from leukocytes in zebrafish

To date, FGF signalling was connected to stimulation of re-epithelialisation and neovascularisation [23], [58], [99], [198]. With the exception of FGF 2 there was little evidence for a function of FGF on fibroblast migration [40], [74]. In our full-thickness wound model, Rebecca Richardson found an almost complete absence of col1a2 expressing fibroblasts in the wound at day four after injury upon block of FGF signalling. However, the other wound healing processes (re-epithelialisation, inflammation and neovascularisation) were completely unaffected and occurred normally. Intriguingly, the block of inflammation by hydrocortisone had the same result and treated fish showed a lack of a granulation tissue [20]. Thus far, it has been an open question whether the two observations are linked, and whether immune cells communicate with and recruit fibroblasts via FGFs. To investigate this signalling axis, treatment of fish ubiquitously expressing a constitutively active FGF receptor 1 in conjunction with hydrocortisone was performed. Constitutive FGF signalling was found to overcome the granulation tissue inhibiting effect of hydrocortisone. This either means FGF is downstream of the immune response or acts in parallel. From the data I obtained in my experiments, it can be hypothesised that leukocytes express and secrete FGF which (either directly or indirectly) causes the activation of fibroblasts in close vicinity to the wound. The activation of fibroblasts then is observable by the active migration of fibroblasts into the injured tissues, the locally increased proliferation (Fig. 5.23) and an increased collagen production [20]. Initial steps to shed light on the origin of the FGF in question by examination of csfr1a mutant fish (which are most likely deficient in macrophages considering mouse mutants in this gene [151]) did not result in a decrease of granulation tissue size.

To further investigate and characterise the connection of the immune system and fibroblasts, a model of chronic inflammation in combination with a dominant negative version of the FGF receptor 1 could be used. Given that leukocytes induce fibroblast recruitment the increased FGF secretion due to increased inflammation should not overcome the global block of response to FGF due to inhibited FGF signalling. Thus, an absence of granulation tissue would be expected. With this result the statement that immune cells secrete FGFs which recruit fibroblasts would be more definite and a parallel action of both would be less likely.

Chronic inflammation could be achieved by constant exposure to PAMPs by treatment of wounds with E. coli for instance. However, this exposure would end upon closure of the wound and re-establishment of the epithelial barrier. Injections of bacteria would lead to constant micro-injuries and therefore would not be applicable. Nevertheless, constant exposure of fish to bacteria in the environment with stable epithelial barrier might still increase the leukocyte number. Consequently, it might lead to an 'overshooting' immune response after wounding and a larger granulation tissue. Other means to provoke a chronic inflammation are the treatment with a mixture of hapten 2,4,6-trinitrobenzenesulfonic acid and ethanol as it was described

for induction of colitis in rats [199], [200]. It has to be tested though, if local application of this solution would cause a chronic inflammation and fibrosis in zebrafish epidermis as well. Transgenic approaches most likely have to be of inducible character due to the fact that experiments will be carried out in adult fish and the animals should not be constantly subjected to chronic inflammation. Nevertheless, targets could be NFκB or IKK and hyperactivity of both result in overexpression of pro-inflammatory genes for instance [49], [201], [202].

6.7   Simple collagen modification as key to scar-free healing?

The results obtained in the recent years point to the family of lysyl-hydroxylases as the central decision-point between fibrosis and scar-free healing [15], [108], [121], [203]. Interestingly, activity of these enzymes is described in mechanically more resistant tissues like bone, tendon and cartilage as well as during skin and organ fibrosis [15]. Specifically, *plod2* expression is upregulated in fibroblasts in cutaneous wounds of adult mice. This increase of plod2 expression results from macrophage IL-4Rα signalling and Resistin-like molecule alpha secretion [108]. The zebrafish genome on the other hand does not contain Resistin or Resistin-like encoding genes and thus this signalling axis is not active during cutaneous wound healing of zebrafish. Our studies demonstrate that *plod2b* is not expressed within the granulation tissue despite high collagen production at day five post wounding (Fig. 5.26A and B). Additionally, both biochemical analysis of the collagen crosslinking characteristics and ultrastructural analysis of the collagen fibrils within the granulation tissue indicate a high similarity between fish and *il-4rα* mutant mice (Fig. 5.26C-F). These mouse mutants were shown to have a mechanically deficient granulation tissue leading to haemorrhages underneath the neo-epidermis [108].

The hypothesis is thereby that the granulation tissue of zebrafish contains 'softer' collagen deposits and thus can be resolved easier. This would be the explanation why granulation tissue of zebrafish does not result in a scar. To test this hypothesis, I set out to generate a transgenic line to ectopically express *plod2b* in a ubiquitous, but temporally restricted manner. All examined carriers showed mosaic but nevertheless strong expression during larval stages. In first experiments with injected fish, there were indications for a higher amount of collagen in the dermal compartment of the wound, which could not be confirmed in the following generations (Fig. 5.27 and 5.28). Silencing of the transgene during adulthood rendered the line unusable. The underlying cause for this transgene-silencing could be the CpG mediated methylation and thereby transcriptional inactivation of genomic regions. DNA methylation is a highly dynamic process in zebrafish throughout the life time [204]. However, in comparison to mammals, there is no de-methylation and re-methylation as a somatic reset of gene-silencing patterns [205], [206]. Nevertheless, genes are silenced during development or once it is completed, and for instance germline development (*vasa*) or embryogenesis genes (*c-jun* or *c-myca*) are not necessary anymore [204]. Although *hsp70l* is not necessarily an embryogenesis-relevant promotor, this mechanism could be an explanation for the initial expression of the transgene and the silencing in adult fish. Since Tol2-mediated transgenic integration occurs randomly [207], it is also possible that the construct was inserted into a genomic region which is silenced during later stages and thereby suppresses the *hsp70l* activity and *plod2b* expression. Unfortunately, the majority of research using

zebrafish as model organism mainly uses embryonic and larval stages, hence a silencing of transgenes in adult stages has not been reported frequently.

To further investigate the impact of absent lysyl hydroxylase from the granulation tissue of teleosts and the IL-4Rα – Relm-α – LH2 signalling axis on scar tissue persistence, Katharina Bieker generated transgenic lines expressing mouse resistin-like alpha under control of the heat shock promoter. These lines will be characterised and tested by both *in situ* and immunohistochemistry in near future before wounding experiments take place. Moreover, to exclude the influence of the Gateway assembly method by possible silencing of the transgenes due to the transposon character of the genomic insertion, restriction enzyme-based cloning of the transgene will be done in future as well.

I further injected recombinant Relm-α into the wounds of zebrafish after wounding to examine whether Relm-α can stimulate more persistent granulation tissue in fish. However, due to daily injection and continuous infliction of micro injuries, also the PBS injected control fish exhibited the presence of a granulation tissue at seven days post wounding. Although the area of the granulation tissue was significantly higher in Relm-α injected fish, these results were unreliable, due to a possibly different observation depending on whether the section is close to an injection site or more distant.

6.8   <u>Possible other reasons for the absence of scars</u>

The composition and the character of collagen networks can be one factor influencing the degradation of excessive extracellular matrix during tissue remodelling. Another aspect can be the degradation directly. Although there is no indication for this hypothesis in the literature so far, it could be speculated that different matrix metalloproteases (MMPs) are at work in zebrafish granulation tissue. MMPs degrade extracellular matrix and are required during wound healing for example for migration of leukocytes, fibroblasts, keratinocytes and endothelial cells through the provisional extracellular matrix in the wound [208]. It could also be possible that the MMPs are more active than they are in mammals. These theories can be investigated by *in situ* hybridisation analysis of expression patterns during the time course of healing, ranging from two to ten days post wounding. Quantitative analysis of *mmp* expression can be done by qPCR and activity can possibly be measured by *in vitro* zymography with mouse and fish wound extracts and fluorescent mmp substrate [209].

Further, the epithelial structure could be an indication for a different type of wound healing. Wounds of the same size introduced in oral mucosa and skin heal with striking differences. Oral mucosa can differ in structure in respect to the function. In regions in which mechanical resistance is needed the squamous stratified epithelium shows signs of keratinisation (for example hard palate, gingiva) and resembles the mammalian epidermis. Where flexibility is needed, the epithelium is not keratinised [210]. The latter shows parallels to the zebrafish epidermis since this does not show signs of keratinisation either (with the exception of the mechanically resistant breeding tubercles [7]). Wounds in the mammalian oral mucosa follow the same scheme of wound healing as mammalian skin (haemostasis, inflammation, re-epithelialisation and tissue remodelling), but heal faster and with reduced scar

formation [211], [212]. Wounds in mouse oral mucosa show less infiltrates of leukocytes and less expression of inflammatory cytokines than wounds of back skin with identical size. Additionally, TGF-ß levels are reduced in oral mucosa [213] which was connected to the less fibrotic character of healing in rat wounds [214]. Therefore, it is tempting to speculate the zebrafish shows faster and more perfect healing because the inflammatory response and the remodelling is less pronounced, as it is in the highly similar oral mucosa.

Another theory discussed for a long time was that mammalian foetal wound healing is scar-free due to the outside conditions *in utero*. The foetus is embedded in amniotic fluid and is constantly exposed to a large variety of growth factors. Studies addressing this hypothesis show that extra-uterine development (as it is the case for opossum for instance) does not perturb the foetal scar-free healing of wounds. Further investigation demonstrates that human foetal skin transplanted to subcutaneous locations in adult athymic mice healed without scar tissue, but in cutaneous environment with persistent scars due to the influence of the hosts' cutaneous fibroblasts. Therefore, the scar-free foetal wound healing did not depend on the environment (amniotic fluid) but on the fibroblasts participating in the collagen remodelling (reviewed in [215]). Nevertheless, it is still observed that moisture contributes to accelerated and scar-free wound healing in the clinic and (when tightly balanced) leads to an optimal wound healing environment [216]–[219].

Taken together, it is difficult to directly compare mouse wound healing with zebrafish regeneration, and aspects such as a more effective ECM degradation system, a milder inflammatory response and different pro-fibrotic gene expression profile are challenging to detect. Nonetheless, the striking difference in the outcome of injury in the different species might not be due to the differential expression of one gene encoding for lysyl hydroxylase but rather a combination of several contributing factors. Thus, it is necessary to continue research on both systems to narrow down the candidates and connect the remaining factors in one regulatory network.

6.9   Implications for human wound healing and future directions of adult zebrafish wound healing studies

In medicine, the treatment of wounds occurs daily. Skin wounds can occur through accidents but also surgery. Thus, understanding the underlying processes and knowing the involved signalling cascades is key to an effective treatment. Thus far, TGF-ß mediated effects have not been resolved completely and short-term and long-term effects cannot be dissected completely in mice. Our studies give an important insight into the short-term role of TGF-ß during re-epithelialisation and help to find new approaches to improve re-epithelialisation. Since TGF-ß signalling is not only a key regulator of cell migration but also influences proliferation and later leads to fibrosis [73] a local application of TGF-ß on wounded tissue is most likely not the approach of choice. Instead, downstream effectors can be targeted (activation / inactivation) to improve the migration of keratinocytes during the re-epithelialisation phase. In consequence, wounds close faster, and the risk of infection decreases. In severe cases of injury, fibrotic tissue can cause severe health risks. Due to the less flexible collagen matrix, ruptures can occur. Once a scar ruptures, the wound healing process starts from the beginning and the infection risk is high again. Hence, it is important to avoid fibrosis. This can be achieved on one hand by helping to resolve

the existing scar tissue or on the other hand by avoiding its formation completely. The results presented in this study give important information on possible factors that recruit fibroblasts and determine the character of the future collagen matrix. As demonstrated here, FGF can function as an important activator of wound fibroblasts. This might offer a new approach to affect collagen deposition independent of suppression of the immune response. Furthermore, Relm-α and LH2 have been described by Knipper *et al.* to be essential for a stable and functional granulation tissue [108]. However, this study shows that these two factors are not present in fish granulation tissue which ultimately heals without a scar. Hence, it is tempting to speculate that suppression or inhibition of either Relm-α or LH2 can reduce the risk of scarring. Resolving the impact they have on the scar formation in mammals and the absence of scars in fish can lead to the discovery of new means to avoid scars by influencing the collagen matrix while it is deposited.

Aside from both re-epithelialisation and granulation tissue formation and resolution, the adult zebrafish offers multiple advantages to investigate further open questions of wound healing and regeneration.

As examples I want to mention the keratinocyte overshoot during and after full-thickness wound closure. The neo-epidermis shows a massive increase in the number of cell layers after the wound has closed and re-epithelialised. What happens to the 'excessive' keratinocytes during the regeneration and how is tissue homeostasis ensured? Are they utilised to cover the newly forming scales or do they undergo apoptosis and / or shedding? Likewise, the same question holds true for the fibroblasts which participate in granulation tissue formation but are not needed anymore after day four post injury. What happens to surplus blood vessels during neovascularisation? How is it determined which capillary stays and which one retracts? And finally, pigmentation of mammalian skin is disturbed in some cases after injury but the reestablishment of the zebrafish pigment pattern seems almost flawless after 28 days of healing [20]. Can the cause for this be found in the different location of melanocytes within the skin of mammals or teleosts (epidermis in mammals and dermis in fish)? Do pigment cells such as iridophores, melanocytes and xanthophores follow the same chemotactic cues as keratinocytes and fibroblasts or are they differentially recruited?

Due to the widespread toolbox of genetic manipulation, (injection-independent) small molecule treatment and other more general advantages (low cost, low space demand, fast development) the zebrafish poses a suitable model organism alongside mouse.

7 Material and Methods

7.1 <u>Animal handling</u>

7.1.1 *Fish strains*

For wounding experiments, fish of the hybrid wildtype strain TL/EK with an age above 6 months were used, unless stated otherwise.

Transgenic and mutant fish used during this work include the *Tg(actb2:gfp)zp5* [220], *Tg(hsp70I:dep)fr37* [25], *Tg(hsp70I:dn-fgfr1-egfp)pd1* [221] and *Tg(hsp70I:ca-fgfr1)pd3* [222], as well as *csfr1a* mutants pfe[tm236b] [154].

Carriers of the transgene were identified by ubiquitous GFP fluorescence (*Tg(actb2:gfp)zp5*), heart-specific GFP fluorescence (*Tg(hsp70I:dep)fr37*), ubiquitous GFP fluorescence after heat shock (*Tg(hsp70I:dn-fgfr1-egfp)pd1*), or strong red fluorescence caused by *dsred* expression under control of the zebrafish α-crystallin promoter (*Tg(hsp70I:ca-fgfr1)pd3*).

In larvae, heat shocks were conducted for 30 minutes at 40°C in system water which was pre-warmed in an incubator. Adult fish were heat shocked by transferring them to a self-made water bath, heating the water progressively to 39°C. After the temperature was stable at 39°C the fish were kept at this temperature for 1 hour and constantly monitored due to strong reactions to the increased temperature. Successful heat shocks were confirmed by *gfp* expression or *in situ* hybridisation for the transgene mRNA, if necessary.

Temperature of fish rooms and incubators were constantly kept at 28°C and water quality of the system was monitored at least once per month. Light and dark phases of fish rooms were electronically controlled with a light phase of 14 hours and a dark phase of 10 hours. Feeding of larvae and fish was done by the institute's animal care takers at least twice a day according to the age of the fish with either paramecia and plankton for larvae or artemia, dry food flakes and granulated food for adults.

7.1.2 *Drug treatments*

Inhibitor solutions were set up as a 1000x stock solution in DMSO and added to fresh system water immediately before the treatment. This resulted in the desired final concentration of the respective inhibitor and a DMSO concentration of 0.1%, unless stated otherwise. Adult fish were then treated for 4 hours in the system water containing inhibitor with fresh air supply by bubbler. Due to the restricted volume of inhibitor solution, 3 to 4 fish were treated with inhibitor solution and 3 to 4 fish with 0.1% DMSO as control in parallel. For *in vivo* imaging, 2% low melting point (LMP) agarose in system water was prepared in parallel and kept ready to use at 65°C in a water bath.

T 7.1: Used inhibitors, concentrations and suppliers

Inhibitor / Peptide	Final concentration	Supplier
SB431542	50 µM	Sigma-Aldrich (S4317)
LY364947	50 µM	Sigma-Aldrich (L6293)
GRGDS	1 mM	Bachem (H1345)
Y-27632	50 µM	Merck (SCM075)
ROCKOUT	50 µM	Merck (555553)
SP600125	10 µM	Sigma-Aldrich (S5567)
Capsazepine	100 µM	Sigma-Aldrich (C191)
PF573228	25 µM	Sigma-Aldrich (PZ0117)
PIK90	5 µM	Merck (528117)
Rapamycin	200 nM	Sigma-Aldrich (R0395)
Hydrocortisone	275 µM	Sigma-Aldrich (H4001)

7.1.3 <u>in vivo time lapse imaging of partial-thickness wound closure</u>

The setup for *in vivo* imaging consists of a self-made imaging chamber with an inlet and outlet tube connected to a Gilson minipulse 2 pump, as previously published in [223]. The self-made imaging chamber was a petri dish with a hole on either side, which were introduced with the flame-heated pointy end of a glass Pasteur pipette. The inner surface was roughened for better connection between LMP agarose and the petri dish by flaming the broad end of a glass Pasteur pipette and pressing it on the petri dish several times. To avoid air bubbles travelling through the system, holes with the diameter of the tubing were introduced into a 15 ml falcon tube close to the screw cap. The inflow into the imaging chamber was connected directly to the falcon tube and from there to the pump and the outflow of the imaging chamber.

To prepare the setup for imaging, the tubing was flushed with 70% EtOH followed by system water. Afterwards, the flow rate was adjusted to 3 ml per minute. Then, 47.5 ml of inhibitor solution were split off from the fish treatment and 2.5 ml tricaine was added to a final concentration of 0.016%. This solution was then added to the system to fill the tubing and the falcon tube. The remaining solution in the imaging chamber was used afterwards to anesthetise the first fish. Once the fish was not moving anymore, it was put into the petri dish on the rough area with a floorless, smaller diameter petri dish around it and covered with 10 ml hand-warm LMP agarose. To accelerate solidifying the LMP agarose, the petri dish was kept on ice. After the LMP solidified, the smaller diameter petri dish was removed carefully, LMP around the head was cut away and the inflow tube with a cut 200 µl pipette tip as mouth piece was inserted into the mouth of the zebrafish. Afterwards the petri dish was filled with inhibitor solution containing tricaine and the imaging chamber was placed under a Zeiss Axio Imager.Z1 microscope for fluorescent imaging.

7.1.4 <u>Partial- and full-thickness wounding of adult zebrafish</u>

The scale to be removed was located centred on the dorso-ventral axis and at the height of the anterior base of the anal fin on the anterior-posterior axis. Scale removal wounds were introduced after the fish was anesthetised and embedded in LMP agarose directly under the microscope with low magnification by gently pressing forceps onto a single scale and moving it toward the caudal fin.

If partial-thickness wounding was not used for fluorescent time lapse *in vivo* imaging but for immunohistochemistry, the fish was anesthetized and placed on a humidified sponge beneath a Leica M165FC stereo microscope. With the help of forceps, a single scale was removed in the same location as during *in vivo* imaging.

Full-thickness wounds were inflicted by a dermatology laser (Erbium:YAG MCL29 Dermablate, Asclepion, Jena, Germany). The laser was set to 5 Hz at 500 mJ and the fish were anesthetised with 0.016% tricaine. Once fully anesthetised, the fish were transferred to a petri dish with wet paper towels and the wound was introduced with two pulses at 500 mJ on the flank, dorso-ventrally centred, at the height of the anterior base of the anal fin. Afterwards, the wound was cleaned of scale debris by a lavage with system water and the fish was put back into normal system water.

7.2   Molecular biology methods

7.2.1   Total RNA isolation

Zebrafish larvae or adult tissue was homogenised in TRIzol reagent (Thermo Fisher Scientific) and stored at -80 °C until further processing. RNA isolation was then performed according to the manufacturer's recommendations and stored until use at -80°C.

7.2.2   cDNA synthesis

For reverse transcription, 2 µg of RNA were mixed with 2 µl oligo-dT primers and the reaction was filled up to 10.6 µl with nuclease-free water. This was then incubated at 70 °C for 5 minutes and stored on ice for further 2 minutes. Then, 4µl of 5x first strand buffer (Thermo Fisher), 2 µl 0.1 M DTT (Thermo Fisher), 2 µl 10 mM dNTPs (NEB), 1 µl RNasin (Promega) and 2 µl Superscript II reverse transcriptase (Thermo Fisher) were added. The reaction was then kept at 42 °C for 1.5 hours. The cDNA was then diluted 1:20 and stored at -20°C for further use.

7.2.3   Primers and PCR settings

For amplification of *in situ* hybridisation probe templates as well as DNA fragments for transgenesis, primers and cycler settings were used as stated below. In all cases, the standard PCR cycler settings (T 7.2) were used and necessary adjustments are

given with the primers (T 7.3). The gateway primers consisted of the att sites (red), the Kozak sequence (orange) and the gene-specific part (blue).

T 7.2: Standard PCR cycler settings

	PCR step	Temperature	Duration
	Initial denaturation	96°C	5 min
34 x	Denaturation	96°C	30 sec
	Annealing	58°C	30 sec
	Elongation	72°C	1 min per kb
	Final elongation	72°C	5 min

T 7.3: Primers

Primer description	Sequence	Anneal	Elongation
Dsh-DEP probe for	GGT GTC ACT CTT CAG CCT CT		1 min
Dsh-DEP probe rev	CTC ACC ATC CAC CCT CTG TT		1 min
plod2b probe for	CAA CTT CTG GGG AGC TCT GA		1 min
plod2b probe rev	TCA CGA CTC CTC AAC GTT CA		1 min
plod2b gateway for	G GGG ACA AGT TTG TAC AAA AAA GCA GGC TCA GCC GCC ACC ATG GAG CGG CGT CGG GGT TTT CAC GCG TTC	63 °C	2 min 30 sec
plod2b gateway rev	GGG GAC CAC TTT GTA CAA GAA AGC TGG GTA TTA GGG ATC TAC GAA AGA CAC TGC TAT GTA	63 °C	2 min 30 sec
Dsh-DEP gateway for	G GGG ACA AGT TTG TAC AAA AAA GCA GGC TCA GCC GCC ACC ATG GCC AAA TGC TGG GAC CCT TCC CCT CAG	65 °C	1 min 30 sec
Dsh-DEP gateway rev	GGG GAC CAC TTT GTA CAA GAA AGC TGG GTA TCA CAT GAC ATC CAC AAA GAA CTC GCT AGG	65 °C	1 min 30 sec

7.2.4 *Probe synthesis*

Template cDNA for the gene of interest was cloned into the pGEM-T easy vector (Promega) according to the company's protocol. After plasmid preparation (Macherey-Nagel NucleoSpin Plasmid NoLid), 5 µg of plasmid were linearised and purified by phenol-chloroform extraction. Afterwards 2 µg of linearised plasmid were filled up to 13 µl with nuclease free water and 2 µl 10x transcription buffer (containing

DTT, Boehringer), 2 µl DIG-RNA labelling mix (Roche), 1 µl RNasin (Promega) and 2 µl Sp6 or T7 RNA polymerase were added. The reaction was incubated at 37°C for 2 hours and afterwards treated with DNase to remove the plasmid DNA. Finally, the synthesised RNA probe was cleaned by phenol-chloroform extraction and 1 µl was checked on a 1.5% agarose gel. For long term storage, 20 µl formamid were added to create a 100x stock and this was then kept at -80°C. Shortly before use, 10µl of probe were diluted 1:100 in hybridisation buffer.

7.2.5 *Gateway cloning of plod2b and dishevelled DEP domain*

For transgenesis of zebrafish, the Tol2kit was used according to the published procedures [224]. Regarding the *Tg(hsp70I:dep)^{fr37}*, the plasmid was requested from Masazumi Tada and J. C. Smith [80] and the DEP domain of *Xenopus* dishevelled was amplified with the primers given in T 7.3. The forward primer contained an attB1 site, which is required for efficient recombination later on, as well as a Kozak sequence and a DEP specific sequence. The reverse primer was designed to be specific for DEP and contained further a stop codon and an attB2 site. Zebrafish *plod2b* was amplified from 2 dpf larval cDNA with forward and reverse primers containing attB1, Kozak and attB2 sites and *plod2b* specific parts. Both fragments were amplified with Phusion Taq (NEB) according to the standard PCR protocol (T 7.2) with the changes mentioned with the primers (T 7.3) to avoid errors during amplification. For the BP clonase reaction, the fragment was purified by gel-extraction (Gel purification kit, Macherey Nagel). Thereafter, 50 femtomol of each pDONR221 vector and PCR fragment were combined, filled up to 8 µl with TE buffer and 2 µl of BP clonase were added. The mix was incubated for 2 hours at room temperature and introduced into chemically competent *E. coli* by heat shock at 42°C for 90 seconds. The bacteria were incubated for 1.5 hours at 37°C in LB medium and plated on LB agar plates containing 50 µg / ml kanamycin. The next morning, clones were picked and overnight liquid cultures were prepared. The plasmid was isolated (Plasmidprep, Macherey Nagel) the day after and subsequently verified by sequencing. For the final assembly of the destination vector 20 femtomol of p5E-*hsp70I*, p3A-*polyA*, pDestTol2CG2 and pDONR221 carrying the gene of interest were combined, filled up to 8 µl with TE buffer and 2 µl of LR clonase were added. This reaction was then incubated overnight at room temperature and introduced into *E. coli* the next day. The bacteria were then kept in LB medium at 37°C in a shaker set to 300 rpm and afterwards plated on LB agar plates containing 100 µg / ml ampicillin for overnight incubation at 37°C. The next day, clear clones were picked, cultured in liquid LB medium containing ampicillin and the plasmid was isolated the following day. The presence of hsp70I, gene of interest and polyA signal was assured by control digest with a combination of restriction enzymes cutting in all three modules. Correct clones were injected together with Tol2 recombinase mRNA into 1 cell stage zebrafish embryos. Larvae were sorted on day 2 for strong GFP signal in the heart caused by the *cmlc2:gfp* reporter construct on the pDestTol2CG2 and raised to adulthood. Those fish were then setup for mating with wild types and the pairs were kept separate. The progeny was screened for fluorescence in the heart and raised.

7.3 Histology, immunohistochemistry and *in situ* hybridisation

7.3.1 *Fixation and embedding of larval and adult zebrafish*

Zebrafish larvae were collected in an Eppendorf tube and the excessive embryo medium was removed. After addition of 4% paraformaldehyde (PFA) in PBS, the larvae were incubated at room temperature for 4 hours or at 4 °C overnight. Following this, embryos were washed several times with PBS and transferred to methanol for long-term storage.

Adult fish were sacrificed and the head was removed with razor blades. The body was then transferred to falcon tubes containing 4 % PFA and fixed for 2-3 days at room temperature. After 2 hours of washing with ddH$_2$O with multiple exchanges, the fish were decalcified for 5-7 days with EDTA, exchanging it every third day. Subsequently, the samples were washed for 2 hours with ddH$_2$O again and dehydrated progressively with overnight washing steps of each 30 %, 50 %, 75 % and 90 % EtOH / ddH$_2$O. To finalise the dehydration, the fish were washed 2 times for 2 hours in 100% EtOH and afterwards put into a 1:1 mix of EtOH and Rotihistol overnight. The following day, the samples were treated twice for two hours in 100% Rotihistol and overnight in a mix of Rotihistol and paraffin wax at 65 °C. The solution was replaced the next day with 100% paraffin wax for incubation at 65 °C with daily exchange of the paraffin. Finally, the bodies were placed dorsal side down in an embedding mould, covered with pre-warmed paraffin wax and closed with an embedding cassette. The blocks were then kept at room temperature and sectioned with a Leica RM2255 microtome. If not stated otherwise, the section thickness was 10 µm.

For cryo sections, trimmed tissue of adult fish was embedded in 1.5 % agarose and 15 % sucrose in a petri dish after fixation and decalcification. Following this, the samples were cut out in blocks and kept in 30 % sucrose in PBS at 4 °C for 3 days. Afterwards they were covered with freezing medium on an embedding plate and shock-frozen in -80 °C cold isopentane. The blocks were then sectioned immediately at a thickness of 14 µm on a Leica CM1850 cryostat at -20 °C, air-dried for several hours and stored at 4 °C.

7.3.2 *Immunohistochemistry on whole mounts and sections, western blotting*

Adult fish were wounded, sacrificed and fixed. Afterwards, the fish were washed 3 times with PBST and the body was trimmed to an approximately 1 by 1 cm piece with the wound in the centre. Additionally, the unwounded flank of the fish was removed, leaving only the wounded body half behind for further treatment. Samples which were prepared as described were then incubated for 1 hour at room temperature in 2N HCl (for BrdU) or 1 hour in 10 mM citric acid pH 6.0 for antigen retrieval (for all other antibodies). Subsequently, the samples were transferred to blocking solution and incubated on a shaker at room temperature for 4 hours at least. The primary antibody was diluted 1:500 in blocking solution in the meantime. After the blocking, the

solution was exchanged with the primary antibody solution. The samples were then kept at 4 °C overnight. On the next day, the antibody solution was then collected, the samples washed 3 times for 5 minutes with PBST and the secondary antibody was prepared 1:500 in blocking solution. The secondary antibody solution was added to the samples and incubated for 2 hours at room temperature. Finally, the samples were washed, a 1:1000 dilution of DAPI in PBST was added for 10 minutes and the samples were imaged at a Zeiss LSM710 META confocal microscope.

Paraffin sections of adult fish were dewaxed by treatment with Rotihistol, 100% EtOH, 90% EtOH, 75% EtOH for 10 minutes each and 50% EtOH and ddH$_2$O for 5 minutes each. Following this washing series, the slides were transferred for antigen retrieval to 10 mM citric acid pH 6.0, which was pre-warmed to 65°C. Cryo sections were washed 3 times for 5 minutes with PBS and then transferred to pre-warmed citric acid. For BrdU immunohistochemistry, antigen retrieval was performed by boiling the slides for 15 minutes in 10mM citric acid pH6.0 (microwave, avoiding bubbling) and afterwards 20 minutes cooling at room temperature (slides were kept in the same citric acid solution in which they were boiled and cooled down). After antigen retrieval, the slides were washed 3 times for 5 minutes in PBST and the sections were encircled with a hydrophobic pen. The blocking solution was added to the slides and incubated for 4 hours at room temperature in a humidified chamber. All following steps were performed as described for whole mount samples. The slides were mounted after secondary antibody incubation and washing with PBST (3 times for 5 minutes) with Mowiol containing DAPI (1:1000).

For western blotting, tail fins of rapamycin treated fish were homogenised thoroughly in calcium free Ringer solution (116 mM NaCl, 2.9 mM KCl, 5 mM HEPES, 1 mM EDTA, pH 7.2) and cells dissociated by pipetting several times with a fire-polished Pasteur pipette. The cells were then pelleted by centrifugation at 4°C for 5 minutes at 1.500 rpm and the supernatant was discarded. The pellet was washed by re-suspending it with 300 µl ca-free Ringer, 3 minutes centrifugation (4°C, 1500 rpm) and discarding the supernatant. The cells were then either stored at -80°C or directly re-suspended in cold-spring harbour (CSH) buffer containing protease and phosphatase inhibitors (50 mM Tris HCl pH 7.5, 250 mM NaCl, 1 mM EDTA, 1% Triton-X, 1 tablet Roche cOmplete protease inhibitors). For cell lysis the suspension was kept on ice for 30 minutes. After determination of the protein concentrations the samples were further diluted, loading dye was added and the mix was boiled for 5 minutes. Equal amounts of protein were loaded on a 9% SDS-polyacrylamide gel (stacking gel: 0.9 ml 90% mix [T 9.4], 0.1 ml 30% acrylamide, 5 µl 40% APS, 5 µl TEMED, separating gel: 3.4 ml 60% mix [T 9.4], 1.5 ml 30% acrylamide, 12.5 µl APS, 5 µl TEMED). The gel was run for 60 minutes at 200 V in a chamber containing SDS running buffer (124 mM Tris, 17 mM SDS, 96 mM Glycine) and the nitrocellulose membrane was equilibrated in transfer buffer (48 mM Tris, 39 mM Glycine, 20% MeOH, 1.3 mM SDS). Afterwards, proteins were transferred onto the nitrocellulose membrane for 60 minutes at 100 V. Ponceau S (Sigma-Aldrich) staining was used to ensure the successful transfer and the membrane was washed in ddH$_2$O before blocking with TBST (10 mM Tris pH 7.5, 150 mM NaCl, 4% milk powder, 0.1% Tween 20) for 2 hours at room temperature with agitation. The primary antibodies (Anti pS6-ribosomal protein 1:1000 and anti-alpha tubulin 1:3000, table T 9.5) were added and the membrane was incubated overnight at 4°C. The primary antibodies were collected and the membrane was washed with TBST (3x 10 min). Subsequently, the

membrane was incubated with the secondary antibodies (HRP anti mouse and HRP anti rabbit 1:1000, table T 9.5) for 1 hour at room temperature. After the antibody solution was collected, the membrane was washed with TBST (3x 10 min) and signal detection was performed with the C-DiGit blot scanner (LI-COR) using WesternSure Chemiluminescent substrate (LI-COR). The relative quantity was the determined with FIJI.

T 9.4 Required solutions for SDS-gels

Lower Tris	
Tris	18.2 g
10% SDS	4 ml
Adjust pH (HCl)	pH 8.8
H_2O	Ad 100 ml

Upper Tris	
Tris	6.1 g
10% SDS	3 ml
Adjust pH (HCl)	pH 6.7
H_2O	Ad 100ml

60% Mix	
Lower Tris	200 ml
Glycerine	160 ml
H_2O	120 ml

90% Mix	
Upper Tris	31 ml
H_2O	80 ml

T 9.5: Antibodies

Anti-p63	Biocare Medical CM163C
Anti-Col1	Abcam ab23730
Anti-BrdU	Roche 1170376
Anti-RFP	MBL Life science PM005
Anti-pS6-ribosomal protein	Cell Signalling / NEB 2215
Anti-alpha tubulin	Sigma-Aldrich T5168

Anti-rabbit Alexa Fluor 555	Invitrogen A21428
Anti-rabbit Alexa Fluor 488	Invitrogen A11008
Anti-rabbit Cy3	Invitrogen A10520
Anti-mouse Alexa Fluor 555	Invitrogen A21427
Anti-mouse Alexa Fluor 488	Invitrogen A11001
Anti-mouse Cy3	Invitrogen A10521
Anti-mouse HRP peroxidase conj. Affinipure	Dianova 115-035-003
Anti-rabbit HRP peroxidase conj. Affinipure	Dianova 111-035-003

7.3.3 *Histological staining of adult zebrafish sections*

Paraffin sections of adult zebrafish were rehydrated by a series of washing steps with Rotihistol, 100% - 50% EtOH and ddH$_2$O. Cryo sections were washed several times with ddH$_2$O. Subsequently, the slides were dipped into Gill's Haematoxylin III for 1 minute, rinsed under running tap water for 5 minutes and afterwards transferred to Eosin Y for 4 minutes. Afterwards, the excess Eosin was removed by dipping the sections 5 times into tap water. Then, the sections were dehydrated by sequentially dipping the slides 5 times into 50% EtOH, 10 times into 70% EtOH and incubation in 90% and 100% EtOH for 2 minutes each, followed by a 5 minutes incubation in Rotihistol twice. The dehydrated sections were then mounted with Permount (Fisher Scientific) and kept under the fume hood for drying.

7.3.4 *In situ hybridisation on whole mounts and sections*

Larval zebrafish or fin clips of adult fish were fixed with 4% PFA, washed and dehydrated with a washing series with increasing amount of EtOH and finally transferred to MeOH for storage and removal of endogenous alkaline phosphatase activity. Prior to in situ hybridisation, the larvae were rehydrated with a MeOH/PBS washing series (75%, 50%, 25% and 100% PBS for 5 minutes each). The samples where then digested with proteinase K (10 μg/ml in PBS) for 30 minutes at room temperature and refixed with 4% PFA for 20 minutes. The tissues were then washed 5 times for 5 minutes each with PBST. Afterwards, the samples were treated with hybridisation buffer (hyb+) for 4 hours at 65 °C. To each sample, 200 μl probe was added and incubated overnight at 65 °C in a water bath. The following day, the probe was collected and stored at -20 °C and the samples were rinsed with hyb-. The tissues were then gradually transferred to PBST by 15 minutes washing steps at 65°C each with 75% hyb- / 25% 2x SSCT, 50% hyb- / 50% 2x SSCT, 25% hyb- / 75% 2x SSCT, 100% 2x SSCT and 100% 0.2x SSCT followed by 75% 0.2x SSCT / 25% PBST, 50% 0.2x SSCT / 50% PBST and 25% 0.2x SSCT / 75% PBST for 10 minutes each at room temperature. The samples were then washed for 10 minutes with PBST and blocking solution was added for a 4 hour incubation step at room temperature. The anti-digoxigenin fab fragments were diluted 1:5000 in blocking solution and added to the samples for an overnight incubation at 4°C. The next day, the antibody was discarded and the samples were washed 6 times for 15 minutes

with PBST. Afterwards, washing steps with staining buffer were performed 3 times for 5 minutes each. The larvae or fins were transferred to a 24 well plate and a 1:50 dilution of NBT / BCIP in staining buffer was added to initiate the staining reaction. When the staining was strong enough, the staining solution was discarded and PBST was added 3 times for 5 minutes each. The PBST was then replaced by 100% EtOH for 5 minutes to remove background staining. After a washing step with 50% EtOH and PBST, 4% PFA was added for 4 hours to stop the staining reaction and postfix the tissue. Larvae or fins were then transferred to 80% glycerol and kept in the fridge until imaging.

Rehydrated paraffin sections were washed 2 times for 5 minutes in PBS and then transferred to 10 µg/ml proteinase K in PBS for 10 minutes at 37 °C. Following this, the slides were incubated for 5 minutes in 0.2% glycine and afterwards washed twice for 5 minutes with PBS. At this point, the sections were encircled with a hydrophobic pen and fixed with 10 ml 4% PFA and 100 µl glutaraldehyde. After 2 washing steps with PBS, 80 µl hyb+ was added to each slide, a cover slip was added and the sections were kept at 62°C for 4 hours in a humidified chamber. The hybridisation was started by exchanging the hyb+ solution with 80 µl probe and incubation overnight at 62 °C. On the second day, the probe was collected if possible and the slides were washed twice in 50% formamid / 50% 2x SSC for 20 minutes at 62 °C, 100% 2x SSC for 20 minutes at 62°C and 3 times 5 minutes with PBST at room temperature. The blocking solution was added to the slides and sealed with a cover slip. The blocking phase was performed for 4 hours at room temperature in a humidified chamber. The fab fragments were diluted 1:5000 in blocking solution and 80 µl were added to each slide for overnight incubation at 4 °C. On the third day, the antibody was discarded, the slides were washed 3 times for 5 minutes with PBST and 2 times for 5 minutes with staining buffer. A 1:50 dilution of NBT / BCIP in staining buffer was added afterwards to start the staining reaction. The progress was monitored frequently and the reaction was stopped with several washing steps with PBST and a fixation for 1 hour at room temperature with 4% PFA. The slides were mounted with Mowiol and kept in the fridge until imaging.

7.4 Software, plugins and macros for image and data processing

For processing of the time lapse movies of partial-thickness closure, FIJI software [225] was used with the plugin "Extended Depth of Field" [226], [227]. To accelerate the processing and automate it, I wrote a macro (table T 9.6) which merges the z-stacks of each time point using the EDF plugin and afterwards saves each time point automatically before processing the next frame. This was applicable for multiple time lapse movies without necessary user input.

FIJI was used with other self-written macros to process large numbers of z-stacks (maximum intensity projection and background subtraction shown in table T 9.7, as well as subsequent cell counting with macro in table T 9.8). Other software that was used in this thesis for image processing or generation of schematic representations are Adobe Photoshop CS5, Microsoft Office PowerPoint 2010 and Inkscape.

Further, Microsoft Office programs, such as Word and Excel 2010 were used for data collection and processing (charts and ANOVA).

Statistical analysis was performed with Excel 2010 and the Data analysis plugin as well as the Graphpad Prism Software 7.

T 9.6: FIJI macro for time lapse movie processing

```
//get output directory, number of hyperstacks

x = nImages();

dir1 = getDirectory("Choose Output Directory");


//batch processing loop

for (i=1; i<=x; i+=1) {AutoEDF();}


//Macro core code

function AutoEDF() {

        //get file infos

        name = getTitle();

        getDimensions(dummy, dummy, dummy, b, a);

        //Control output in the log

        write("Current file: " + name);

        write("Frames: " + a);

        write("Slices: " + b);

        write("Output folder:" + dir1);

        // EDF loop

        for(i=1; i<=a; i+=1) {

                run("Duplicate...", "title=[" + name + "] duplicate slices=1-"+b+" frames=" +i);

                run("Enhance Contrast", "saturated=0.35");

                run("Easy mode...", "quality='3' topology='0' show-topology='off' show-view='off'");

                // Wait for EDF to be done

                while(!isOpen("Output")) {wait(500);}

                // Feedback for EDF processing and brightness/contrast enhancement

                write("Frame # " + i + " successfully processed!");

                selectWindow("Output");

                run("Enhance Contrast", "saturated=0.35");
```

```
            // Save, close

            saveAs("Tiff", dir1 + "\\" + name + "_" + i + ".tif");

            close();

            close();

            selectWindow(name);

    }

    // Close the hyperstack when finished

    close();

    write("Processing complete! Starting next hyperstack...");

    wait(2000);

}
```

T 9.7: FIJI macro for z-stack processing of BrdU images

```
//get output directory, number of hyperstacks

x = nImages();

dir1 = getDirectory("Choose Output Directory");

//batch processing loop

for (i=001; i<=x; i++) {Automergezstack();}

function Automergezstack() {

        title = getTitle();

        if (isOpen("Original Metadata - " + title)) {

                selectWindow("Original Metadata - " + title);

                run("Close");

                selectWindow(title);}

        run("Split Channels");

        selectWindow("C1-" + title);

        run("Blue");

        run("Z Project...", "projection=[Max Intensity]");

        run("Subtract Background...", "rolling=5");

        selectWindow("C2-" + title);

        run("Z Project...", "projection=[Max Intensity]");

        run("Green");

        run("Subtract Background...", "rolling=5");

        if (i>99) {selectWindow("MAX_C1-" + title);

                saveAs("Tiff", dir1 + "\\" + i + "_C1.tif");

                z = "" + i + "_C2.tif";

                selectWindow("MAX_C2-" + title);

                saveAs("Tiff", dir1 + "\\" + i + "_C2.tif");

                y = "" + i + "_C1.tif";}

        else if (i>9) {selectWindow("MAX_C1-" + title);

                saveAs("Tiff", dir1 + "\\0" + i + "_C1.tif");

                z = "0" + i + "_C2.tif";

                selectWindow("MAX_C2-" + title);

                saveAs("Tiff", dir1 + "\\0" + i + "_C2.tif");

                y = "0" + i + "_C1.tif";}
```

```
else {selectWindow("MAX_C1-" + title);

        saveAs("Tiff", dir1 + "\\00" + i + "_C1.tif");

        z = "00" + i + "_C2.tif";

        selectWindow("MAX_C2-" + title);

        saveAs("Tiff", dir1 + "\\00" + i + "_C2.tif");

        y = "00" + i + "_C1.tif";}

run("Merge Channels...", "c1=[*None*] c2=[" + z + "] c3=[" + y + "]");

selectWindow("RGB");

if (i>99) {saveAs("Tiff", dir1 + "\\" + i + "_MIP.tif");}

else if (i>9) {saveAs("Tiff", dir1 + "\\0" + i + "_MIP.tif");}

else {saveAs("Tiff", dir1 + "\\00" + i + "_MIP.tif");}

run("Close");

selectWindow("C1-"+title);

run("Close");

selectWindow("C2-"+title);

run("Close");
}
```

T 9.8: Automated cell counting of DAPI and BrdU channels

```
x = nImages();

dir1 = getDirectory("Choose Output Directory");

run("Set Measurements...", "area display redirect=None decimal=2");

for (i=1; i<=x; i+=1){process();}

function process(){

        title=getTitle();

        run("8-bit");

        //run("Brightness/Contrast...");

        run("Enhance Contrast", "saturated=0.35");

        run("Apply LUT");

        run("Subtract Background...", "rolling=10 sliding");
```

```
run("Despeckle");

run("Despeckle");

run("Remove Outliers...", "radius=5 threshold=5 which=Bright");

setOption("BlackBackground", true);

run("Make Binary");

run("Close-");

run("Dilate");

run("Dilate");

run("Watershed");

run("Set Scale...", "distance=0 known=0 pixel=1 unit=pixel");

run("Analyze Particles...", "size=30-Infinity display add");

run("From ROI Manager");

run("Flatten");

saveAs("TIFF", dir1 + "\\" + title + "_ROI.tif");

run("Close");

selectWindow("Results");

saveAs("Measurements", dir1 + "\\" + title + ".xls");

run("Close");

selectWindow(title);

run("Close");

selectWindow("ROI Manager");

run("Close");
}
```

8 Literature

[1]   R. B. Presland and R. J. Jurevic, "Making sense of the epithelial barrier: what molecular biology and genetics tell us about the functions of oral mucosal and epidermal tissues.," *J. Dent. Educ.*, vol. 66, no. 4, pp. 564–74, Apr. 2002.

[2]   J. A. Mack, S. Anand, and E. V. Maytin, "Proliferation and cornification during development of the mammalian epidermis.," *Birth Defects Res. C. Embryo Today*, vol. 75, no. 4, pp. 314–29, Dec. 2005.

[3]   A. E. Kalinin, A. V. Kajava, and P. M. Steinert, "Epithelial barrier function: assembly and structural features of the cornified cell envelope.," *Bioessays*, vol. 24, no. 9, pp. 789–800, Sep. 2002.

[4]   E. Candi, R. Schmidt, and G. Melino, "The cornified envelope: a model of cell death in the skin.," *Nat. Rev. Mol. Cell Biol.*, vol. 6, no. 4, pp. 328–40, Apr. 2005.

[5]   C. Blanpain and E. Fuchs, "Epidermal homeostasis: a balancing act of stem cells in the skin.," *Nat. Rev. Mol. Cell Biol.*, vol. 10, no. 3, pp. 207–17, Mar. 2009.

[6]   a Kalinin, L. N. Marekov, and P. M. Steinert, "Assembly of the epidermal cornified cell envelope.," *J. Cell Sci.*, vol. 114, no. Pt 17, pp. 3069–70, Sep. 2001.

[7]   B. Fischer *et al.*, "p53 and TAp63 promote keratinocyte proliferation and differentiation in breeding tubercles of the zebrafish.," *PLoS Genet.*, vol. 10, no. 1, p. e1004048, Jan. 2014.

[8]   W.-J. Chang and P.-P. Hwang, "Development of zebrafish epidermis.," *Birth Defects Res. C. Embryo Today*, vol. 93, no. 3, pp. 205–14, Sep. 2011.

[9]   D. Le Guellec, G. Morvan-Dubois, and J.-Y. Sire, "Skin development in bony fish with particular emphasis on collagen deposition in the dermis of the zebrafish (Danio rerio).," *Int. J. Dev. Biol.*, vol. 48, no. 2–3, pp. 217–31, 2004.

[10]   R. C. Henrikson and A. G. Matoltsy, "The fine structure of teleost epidermis. 1. Introduction and filament-containing cells.," *J. Ultrastruct. Res.*, vol. 21, no. 3, pp. 194–212, Dec. 1967.

[11]   A. Sharma, K. I. Anderson, and D. J. Müller, "Actin microridges characterized by laser scanning confocal and atomic force microscopy.," *FEBS Lett.*, vol. 579, no. 9, pp. 2001–8, Mar. 2005.

[12]   A. Haake, G. A. Scott, and K. A. Holbrook, "Structure and function of the skin: overview of the epidermis and dermis," in *The biology of the skin*, R. K. Freinkel and D. T. Woodley, Eds. New York / London: The Parthenon Publishing Group, 2001, pp. 19–45.

[13]   F. Ramirez and H. C. Dietz, "Marfan syndrome: from molecular pathogenesis to clinical treatment.," *Curr. Opin. Genet. Dev.*, vol. 17, no. 3, pp. 252–8, Jun. 2007.

[14]   S. P. Robins, "Functional properties of collagen and elastin.," *Baillieres. Clin. Rheumatol.*, vol. 2, no. 1, pp. 1–36, Apr. 1988.

[15]   A. J. van der Slot *et al.*, "Identification of PLOD2 as telopeptide lysyl hydroxylase, an important enzyme in fibrosis.," *J. Biol. Chem.*, vol. 278, no. 42, pp. 40967–72, Oct. 2003.

[16]   M. Yamauchi and M. Sricholpech, "Lysine post-translational modifications of

collagen.," *Essays Biochem.*, vol. 52, pp. 113–33, 2012.

[17] R. Cerio, C. E. Griffiths, K. D. Cooper, B. J. Nickoloff, and J. T. Headington, "Characterization of factor XIIIa positive dermal dendritic cells in normal and inflamed skin.," *Br. J. Dermatol.*, vol. 121, no. 4, pp. 421–31, Oct. 1989.

[18] S. A. Eming, M. Hammerschmidt, T. Krieg, and A. Roers, "Interrelation of immunity and tissue repair or regeneration.," *Semin. Cell Dev. Biol.*, vol. 20, no. 5, pp. 517–27, Jul. 2009.

[19] J.-Y. Sire and M.-A. Akimenko, "Scale development in fish: a review, with description of sonic hedgehog (shh) expression in the zebrafish (Danio rerio).," *Int. J. Dev. Biol.*, vol. 48, no. 2–3, pp. 233–47, 2004.

[20] R. Richardson, K. Slanchev, C. Kraus, P. Knyphausen, S. Eming, and M. Hammerschmidt, "Adult zebrafish as a model system for cutaneous wound-healing research.," *J. Invest. Dermatol.*, vol. 133, no. 6, pp. 1655–65, Jun. 2013.

[21] G. C. Gurtner, S. Werner, Y. Barrandon, and M. T. Longaker, "Wound repair and regeneration.," *Nature*, vol. 453, no. 7193, pp. 314–21, May 2008.

[22] P. Martin, "Wound healing--aiming for perfect skin regeneration.," *Science*, vol. 276, no. 5309, pp. 75–81, Apr. 1997.

[23] A. J. Singer and R. A. Clark, "Cutaneous wound healing.," *N. Engl. J. Med.*, vol. 341, no. 10, pp. 738–46, Sep. 1999.

[24] T. J. Shaw and P. Martin, "Wound repair at a glance.," *J. Cell Sci.*, vol. 122, no. Pt 18, pp. 3209–13, Sep. 2009.

[25] R. Richardson *et al.*, "Re-epithelialization of cutaneous wounds in adult zebrafish combines mechanisms of wound closure in embryonic and adult mammals.," *Development*, vol. 143, no. 12, pp. 2077–88, 2016.

[26] A. T. Nurden, P. Nurden, M. Sanchez, I. Andia, and E. Anitua, "Platelets and wound healing.," *Front. Biosci.*, vol. 13, no. i, pp. 3532–48, May 2008.

[27] P. Martin and J. Lewis, "Actin cables and epidermal movement in embryonic wound healing.," *Nature*, vol. 360, no. 6400, pp. 179–83, Nov. 1992.

[28] P. Martin and S. M. Parkhurst, "Parallels between tissue repair and embryo morphogenesis.," *Development*, vol. 131, no. 13, pp. 3021–34, Jul. 2004.

[29] P. Kakanj *et al.*, "Insulin and TOR signal in parallel through FOXO and S6K to promote epithelial wound healing.," *Nat. Commun.*, vol. 7, p. 12972, Oct. 2016.

[30] W. J. Gault, B. Enyedi, and P. Niethammer, "Osmotic surveillance mediates rapid wound closure through nucleotide release.," *J. Cell Biol.*, vol. 207, no. 6, pp. 767–82, Dec. 2014.

[31] S.-Y. Seong and P. Matzinger, "Hydrophobicity: an ancient damage-associated molecular pattern that initiates innate immune responses.," *Nat. Rev. Immunol.*, vol. 4, no. 6, pp. 469–78, Jun. 2004.

[32] B. Enyedi, S. Kala, T. Nikolich-Zugich, and P. Niethammer, "Tissue damage detection by osmotic surveillance.," *Nat. Cell Biol.*, vol. 15, no. 9, pp. 1123–30, Sep. 2013.

[33] R. Mori, T. J. Shaw, and P. Martin, "Molecular mechanisms linking wound inflammation and fibrosis: knockdown of osteopontin leads to rapid repair and reduced scarring," *J. Exp. Med.*, vol. 205, no. 1, pp. 43–51, 2008.

[34] S. J. Leibovich and R. Ross, "The role of the macrophage in wound repair. A study with hydrocortisone and antimacrophage serum.," *Am. J. Pathol.*, vol. 78, no. 1, pp. 71–100, Jan. 1975.

[35] P. Martin and S. J. Leibovich, "Inflammatory cells during wound repair: the good, the bad and the ugly.," *Trends Cell Biol.*, vol. 15, no. 11, pp. 599–607, Nov. 2005.

[36] J. V. Dovi, A. M. Szpaderska, and L. A. DiPietro, "Neutrophil function in the healing wound: adding insult to injury?," *Thromb. Haemost.*, vol. 92, no. 2, pp. 275–80, Aug. 2004.

[37] V. Brinkmann, "Neutrophil Extracellular Traps Kill Bacteria," *Science (80-.).*, vol. 303, no. 5663, pp. 1532–1535, 2004.

[38] G. Filio-Rodríguez *et al.*, "In vivo induction of neutrophil extracellular traps by Mycobacterium tuberculosis in a guinea pig model.," *Innate Immun.*, vol. 23, no. 7, p. 1753425917732406, Jan. 2017.

[39] S. K. Jorch and P. Kubes, "An emerging role for neutrophil extracellular traps in noninfectious disease.," *Nat. Med.*, vol. 23, no. 3, pp. 279–287, Mar. 2017.

[40] S. Barrientos, O. Stojadinovic, M. S. Golinko, H. Brem, and M. Tomic-Canic, "Growth factors and cytokines in wound healing.," *Wound Repair Regen.*, vol. 16, no. 5, pp. 585–601, 2008.

[41] J. A. Schmidt, S. B. Mizel, D. Cohen, and I. Green, "Interleukin 1, a potential regulator of fibroblast proliferation.," *J. Immunol.*, vol. 128, no. 5, pp. 2177–82, May 1982.

[42] E. W. Raines, S. K. Dower, and R. Ross, "Interleukin-1 mitogenic activity for fibroblasts and smooth muscle cells is due to PDGF-AA.," *Science*, vol. 243, no. 4889, pp. 393–6, Jan. 1989.

[43] C. A. Dinarello, "Biology of interleukin 1.," *FASEB J.*, vol. 2, no. 2, pp. 108–15, Feb. 1988.

[44] M. R. Duncan and B. Berman, "Differential regulation of collagen, glycosaminoglycan, fibronectin, and collagenase activity production in cultured human adult dermal fibroblasts by interleukin 1-alpha and beta and tumor necrosis factor-alpha and beta," *J. Invest. Dermatol.*, vol. 92, no. 5, pp. 699–706, May 1989.

[45] J. M. Dayer, B. de Rochemonteix, B. Burrus, S. Demczuk, and C. A. Dinarello, "Human recombinant interleukin 1 stimulates collagenase and prostaglandin E2 production by human synovial cells.," *J. Clin. Invest.*, vol. 77, no. 2, pp. 645–8, Feb. 1986.

[46] A. E. Postlethwaite, R. Raghow, G. P. Stricklin, H. Poppleton, J. M. Seyer, and A. H. Kang, "Modulation of fibroblast functions by interleukin 1: increased steady-state accumulation of type I procollagen messenger RNAs and stimulation of other functions but not chemotaxis by human recombinant interleukin 1 alpha and beta.," *J. Cell Biol.*, vol. 106, no. 2, pp. 311–8, Feb. 1988.

[47] A. E. Postlethwaite and J. M. Seyer, "Stimulation of fibroblast chemotaxis by human recombinant tumor necrosis factor alpha (TNF-alpha) and a synthetic TNF-alpha 31-68 peptide.," *J. Exp. Med.*, vol. 172, no. 6, pp. 1749–56, Dec. 1990.

[48] M. Egawa *et al.*, "Inflammatory monocytes recruited to allergic skin acquire an anti-inflammatory M2 phenotype via basophil-derived interleukin-4.," *Immunity*, vol. 38, no. 3, pp. 570–80, Mar. 2013.

[49]   M. Pasparakis, I. Haase, and F. O. Nestle, "Mechanisms regulating skin immunity and inflammation.," *Nat. Rev. Immunol.*, vol. 14, no. 5, pp. 289–301, May 2014.

[50]   J. Fuentes-Duculan *et al.*, "A subpopulation of CD163-positive macrophages is classically activated in psoriasis.," *J. Invest. Dermatol.*, vol. 130, no. 10, pp. 2412–22, Oct. 2010.

[51]   R. P. Kataru *et al.*, "Critical role of CD11b+ macrophages and VEGF in inflammatory lymphangiogenesis, antigen clearance, and inflammation resolution.," *Blood*, vol. 113, no. 22, pp. 5650–9, May 2009.

[52]   K. Buchmann, "Evolution of Innate Immunity: Clues from Invertebrates via Fish to Mammals.," *Front. Immunol.*, vol. 5, no. SEP, p. 459, 2014.

[53]   N. V. Ogryzko *et al.*, "Zebrafish tissue injury causes upregulation of interleukin-1 and caspase-dependent amplification of the inflammatory response.," *Dis. Model. Mech.*, vol. 7, no. 2, pp. 259–64, Feb. 2014.

[54]   J. Watzke, K. Schirmer, and S. Scholz, "Bacterial lipopolysaccharides induce genes involved in the innate immune response in embryos of the zebrafish (Danio rerio).," *Fish Shellfish Immunol.*, vol. 23, no. 4, pp. 901–5, Oct. 2007.

[55]   M. Seppola, A. N. Larsen, K. Steiro, B. Robertsen, and I. Jensen, "Characterisation and expression analysis of the interleukin genes, IL-1beta, IL-8 and IL-10, in Atlantic cod (Gadus morhua L.).," *Mol. Immunol.*, vol. 45, no. 4, pp. 887–97, Feb. 2008.

[56]   D.-C. Zhang, Y.-Q. Shao, Y.-Q. Huang, and S.-G. Jiang, "Cloning, characterization and expression analysis of interleukin-10 from the zebrafish (Danio rerion).," *J. Biochem. Mol. Biol.*, vol. 38, no. 5, pp. 571–6, Sep. 2005.

[57]   L. Zhu, P. Pan, W. Fang, J. Shao, and L. Xiang, "Essential role of IL-4 and IL-4Rα interaction in adaptive immunity of zebrafish: insight into the origin of Th2-like regulatory mechanism in ancient vertebrates.," *J. Immunol.*, vol. 188, no. 11, pp. 5571–84, Jun. 2012.

[58]   M. G. Tonnesen, X. Feng, and R. A. F. Clark, "Angiogenesis in wound healing.," *J. Investig. dermatology. Symp. Proc.*, vol. 5, no. 1, pp. 40–6, Dec. 2000.

[59]   R. Abe, S. C. Donnelly, T. Peng, R. Bucala, and C. N. Metz, "Peripheral blood fibrocytes: differentiation pathway and migration to wound sites.," *J. Immunol.*, vol. 166, no. 12, pp. 7556–62, Jun. 2001.

[60]   K. J. L. Fernandes *et al.*, "A dermal niche for multipotent adult skin-derived precursor cells.," *Nat. Cell Biol.*, vol. 6, no. 11, pp. 1082–93, Nov. 2004.

[61]   R. Roy, B. Zhang, and M. A. Moses, "Making the cut: protease-mediated regulation of angiogenesis.," *Exp. Cell Res.*, vol. 312, no. 5, pp. 608–22, Mar. 2006.

[62]   N. Hattori *et al.*, "MMP-13 plays a role in keratinocyte migration, angiogenesis, and contraction in mouse skin wound healing.," *Am. J. Pathol.*, vol. 175, no. 2, pp. 533–46, Aug. 2009.

[63]   S. A. Eming, B. Brachvogel, T. Odorisio, and M. Koch, "Regulation of angiogenesis: wound healing as a model.," *Prog. Histochem. Cytochem.*, vol. 42, no. 3, pp. 115–70, 2007.

[64]   P. Alberts, B. Johnson, A. Lewis, J. Raff, M. Roberts, K. Walter, "Specialized tissues, Stem Cells, and Tissue Renewal," in *Molecular Biology of the Cell, 5th Edition*, 5th ed., New York: Garland Science, 2008, pp. 1467–1468.

[65] A. Atala, D. J. Irvine, M. Moses, and S. Shaunak, "Wound Healing Versus Regeneration: Role of the Tissue Environment in Regenerative Medicine.," *MRS Bull.*, vol. 35, no. 8, pp. 597–606, Aug. 2010.

[66] V. Kroehne, D. Freudenreich, S. Hans, J. Kaslin, and M. Brand, "Regeneration of the adult zebrafish brain from neurogenic radial glia-type progenitors.," *Development*, vol. 138, no. 22, pp. 4831–41, Nov. 2011.

[67] S. Ausoni and S. Sartore, "From fish to amphibians to mammals: in search of novel strategies to optimize cardiac regeneration.," *J. Cell Biol.*, vol. 184, no. 3, pp. 357–64, Feb. 2009.

[68] F. Chablais and A. Jazwinska, "The regenerative capacity of the zebrafish heart is dependent on TGFβ signaling.," *Development*, vol. 139, no. 11, pp. 1921–30, Jun. 2012.

[69] S. M. LEVENSON, E. F. GEEVER, L. V CROWLEY, J. F. OATES, C. W. BERARD, and H. ROSEN, "THE HEALING OF RAT SKIN WOUNDS.," *Ann. Surg.*, vol. 161, pp. 293–308, Feb. 1965.

[70] M. A. Laflamme and C. E. Murry, "Heart regeneration.," *Nature*, vol. 473, no. 7347, pp. 326–35, May 2011.

[71] J. Silver and J. H. Miller, "Regeneration beyond the glial scar.," *Nat. Rev. Neurosci.*, vol. 5, no. 2, pp. 146–56, Feb. 2004.

[72] K. Miyazono, H. Ichijo, and C. H. Heldin, "Transforming growth factor-beta: latent forms, binding proteins and receptors.," *Growth Factors*, vol. 8, no. 1, pp. 11–22, 1993.

[73] A. B. Roberts, "Transforming growth factor-beta: activity and efficacy in animal models of wound healing.," *Wound Repair Regen.*, vol. 3, no. 4, pp. 408–18, 1995.

[74] S. Werner and R. Grose, "Regulation of wound healing by growth factors and cytokines.," *Physiol. Rev.*, vol. 83, no. 3, pp. 835–70, Jul. 2003.

[75] P. A. Hebda, "Stimulatory effects of transforming growth factor-beta and epidermal growth factor on epidermal cell outgrowth from porcine skin explant cultures.," *J. Invest. Dermatol.*, vol. 91, no. 5, pp. 440–5, Nov. 1988.

[76] G. S. Ashcroft *et al.*, "Mice lacking Smad3 show accelerated wound healing and an impaired local inflammatory response.," *Nat. Cell Biol.*, vol. 1, no. 5, pp. 260–6, Sep. 1999.

[77] L. Yang *et al.*, "Smad4 disruption accelerates keratinocyte reepithelialization in murine cutaneous wound repair.," *Histochem. Cell Biol.*, vol. 138, no. 4, pp. 573–82, Oct. 2012.

[78] C. B. Kimmel, W. W. Ballard, S. R. Kimmel, B. Ullmann, and T. F. Schilling, "Stages of embryonic development of the zebrafish.," *Dev. Dyn.*, vol. 203, no. 3, pp. 253–310, Jul. 1995.

[79] C. P. Heisenberg *et al.*, "Silberblick/Wnt11 mediates convergent extension movements during zebrafish gastrulation.," *Nature*, vol. 405, no. 6782, pp. 76–81, May 2000.

[80] M. Tada and J. C. Smith, "Xwnt11 is a target of Xenopus Brachyury: regulation of gastrulation movements via Dishevelled, but not through the canonical Wnt pathway.," *Development*, vol. 127, no. 10, pp. 2227–38, May 2000.

[81] M. Boutros and M. Mlodzik, "Dishevelled: at the crossroads of divergent intracellular

signaling pathways.," *Mech. Dev.*, vol. 83, no. 1–2, pp. 27–37, May 1999.

[82] J. B. Wallingford and R. Habas, "The developmental biology of Dishevelled: an enigmatic protein governing cell fate and cell polarity.," *Development*, vol. 132, no. 20, pp. 4421–36, Oct. 2005.

[83] K. A. Wharton, "Runnin' with the Dvl: proteins that associate with Dsh/Dvl and their significance to Wnt signal transduction.," *Dev. Biol.*, vol. 253, no. 1, pp. 1–17, Jan. 2003.

[84] M. D. Gordon and R. Nusse, "Wnt signaling: multiple pathways, multiple receptors, and multiple transcription factors.," *J. Biol. Chem.*, vol. 281, no. 32, pp. 22429–33, Aug. 2006.

[85] J. D. Axelrod, J. R. Miller, J. M. Shulman, R. T. Moon, and N. Perrimon, "Differential recruitment of Dishevelled provides signaling specificity in the planar cell polarity and Wingless signaling pathways.," *Genes Dev.*, vol. 12, no. 16, pp. 2610–22, Aug. 1998.

[86] J. Caddy *et al.*, "Epidermal wound repair is regulated by the planar cell polarity signaling pathway.," *Dev. Cell*, vol. 19, no. 1, pp. 138–47, Jul. 2010.

[87] F. Marlow, J. Topczewski, D. Sepich, and L. Solnica-Krezel, "Zebrafish Rho kinase 2 acts downstream of Wnt11 to mediate cell polarity and effective convergence and extension movements.," *Curr. Biol.*, vol. 12, no. 11, pp. 876–84, Jun. 2002.

[88] S.-L. Lai, C.-N. Chang, P.-J. Wang, and S.-J. Lee, "Rho mediates cytokinesis and epiboly via ROCK in zebrafish.," *Mol. Reprod. Dev.*, vol. 71, no. 2, pp. 186–96, Jun. 2005.

[89] S. Edlund, M. Landström, C. Heldin, and P. Aspenström, "Transforming growth factor-beta-induced mobilization of actin cytoskeleton requires signaling by small GTPases Cdc42 and RhoA.," *Mol. Biol. Cell*, vol. 13, no. 3, pp. 902–14, Mar. 2002.

[90] N. Okumura *et al.*, "Enhancement of corneal endothelium wound healing by Rho-associated kinase (ROCK) inhibitor eye drops.," *Br. J. Ophthalmol.*, vol. 95, no. 7, pp. 1006–9, Jul. 2011.

[91] A. Pipparelli, Y. Arsenijevic, G. Thuret, P. Gain, M. Nicolas, and F. Majo, "ROCK inhibitor enhances adhesion and wound healing of human corneal endothelial cells.," *PLoS One*, vol. 8, no. 4, p. e62095, 2013.

[92] J. Yin and F.-S. X. Yu, "Rho kinases regulate corneal epithelial wound healing.," *Am. J. Physiol. Cell Physiol.*, vol. 295, no. 2, pp. C378-87, Aug. 2008.

[93] I. Boucher, C. Rich, A. Lee, M. Marcincin, and V. Trinkaus-Randall, "The P2Y2 receptor mediates the epithelial injury response and cell migration.," *Am. J. Physiol. Cell Physiol.*, vol. 299, no. 2, pp. C411-21, Aug. 2010.

[94] S. P. Humphrey and R. T. Williamson, "A review of saliva: normal composition, flow, and function.," *J. Prosthet. Dent.*, vol. 85, no. 2, pp. 162–9, Feb. 2001.

[95] J. Hatzold *et al.,* "Tumor suppression in basal keratinocytes via dual non-cell-autonomous functions of a Na,K-ATPase beta subunit.," *Elife*, vol. 5, no. MAY2016, pp. 1–30, May 2016.

[96] J. Hopkinson-Woolley, D. Hughes, S. Gordon, and P. Martin, "Macrophage recruitment during limb development and wound healing in the embryonic and foetal mouse.," *J. Cell Sci.*, vol. 107 (Pt 5, pp. 1159–67, May 1994.

[97] S. E. Mutsaers, J. E. Bishop, G. McGrouther, and G. J. Laurent, "Mechanisms of tissue repair: from wound healing to fibrosis.," *Int. J. Biochem. Cell Biol.*, vol. 29, no. 1, pp. 5–17, Jan. 1997.

[98] D. Gay *et al.*, "Fgf9 from dermal γδ T cells induces hair follicle neogenesis after wounding.," *Nat. Med.*, vol. 19, no. 7, pp. 916–23, Jul. 2013.

[99] S. Werner, K. G. Peters, M. T. Longaker, F. Fuller-Pace, M. J. Banda, and L. T. Williams, "Large induction of keratinocyte growth factor expression in the dermis during wound healing.," *Proc. Natl. Acad. Sci. U. S. A.*, vol. 89, no. 15, pp. 6896–900, Aug. 1992.

[100] S. Werner *et al.*, "The function of KGF in morphogenesis of epithelium and reepithelialization of wounds.," *Science*, vol. 266, no. 5186, pp. 819–22, Nov. 1994.

[101] I. N. Holcomb *et al.*, "FIZZ1, a novel cysteine-rich secreted protein associated with pulmonary inflammation, defines a new gene family.," *EMBO J.*, vol. 19, no. 15, pp. 4046–55, Aug. 2000.

[102] C. M. Steppan *et al.*, "A family of tissue-specific resistin-like molecules.," *Proc. Natl. Acad. Sci. U. S. A.*, vol. 98, no. 2, pp. 502–6, Jan. 2001.

[103] B. Gerstmayer *et al.*, "Identification of RELMgamma, a novel resistin-like molecule with a distinct expression pattern.," *Genomics*, vol. 81, no. 6, pp. 588–95, Jun. 2003.

[104] M. G. Nair *et al.*, "Alternatively activated macrophage-derived RELM-{alpha} is a negative regulator of type 2 inflammation in the lung.," *J. Exp. Med.*, vol. 206, no. 4, pp. 937–52, Apr. 2009.

[105] A. Munitz *et al.*, "Resistin-like molecule alpha enhances myeloid cell activation and promotes colitis.," *J. Allergy Clin. Immunol.*, vol. 122, no. 6, p. 1200–1207.e1, Dec. 2008.

[106] T. Liu *et al.*, "FIZZ2/RELM-β induction and role in pulmonary fibrosis.," *J. Immunol.*, vol. 187, no. 1, pp. 450–61, Jul. 2011.

[107] A. Tarkowski, J. Bjersing, A. Shestakov, and M. I. Bokarewa, "Resistin competes with lipopolysaccharide for binding to toll-like receptor 4.," *J. Cell. Mol. Med.*, vol. 14, no. 6B, pp. 1419–31, Jun. 2010.

[108] J. A. Knipper *et al.*, "Interleukin-4 Receptor α Signaling in Myeloid Cells Controls Collagen Fibril Assembly in Skin Repair.," *Immunity*, vol. 43, no. 4, pp. 803–16, Oct. 2015.

[109] J. Myllyharju and K. I. Kivirikko, "Collagens, modifying enzymes and their mutations in humans, flies and worms.," *Trends Genet.*, vol. 20, no. 1, pp. 33–43, Jan. 2004.

[110] V. A. Schneider and M. Granato, "Genomic structure and embryonic expression of zebrafish lysyl hydroxylase 1 and lysyl hydroxylase 2.," *Matrix Biol.*, vol. 26, no. 1, pp. 12–9, Jan. 2007.

[111] H. N. Yeowell and L. C. Walker, "Mutations in the lysyl hydroxylase 1 gene that result in enzyme deficiency and the clinical phenotype of Ehlers-Danlos syndrome type VI.," *Mol. Genet. Metab.*, vol. 71, no. 1–2, pp. 212–24, 2000.

[112] C. Giunta, A. Randolph, L. I. Al-Gazali, H. G. Brunner, M. E. Kraenzlin, and B. Steinmann, "Nevo syndrome is allelic to the kyphoscoliotic type of the Ehlers-Danlos syndrome (EDS VIA).," *Am. J. Med. Genet. A*, vol. 133A, no. 2, pp. 158–64, Mar. 2005.

[113] R. E. Brenner, U. Vetter, H. Stöss, P. K. Müller, and W. M. Teller, "Defective collagen fibril formation and mineralization in osteogenesis imperfecta with congenital joint contractures (Bruck syndrome).," *Eur. J. Pediatr.*, vol. 152, no. 6, pp. 505–8, Jun. 1993.

[114] E. J. Breslau-Siderius, R. H. Engelbert, G. Pals, and J. A. van der Sluijs, "Bruck syndrome: a rare combination of bone fragility and multiple congenital joint contractures.," *J. Pediatr. Orthop. B*, vol. 7, no. 1, pp. 35–8, Jan. 1998.

[115] J. G. Leroy *et al.*, "Bruck syndrome: neonatal presentation and natural course in three patients.," *Pediatr. Radiol.*, vol. 28, no. 10, pp. 781–9, Oct. 1998.

[116] E. McPherson and M. Clemens, "Bruck syndrome (osteogenesis imperfecta with congenital joint contractures): review and report on the first North American case.," *Am. J. Med. Genet.*, vol. 70, no. 1, pp. 28–31, May 1997.

[117] R. Ha-Vinh *et al.*, "Phenotypic and molecular characterization of Bruck syndrome (osteogenesis imperfecta with contractures of the large joints) caused by a recessive mutation in PLOD2.," *Am. J. Med. Genet. A*, vol. 131, no. 2, pp. 115–20, Dec. 2004.

[118] A. M. Salo *et al.*, "A connective tissue disorder caused by mutations of the lysyl hydroxylase 3 gene.," *Am. J. Hum. Genet.*, vol. 83, no. 4, pp. 495–503, Oct. 2008.

[119] M. Risteli *et al.*, "Reduction of lysyl hydroxylase 3 causes deleterious changes in the deposition and organization of extracellular matrix.," *J. Biol. Chem.*, vol. 284, no. 41, pp. 28204–11, Oct. 2009.

[120] D. R. Eyre, T. J. Koob, and K. P. Van Ness, "Quantitation of hydroxypyridinium crosslinks in collagen by high-performance liquid chromatography.," *Anal. Biochem.*, vol. 137, no. 2, pp. 380–8, Mar. 1984.

[121] J. Brinckmann *et al.*, "Overhydroxylation of lysyl residues is the initial step for altered collagen cross-links and fibril architecture in fibrotic skin.," *J. Invest. Dermatol.*, vol. 113, no. 4, pp. 617–21, Oct. 1999.

[122] P. L. Leopold, J. Vincent, and H. Wang, "A comparison of epithelial-to-mesenchymal transition and re-epithelialization.," *Semin. Cancer Biol.*, vol. 22, no. 5–6, pp. 471–83, Oct. 2012.

[123] J. Gailit, M. P. Welch, and R. A. Clark, "TGF-beta 1 stimulates expression of keratinocyte integrins during re-epithelialization of cutaneous wounds.," *J. Invest. Dermatol.*, vol. 103, no. 2, pp. 221–7, Aug. 1994.

[124] J. Gailit and R. A. Clark, "Wound repair in the context of extracellular matrix.," *Curr. Opin. Cell Biol.*, vol. 6, no. 5, pp. 717–25, Oct. 1994.

[125] G. J. Inman *et al.*, "SB-431542 is a potent and specific inhibitor of transforming growth factor-beta superfamily type I activin receptor-like kinase (ALK) receptors ALK4, ALK5, and ALK7.," *Mol. Pharmacol.*, vol. 62, no. 1, pp. 65–74, Jul. 2002.

[126] J. S. Sawyer *et al.*, "Synthesis and activity of new aryl- and heteroaryl-substituted pyrazole inhibitors of the transforming growth factor-beta type I receptor kinase domain.," *J. Med. Chem.*, vol. 46, no. 19, pp. 3953–6, Sep. 2003.

[127] R. O. Hynes, "Integrins: Versatility, modulation, and signaling in cell adhesion," *Cell*, vol. 69, no. 1, pp. 11–25, 1992.

[128] R. Pytela, M. D. Pierschbacher, M. H. Ginsberg, E. F. Plow, and E. Ruoslahti, "Platelet membrane glycoprotein IIb/IIIa: member of a family of Arg-Gly-Asp--specific adhesion

receptors.," *Science*, vol. 231, no. 4745, pp. 1559–62, Mar. 1986.

[129] R. Pytela, "Amino acid sequence of the murine Mac-1 alpha chain reveals homology with the integrin family and an additional domain related to von Willebrand factor.," *EMBO J.*, vol. 7, no. 5, pp. 1371–8, May 1988.

[130] D. S. Grant, K. Tashiro, B. Segui-Real, Y. Yamada, G. R. Martin, and H. K. Kleinman, "Two different laminin domains mediate the differentiation of human endothelial cells into capillary-like structures in vitro.," *Cell*, vol. 58, no. 5, pp. 933–43, Sep. 1989.

[131] S. Dedhar, "Signal transduction via the beta 1 integrins is a required intermediate in interleukin-1 beta induction of alkaline phosphatase activity in human osteosarcoma cells.," *Exp. Cell Res.*, vol. 183, no. 1, pp. 207–14, Jul. 1989.

[132] J. Lawler, R. Weinstein, and R. O. Hynes, "Cell attachment to thrombospondin: the role of ARG-GLY-ASP, calcium, and integrin receptors.," *J. Cell Biol.*, vol. 107, no. 6 Pt 1, pp. 2351–61, Dec. 1988.

[133] A. Miyauchi *et al.*, "Recognition of osteopontin and related peptides by an alpha v beta 3 integrin stimulates immediate cell signals in osteoclasts.," *J. Biol. Chem.*, vol. 266, no. 30, pp. 20369–74, Oct. 1991.

[134] M. P. Harris, N. Rohner, H. Schwarz, S. Perathoner, P. Konstantinidis, and C. Nüsslein-Volhard, "Zebrafish eda and edar mutants reveal conserved and ancestral roles of ectodysplasin signaling in vertebrates.," *PLoS Genet.*, vol. 4, no. 10, p. e1000206, Oct. 2008.

[135] J. Huelsken and J. Behrens, "The Wnt signalling pathway," *J. Cell Sci.*, vol. 115, no. 21, pp. 3977–3978, Nov. 2002.

[136] M. Amano, Y. Fukata, and K. Kaibuchi, "Regulation and functions of Rho-associated kinase.," *Exp. Cell Res.*, vol. 261, no. 1, pp. 44–51, Nov. 2000.

[137] J. G. Homsy, H. Jasper, X. G. Peralta, H. Wu, D. P. Kiehart, and D. Bohmann, "JNK signaling coordinates integrin and actin functions during Drosophila embryogenesis," *Dev. Dyn.*, vol. 235, no. 2, pp. 427–434, 2006.

[138] M. J. Marinissen, M. Chiariello, T. Tanos, O. Bernard, S. Narumiya, and J. S. Gutkind, "The small GTP-binding protein RhoA regulates c-jun by a ROCK-JNK signaling axis.," *Mol. Cell*, vol. 14, no. 1, pp. 29–41, Apr. 2004.

[139] J. C. Yarrow, G. Totsukawa, G. T. Charras, and T. J. Mitchison, "Screening for cell migration inhibitors via automated microscopy reveals a Rho-kinase inhibitor.," *Chem. Biol.*, vol. 12, no. 3, pp. 385–95, Mar. 2005.

[140] M. Boutros, N. Paricio, D. I. Strutt, and M. Mlodzik, "Dishevelled activates JNK and discriminates between JNK pathways in planar polarity and wingless signaling.," *Cell*, vol. 94, no. 1, pp. 109–18, Jul. 1998.

[141] H. Kobayashi, S. Aiba, Y. Yoshino, and H. Tagami, "Acute cutaneous barrier disruption activates epidermal p44/42 and p38 mitogen-activated protein kinases in human and hairless guinea pig skin.," *Exp. Dermatol.*, vol. 12, no. 6, pp. 734–46, Dec. 2003.

[142] S. Yano, M. Komine, M. Fujimoto, H. Okochi, and K. Tamaki, "Mechanical stretching in vitro regulates signal transduction pathways and cellular proliferation in human epidermal keratinocytes.," *J. Invest. Dermatol.*, vol. 122, no. 3, pp. 783–90, Mar. 2004.

[143] S. Ugawa, Y. Ishida, T. Ueda, Y. Yu, and S. Shimada, "Hypotonic stimuli enhance

proton-gated currents of acid-sensing ion channel-1b.," *Biochem. Biophys. Res. Commun.*, vol. 367, no. 3, pp. 530–4, Mar. 2008.

[144] J. Vriens, H. Watanabe, A. Janssens, G. Droogmans, T. Voets, and B. Nilius, "Cell swelling, heat, and chemical agonists use distinct pathways for the activation of the cation channel TRPV4," *Proc. Natl. Acad. Sci.*, vol. 101, no. 1, pp. 396–401, 2004.

[145] M. Oike, M. Watanabe, and C. Kimura, "Involvement of heparan sulfate proteoglycan in sensing hypotonic stress in bovine aortic endothelial cells.," *Biochim. Biophys. Acta*, vol. 1780, no. 10, pp. 1148–55, Oct. 2008.

[146] S. Ahmad, A. Ahmad, M. Ghosh, C. C. Leslie, and C. W. White, "Extracellular ATP-mediated signaling for survival in hyperoxia-induced oxidative stress.," *J. Biol. Chem.*, vol. 279, no. 16, pp. 16317–25, Apr. 2004.

[147] D. M. Graham, L. Huang, K. R. Robinson, and M. a Messerli, "Epidermal keratinocyte polarity and motility require Ca^{2+} influx through TRPV1.," *J. Cell Sci.*, vol. 126, no. Pt 20, pp. 4602–13, Oct. 2013.

[148] X. C. Yang and F. Sachs, "Block of stretch-activated ion channels in Xenopus oocytes by gadolinium and calcium ions.," *Science*, vol. 243, no. 4894 Pt 1, pp. 1068–71, Feb. 1989.

[149] X. Zhao and J.-L. Guan, "Focal adhesion kinase and its signaling pathways in cell migration and angiogenesis.," *Adv. Drug Deliv. Rev.*, vol. 63, no. 8, pp. 610–5, Jul. 2011.

[150] P. Ducy and G. Karsenty, "Genetic control of cell differentiation in the skeleton.," *Curr. Opin. Cell Biol.*, vol. 10, no. 5, pp. 614–9, Oct. 1998.

[151] H. Yoshida *et al.*, "The murine mutation osteopetrosis is in the coding region of the macrophage colony stimulating factor gene.," *Nature*, vol. 345, no. 6274, pp. 442–4, May 1990.

[152] D. M. Parichy, D. G. Ransom, B. Paw, L. I. Zon, and S. L. Johnson, "An orthologue of the kit-related gene fms is required for development of neural crest-derived xanthophores and a subpopulation of adult melanocytes in the zebrafish, Danio rerio.," *Development*, vol. 127, no. 14, pp. 3031–44, Jul. 2000.

[153] D. M. Parichy and J. M. Turner, "Temporal and cellular requirements for Fms signaling during zebrafish adult pigment pattern development.," *Development*, vol. 130, no. 5, pp. 817–33, Mar. 2003.

[154] J. Odenthal *et al.*, "Mutations affecting xanthophore pigmentation in the zebrafish, Danio rerio.," *Development*, vol. 123, pp. 391–8, Dec. 1996.

[155] S. Lamouille, J. Xu, and R. Derynck, "Molecular mechanisms of epithelial-mesenchymal transition.," *Nat. Rev. Mol. Cell Biol.*, vol. 15, no. 3, pp. 178–96, Mar. 2014.

[156] K. Räsänen and A. Vaheri, "TGF-beta1 causes epithelial-mesenchymal transition in HaCaT derivatives, but induces expression of COX-2 and migration only in benign, not in malignant keratinocytes.," *J. Dermatol. Sci.*, vol. 58, no. 2, pp. 97–104, May 2010.

[157] R. M. Koch, N. S. Roche, W. T. Parks, G. S. Ashcroft, J. J. Letterio, and a B. Roberts, "Incisional wound healing in transforming growth factor-beta1 null mice.," *Wound Repair Regen.*, vol. 8, no. 3, pp. 179–91, 2000.

[158] A. G. Matoltsy and C. B. Viziam, "Further observations on epithelialization of small

wounds: an autoradiographic study of incorporation and distribution of 3H-thymidine in the epithelium covering skin wounds.," *J. Invest. Dermatol.*, vol. 55, no. 1, pp. 20–5, Jul. 1970.

[159] M. Lévesque, E. Villiard, and S. Roy, "Skin wound healing in axolotls: a scarless process.," *J. Exp. Zool. B. Mol. Dev. Evol.*, vol. 314, no. 8, pp. 684–97, Dec. 2010.

[160] G. F. Pierce *et al.*, "Stimulation of all epithelial elements during skin regeneration by keratinocyte growth factor.," *J. Exp. Med.*, vol. 179, no. 3, pp. 831–40, Mar. 1994.

[161] Y. Shirakata *et al.*, "Heparin-binding EGF-like growth factor accelerates keratinocyte migration and skin wound healing.," *J. Cell Sci.*, vol. 118, no. Pt 11, pp. 2363–70, Jun. 2005.

[162] R. Kalluri and R. a Weinberg, "The basics of epithelial-mesenchymal transition.," *J. Clin. Invest.*, vol. 119, no. 6, pp. 1420–8, Jun. 2009.

[163] C. M. DiPersio, R. Zheng, J. Kenney, and L. Van De Water, "Integrin-mediated regulation of epidermal wound functions.," *Cell Tissue Res.*, vol. 365, no. 3, pp. 467–82, Sep. 2016.

[164] P. Caswell and J. Norman, "Endocytic transport of integrins during cell migration and invasion.," *Trends Cell Biol.*, vol. 18, no. 6, pp. 257–63, Jun. 2008.

[165] R. E. Bridgewater, J. C. Norman, and P. T. Caswell, "Integrin trafficking at a glance.," *J. Cell Sci.*, vol. 125, no. Pt 16, pp. 3695–701, Aug. 2012.

[166] M. Roberts, S. Barry, A. Woods, P. van der Sluijs, and J. Norman, "PDGF-regulated rab4-dependent recycling of alphavbeta3 integrin from early endosomes is necessary for cell adhesion and spreading.," *Curr. Biol.*, vol. 11, no. 18, pp. 1392–402, Sep. 2001.

[167] M. S. Roberts, A. J. Woods, T. C. Dale, P. Van Der Sluijs, and J. C. Norman, "Protein kinase B/Akt acts via glycogen synthase kinase 3 to regulate recycling of alpha v beta 3 and alpha 5 beta 1 integrins.," *Mol. Cell. Biol.*, vol. 24, no. 4, pp. 1505–15, Feb. 2004.

[168] A. Quilhac and J. Y. Sire, "Spreading, proliferation, and differentiation of the epidermis after wounding a cichlid fish, Hemichromis bimaculatus.," *Anat. Rec.*, vol. 254, no. 3, pp. 435–51, Mar. 1999.

[169] Y. Shimizu *et al.*, "ROCK-I regulates closure of the eyelids and ventral body wall by inducing assembly of actomyosin bundles," *J. Cell Biol.*, vol. 168, no. 6, pp. 941–953, 2005.

[170] M. Bosch, F. Serras, E. Martín-Blanco, and J. Baguñà, "JNK signaling pathway required for wound healing in regenerating Drosophila wing imaginal discs.," *Dev. Biol.*, vol. 280, no. 1, pp. 73–86, Apr. 2005.

[171] A. Taruno, N. Niisato, and Y. Marunaka, "Hypotonicity stimulates renal epithelial sodium transport by activating JNK via receptor tyrosine kinases.," *Am. J. Physiol. Renal Physiol.*, vol. 293, no. 1, pp. F128-38, Jul. 2007.

[172] B. Nilius and G. Droogmans, "Amazing chloride channels: an overview.," *Acta Physiol. Scand.*, vol. 177, no. 2, pp. 119–47, Feb. 2003.

[173] J. Riedl *et al.*, "Lifeact: a versatile marker to visualize F-actin.," *Nat. Methods*, vol. 5, no. 7, pp. 605–7, Jul. 2008.

[174] P. Lam and A. Huttenlocher, "Interstitial leukocyte migration in vivo.," *Curr. Opin. Cell Biol.*, vol. 25, no. 5, pp. 650–8, Oct. 2013.

[175] G. T. Eisenhoffer *et al.*, "Crowding induces live cell extrusion to maintain homeostatic cell numbers in epithelia.," *Nature*, vol. 484, no. 7395, pp. 546–9, Apr. 2012.

[176] K. Tousova, L. Vyklicky, K. Susankova, J. Benedikt, and V. Vlachova, "Gadolinium activates and sensitizes the vanilloid receptor TRPV1 through the external protonation sites.," *Mol. Cell. Neurosci.*, vol. 30, no. 2, pp. 207–17, Oct. 2005.

[177] L. Tian *et al.*, "Imaging neural activity in worms, flies and mice with improved GCaMP calcium indicators.," *Nat. Methods*, vol. 6, no. 12, pp. 875–81, Dec. 2009.

[178] S. K. Yoo, C. M. Freisinger, D. C. LeBert, and A. Huttenlocher, "Early redox, Src family kinase, and calcium signaling integrate wound responses and tissue regeneration in zebrafish.," *J. Cell Biol.*, vol. 199, no. 2, pp. 225–34, Oct. 2012.

[179] V. W. Wong *et al.*, "Focal adhesion kinase links mechanical force to skin fibrosis via inflammatory signaling.," *Nat. Med.*, vol. 18, no. 1, pp. 148–52, Dec. 2011.

[180] D. Kwak *et al.*, "Osmotic stress regulates mammalian target of rapamycin (mTOR) complex 1 via c-Jun N-terminal Kinase (JNK)-mediated Raptor protein phosphorylation.," *J. Biol. Chem.*, vol. 287, no. 22, pp. 18398–407, May 2012.

[181] K. Sossey-Alaoui, X. Li, T. A. Ranalli, and J. K. Cowell, "WAVE3-mediated cell migration and lamellipodia formation are regulated downstream of phosphatidylinositol 3-kinase," *J. Biol. Chem.*, vol. 280, no. 23, pp. 21748–21755, 2005.

[182] S.-C. Yip *et al.*, "The distinct roles of Ras and Rac in PI 3-kinase-dependent protrusion during EGF-stimulated cell migration," *J. Cell Sci.*, vol. 120, no. 17, pp. 3138–3146, 2007.

[183] G. Fenteany and M. Glogauer, "Cytoskeletal remodeling in leukocyte function," *Curr. Opin. Hematol.*, vol. 11, no. 1, pp. 15–24, 2004.

[184] G. Xue and B. A. Hemmings, "PKB/akt-dependent regulation of cell motility," *J. Natl. Cancer Inst.*, vol. 105, no. 6, pp. 393–404, 2013.

[185] A. Enomoto, J. Ping, and M. Takahashi, "Girdin, a novel actin-binding protein, and its family of proteins possess versatile functions in the Akt and Wnt signaling pathways," *Ann. N. Y. Acad. Sci.*, vol. 1086, pp. 169–184, 2006.

[186] R. Cipriano, K. L. S. Miskimen, B. L. Bryson, C. R. Foy, C. A. Bartel, and M. W. Jackson, "FAM83B-mediated activation of PI3K/AKT and MAPK signaling cooperates to promote epithelial cell transformation and resistance to targeted therapies.," *Oncotarget*, vol. 4, no. 5, pp. 729–38, May 2013.

[187] E. U. Frevert, C. Bjørbaek, C. L. Venable, S. R. Keller, and B. B. Kahn, "Targeting of constitutively active phosphoinositide 3-kinase to GLUT4-containing vesicles in 3T3-L1 adipocytes.," *J. Biol. Chem.*, vol. 273, no. 39, pp. 25480–7, Sep. 1998.

[188] Q. Hu, A. Klippel, A. J. Muslin, W. J. Fantl, and L. T. Williams, "Ras-dependent induction of cellular responses by constitutively active phosphatidylinositol-3 kinase.," *Science*, vol. 268, no. 5207, pp. 100–2, Apr. 1995.

[189] A. D. Kohn, S. A. Summers, M. J. Birnbaum, and R. A. Roth, "Expression of a constitutively active Akt Ser/Thr kinase in 3T3-L1 adipocytes stimulates glucose uptake and glucose transporter 4 translocation.," *J. Biol. Chem.*, vol. 271, no. 49, pp. 31372–8, Dec. 1996.

[190] C. A. Eyster, Q. S. Duggins, and A. L. Olson, "Expression of constitutively active Akt/protein kinase B signals GLUT4 translocation in the absence of an intact actin cytoskeleton.," *J. Biol. Chem.*, vol. 280, no. 18, pp. 17978–85, May 2005.

[191] A. I. Flores *et al.*, "Constitutively active Akt induces enhanced myelination in the CNS.," *J. Neurosci.*, vol. 28, no. 28, pp. 7174–83, Jul. 2008.

[192] M. G. Kharas *et al.*, "Constitutively active AKT depletes hematopoietic stem cells and induces leukemia in mice.," *Blood*, vol. 115, no. 7, pp. 1406–15, Feb. 2010.

[193] B. Ju, J. Spitsbergen, C. J. Eden, M. R. Taylor, and W. Chen, "Co-activation of hedgehog and AKT pathways promote tumorigenesis in zebrafish.," *Mol. Cancer*, vol. 8, p. 40, Jun. 2009.

[194] M. Oike, C. Kimura, T. Koyama, M. Yoshikawa, and Y. Ito, "Hypotonic stress-induced dual Ca(2+) responses in bovine aortic endothelial cells.," *Am. J. Physiol. Heart Circ. Physiol.*, vol. 279, no. 2, pp. H630-8, Aug. 2000.

[195] E. M. Schwiebert and A. Zsembery, "Extracellular ATP as a signaling molecule for epithelial cells.," *Biochim. Biophys. Acta*, vol. 1615, no. 1–2, pp. 7–32, Sep. 2003.

[196] A. G. Szent-Györgyi, "Calcium regulation of muscle contraction.," *Biophys. J.*, vol. 15, no. 7, pp. 707–23, Jul. 1975.

[197] F.-C. Tsai, G.-H. Kuo, S.-W. Chang, and P.-J. Tsai, "Ca2+ signaling in cytoskeletal reorganization, cell migration, and cancer metastasis.," *Biomed Res. Int.*, vol. 2015, p. 409245, 2015.

[198] L. Staiano-Coico *et al.*, "Human keratinocyte growth factor effects in a porcine model of epidermal wound healing.," *J. Exp. Med.*, vol. 178, no. 3, pp. 865–78, Sep. 1993.

[199] G. P. Morris, P. L. Beck, M. S. Herridge, W. T. Depew, M. R. Szewczuk, and J. L. Wallace, "Hapten-induced model of chronic inflammation and ulceration in the rat colon.," *Gastroenterology*, vol. 96, no. 3, pp. 795–803, Mar. 1989.

[200] L. R. Fitzpatrick, K. Meirelles, J. S. Small, F. J. Puleo, W. A. Koltun, and R. N. Cooney, "A new model of chronic hapten-induced colitis in young rats.," *J. Pediatr. Gastroenterol. Nutr.*, vol. 50, no. 3, pp. 240–50, Mar. 2010.

[201] A. Wullaert, M. C. Bonnet, and M. Pasparakis, "NF-κB in the regulation of epithelial homeostasis and inflammation.," *Cell Res.*, vol. 21, no. 1, pp. 146–58, Jan. 2011.

[202] M. Pasparakis, "Regulation of tissue homeostasis by NF-kappaB signalling: implications for inflammatory diseases.," *Nat. Rev. Immunol.*, vol. 9, no. 11, pp. 778–88, Nov. 2009.

[203] A. J. van der Slot *et al.*, "Increased formation of pyridinoline cross-links due to higher telopeptide lysyl hydroxylase levels is a general fibrotic phenomenon.," *Matrix Biol.*, vol. 23, no. 4, pp. 251–7, Jul. 2004.

[204] X. Fang, J. Corrales, C. Thornton, B. E. Scheffler, and K. L. Willett, "Global and gene specific DNA methylation changes during zebrafish development.," *Comp. Biochem. Physiol. B. Biochem. Mol. Biol.*, vol. 166, no. 1, pp. 99–108, Sep. 2013.

[205] A. Bird, "DNA methylation patterns and epigenetic memory.," *Genes Dev.*, vol. 16, no. 1, pp. 6–21, Jan. 2002.

[206] D. Macleod, V. H. Clark, and A. Bird, "Absence of genome-wide changes in DNA methylation during development of the zebrafish.," *Nat. Genet.*, vol. 23, no. 2, pp. 139–

40, Oct. 1999.

[207] M. L. Suster, G. Abe, A. Schouw, and K. Kawakami, "Transposon-mediated BAC transgenesis in zebrafish.," *Nat. Protoc.*, vol. 6, no. 12, pp. 1998–2021, Dec. 2011.

[208] M. G. Rohani and W. C. Parks, "Matrix remodeling by MMPs during wound repair.," *Matrix Biol.*, vol. 44–46, pp. 113–21, 2015.

[209] J. Y. Keow, K. M. Herrmann, and B. D. Crawford, "Differential in vivo zymography: a method for observing matrix metalloproteinase activity in the zebrafish embryo.," *Matrix Biol.*, vol. 30, no. 3, pp. 169–77, Apr. 2011.

[210] C. A. Squier and M. J. Kremer, "Biology of oral mucosa and esophagus.," *J. Natl. Cancer Inst. Monogr.*, vol. 29, no. 29, pp. 7–15, 2001.

[211] J. J. Sciubba, J. P. Waterhouse, and J. Meyer, "A fine structural comparison of the healing of incisional wounds of mucosa and skin.," *J. Oral Pathol.*, vol. 7, no. 4, pp. 214–27, Aug. 1978.

[212] L. J. Walsh, P. R. L'Estrange, and G. J. Seymour, "High magnification in situ viewing of wound healing in oral mucosa.," *Aust. Dent. J.*, vol. 41, no. 2, pp. 75–9, Apr. 1996.

[213] A. M. Szpaderska, J. D. Zuckerman, and L. A. DiPietro, "Differential injury responses in oral mucosal and cutaneous wounds.," *J. Dent. Res.*, vol. 82, no. 8, pp. 621–6, Aug. 2003.

[214] M. Shah, D. M. Foreman, and M. W. Ferguson, "Neutralisation of TGF-beta 1 and TGF-beta 2 or exogenous addition of TGF-beta 3 to cutaneous rat wounds reduces scarring.," *J. Cell Sci.*, vol. 108 (Pt 3, pp. 985–1002, Mar. 1995.

[215] K. M. Bullard, M. T. Longaker, and H. P. Lorenz, "Fetal wound healing: current biology.," *World J. Surg.*, vol. 27, no. 1, pp. 54–61, Jan. 2003.

[216] F. K. Field and M. D. Kerstein, "Overview of wound healing in a moist environment.," *Am. J. Surg.*, vol. 167, no. 1A, p. 2S–6S, Jan. 1994.

[217] J. Boateng and O. Catanzano, "Advanced Therapeutic Dressings for Effective Wound Healing--A Review.," *J. Pharm. Sci.*, vol. 104, no. 11, pp. 3653–80, Nov. 2015.

[218] J. Hurlow, K. Couch, K. Laforet, L. Bolton, D. Metcalf, and P. Bowler, "Clinical Biofilms: A Challenging Frontier in Wound Care.," *Adv. wound care*, vol. 4, no. 5, pp. 295–301, May 2015.

[219] G. Han and R. Ceilley, "Chronic Wound Healing: A Review of Current Management and Treatments.," *Adv. Ther.*, vol. 34, no. 3, pp. 599–610, Mar. 2017.

[220] S. Reischauer, M. P. Levesque, C. Nüsslein-Volhard, and M. Sonawane, "Lgl2 executes its function as a tumor suppressor by regulating ErbB signaling in the zebrafish epidermis.," *PLoS Genet.*, vol. 5, no. 11, p. e1000720, Nov. 2009.

[221] Y. Lee, S. Grill, A. Sanchez, M. Murphy-Ryan, and K. D. Poss, "Fgf signaling instructs position-dependent growth rate during zebrafish fin regeneration," *Development*, vol. 132, no. 23, pp. 5173–5183, Dec. 2005.

[222] S. R. Marques, Y. Lee, K. D. Poss, and D. Yelon, "Reiterative roles for FGF signaling in the establishment of size and proportion of the zebrafish heart.," *Dev. Biol.*, vol. 321, no. 2, pp. 397–406, Sep. 2008.

[223] C. Xu *et al.*, "Arteries are formed by vein-derived endothelial tip cells.," *Nat. Commun.*, vol. 5, p. 5758, Dec. 2014.

[224] K. M. Kwan *et al.*, "The Tol2kit: a multisite gateway-based construction kit for Tol2 transposon transgenesis constructs.," *Dev. Dyn.*, vol. 236, no. 11, pp. 3088–99, Nov. 2007.

[225] J. Schindelin *et al.*, "Fiji: an open-source platform for biological-image analysis.," *Nat. Methods*, vol. 9, no. 7, pp. 676–82, Jun. 2012.

[226] F. Aguet, D. Van De Ville, and M. Unser, "Model-based 2.5-d deconvolution for extended depth of field in brightfield microscopy.," *IEEE Trans. Image Process.*, vol. 17, no. 7, pp. 1144–53, Jul. 2008.

[227] B. Forster, D. Van De Ville, J. Berent, D. Sage, and M. Unser, "Complex wavelets for extended depth-of-field: a new method for the fusion of multichannel microscopy images.," *Microsc. Res. Tech.*, vol. 65, no. 1–2, pp. 33–42, Sep. 2004.

[228] K. J. Clark *et al.*, "In vivo protein trapping produces a functional expression codex of the vertebrate proteome.," *Nat. Methods*, vol. 8, no. 6, pp. 506–15, Jun. 2011.

[229] S. C. McMillan *et al.*, "Regeneration of breeding tubercles on zebrafish pectoral fins requires androgens and two waves of revascularization.," *Development*, vol. 140, no. 21, pp. 4323–34, Nov. 2013.

[230] S. V. Strelkov, H. Herrmann, and U. Aebi, "Molecular architecture of intermediate filaments.," *Bioessays*, vol. 25, no. 3, pp. 243–51, Mar. 2003.

[231] E. Fuchs and S. Raghavan, "Getting under the skin of epidermal morphogenesis.," *Nat. Rev. Genet.*, vol. 3, no. 3, pp. 199–209, Mar. 2002.

[232] H. H. Bragulla and D. G. Homberger, "Structure and functions of keratin proteins in simple, stratified, keratinized and cornified epithelia.," *J. Anat.*, vol. 214, no. 4, pp. 516–59, Apr. 2009.

[233] M. Ruse, A. Lambert, N. Robinson, D. Ryan, K. J. Shon, and R. L. Eckert, "S100A7, S100A10, and S100A11 are transglutaminase substrates.," *Biochemistry*, vol. 40, no. 10, pp. 3167–73, Mar. 2001.

[234] R. L. Eckert, A.-M. Broome, M. Ruse, N. Robinson, D. Ryan, and K. Lee, "S100 proteins in the epidermis.," *J. Invest. Dermatol.*, vol. 123, no. 1, pp. 23–33, Jul. 2004.

[235] Z. Nemes and P. M. Steinert, "Bricks and mortar of the epidermal barrier.," *Exp. Mol. Med.*, vol. 31, no. 1, pp. 5–19, Mar. 1999.

[236] A. M. Kraemer, L. R. Saraiva, and S. I. Korsching, "Structural and functional diversification in the teleost S100 family of calcium-binding proteins.," *BMC Evol. Biol.*, vol. 8, p. 48, Feb. 2008.

[237] J. Bakkers, M. Hild, C. Kramer, M. Furutani-Seiki, and M. Hammerschmidt, "Zebrafish DeltaNp63 is a direct target of Bmp signaling and encodes a transcriptional repressor blocking neural specification in the ventral ectoderm.," *Dev. Cell*, vol. 2, no. 5, pp. 617–27, May 2002.

[238] B. L. Hogan, "Bone morphogenetic proteins: multifunctional regulators of vertebrate development.," *Genes Dev.*, vol. 10, no. 13, pp. 1580–94, Jul. 1996.

[239] M. C. Mullins *et al.*, "Genes establishing dorsoventral pattern formation in the zebrafish embryo: the ventral specifying genes.," *Development*, vol. 123, no. 1995, pp. 81–93, Dec. 1996.

[240] V. H. Nguyen, B. Schmid, J. Trout, S. A. Connors, M. Ekker, and M. C. Mullins,

"Ventral and lateral regions of the zebrafish gastrula, including the neural crest progenitors, are established by a bmp2b/swirl pathway of genes.," *Dev. Biol.*, vol. 199, no. 1, pp. 93–110, Jul. 1998.

[241] M. Fürthauer, B. Thisse, and C. Thisse, "Three different noggin genes antagonize the activity of bone morphogenetic proteins in the zebrafish embryo.," *Dev. Biol.*, vol. 214, no. 1, pp. 181–96, Oct. 1999.

[242] I. H. A. Ali and D. P. Brazil, "Bone morphogenetic proteins and their antagonists: current and emerging clinical uses.," *Br. J. Pharmacol.*, vol. 171, no. 15, pp. 3620–32, Aug. 2014.

[243] C. Brocker, D. Thompson, A. Matsumoto, D. W. Nebert, and V. Vasiliou, "Evolutionary divergence and functions of the human interleukin (IL) gene family.," *Hum. Genomics*, vol. 5, no. 1, pp. 30–55, Oct. 2010.

[244] S. Werner, "Keratinocyte growth factor: a unique player in epithelial repair processes.," *Cytokine Growth Factor Rev.*, vol. 9, no. 2, pp. 153–65, Jun. 1998.

[245] S. Werner and H. Smola, "Paracrine regulation of keratinocyte proliferation and differentiation.," *Trends Cell Biol.*, vol. 11, no. 4, pp. 143–6, Apr. 2001.

[246] H.-H. Li *et al.*, "Interleukin-19 upregulates keratinocyte growth factor and is associated with psoriasis.," *Br. J. Dermatol.*, vol. 153, no. 3, pp. 591–5, Sep. 2005.

[247] Y. Zhang *et al.*, "Processing and activation of pro-interleukin-16 by caspase-3.," *J. Biol. Chem.*, vol. 273, no. 2, pp. 1144–9, Jan. 1998.

[248] N. A. Thornberry *et al.*, "A novel heterodimeric cysteine protease is required for interleukin-1 beta processing in monocytes.," *Nature*, vol. 356, no. 6372, pp. 768–74, Apr. 1992.

9 Appendix

9.1 <u>Superficial keratinocyte changes during epidermal wound closure</u>

Rebecca Richardson and colleagues described that the characteristic microridges on the apical surface of the superficial keratinocytes disappear progressively after laser injury and the cells themselves elongate in a directed manner [25]. It was found during wound healing of the cichlid fish *Hemichromis bimaculatus* that intermediate cells can either acquire basal keratinocyte function or superficial cell characteristics [168]. However, it is not well described what happens to the superficial keratinocytes after the closure of full-thickness wounds in zebrafish. Our investigation shows that there is a relief in tissue tension almost immediately as the wound closes caused by intercalation of intermediate cells basal keratinocytes. But there is no indication that intermediate cells intercalate with superficial cells in our wound models. This implies that the massive cell elongation and flattening of the superficial keratinocytes is not immediately resolved and causes a potential weakness of the epidermal barrier at least in the initial closure phase. Concomitantly, this means a higher risk of further injuries and micro-ruptures to the animal. It remains unclear, how long exactly this tissue tension persists on the superficial cells and when or how it is counteracted. Initial time lapse imaging of full-thickness wound closure by Philipp Knyphausen showed that the neo-epidermis most likely is not subjected to the described tissue tension due to an overshoot reaction during closure [25]. However, the adjacent epidermis has not been examined beyond the initial closing phase in our studies. Hence, investigation needs to be extended to at least four days after injury to find out when the flattening of the wound-adjacent superficial keratinocytes is back to normal levels and when the microridges are back. This however only answers when the tension is released but more interesting would be how it is resolved. Most likely this is achieved by an increase of proliferation. It will be intriguing to find out whether exclusively the superficial cells give rise to new superficial keratinocytes by horizontal proliferation or whether the intermediate or basal keratinocytes contribute to the replenishment of the outermost layer as well in a vertical proliferation and 'differentiation'-like manner. The latter could be visualised by lineage tracing experiments using for example *krt19* or *p63* driven creERT2 in combination with floxed GFP or RFP transgenic lines.

In future, it would be interesting to see if superficial keratinocytes undergo de-differentiation to some degree and if the loss of microridges is a sign for that. As mentioned in the introduction, microridges are 100 nm high elevations on the apical surface of superficial keratinocytes mainly formed by an actin bundle network [11]. The loss of microridges could imply a complete reorganisation of the whole cytoskeleton, firstly to recruit more cell membrane to be used to for cell elongation and increase of the cell surface. Secondly it could result in more free actin to prepare the cell for higher motility by making it less rigid and more flexible.

Another indicator for a de-differentiation, the superficial keratinocyte-specific transgenic line *krt4:gfp*, thus far did not give an indication for a decreased *krt4* promoter activity. Nevertheless, other markers for superficial keratinocytes such as S100 proteins might be altered and be a read-out for a more flexible intermediate filament cytoskeleton.

Indications for possible changes in the characteristics of superficial keratinocytes where found during a collaboration with the Steven Ekker lab at the Mayo Clinic in Rochester, Minnesota. This lab utilised a transposon-based mutagenesis approach which caused gene trapping with concomitant generation of a fusion protein with RFP. This made it possible to examine gene function and simultaneously observe expression patterns [228]. One of these lines, GBT1010 showed strong expression of the fusion protein in the superficial keratinocytes which completely disappeared from the neo-epidermis at 8 hours after full-thickness wounding but not the adjacent keratinocytes. The expression was restored at four days post wounding. Re-epithelialisation, however, was not affected in this line (unpublished data, Fig. 9.1). Initial attempts to locate the site of integration indicate an intergenic insertion in close vicinity to a close relative to the S100 protein family, the *ictacalcin2* gene, but was not confirmed yet. Nevertheless, this demonstrates that the changes in superficial keratinocytes go beyond elongation and the loss of microridges.
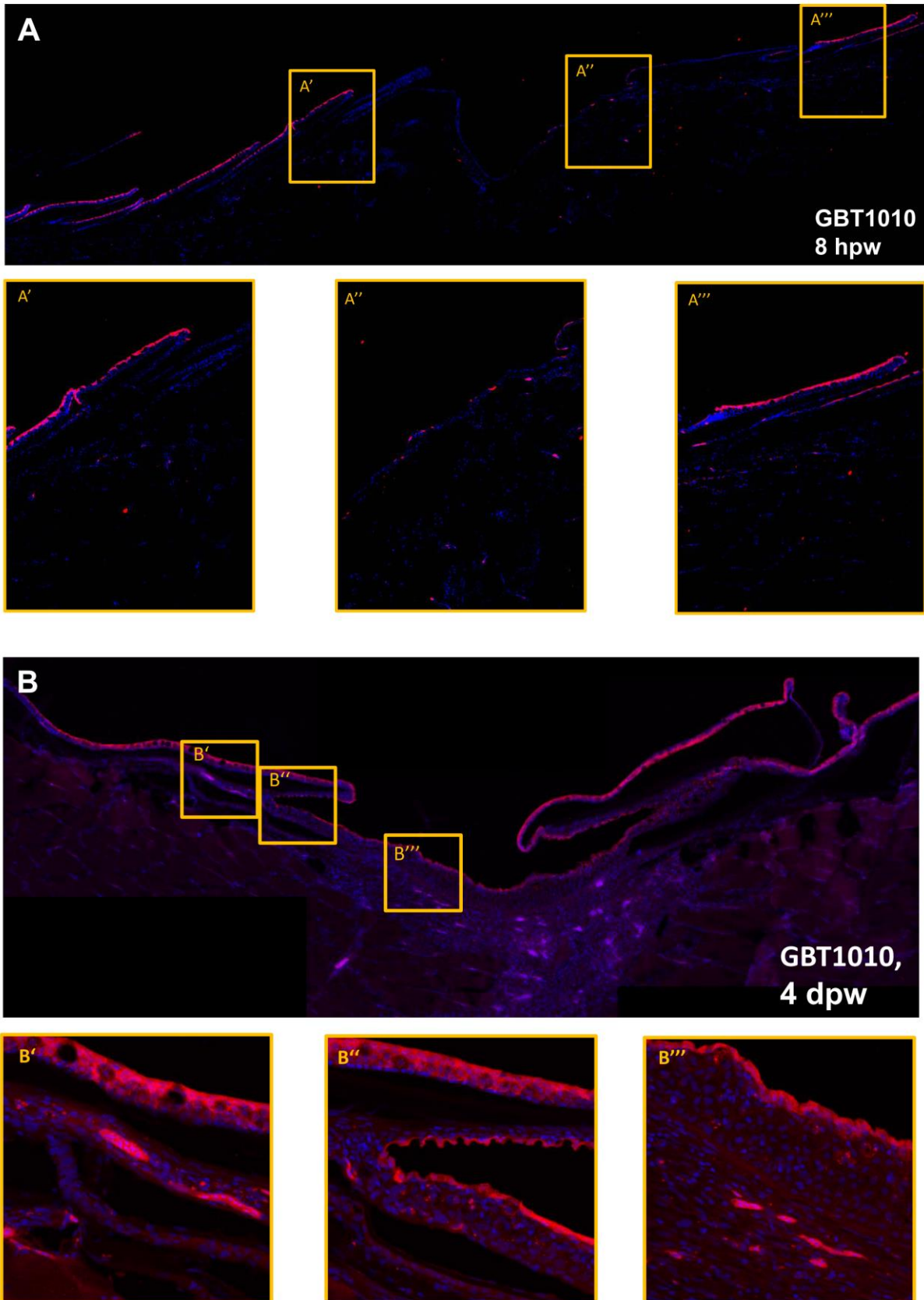
Figure 9.1: RFP signal of GBT1010 at eight hours (**A**) and four days post wounding (**B**). The RFP signal was found in the outermost layer of the epidermis, on the apical side of the scales in unwounded regions (**A'** and **A'''**) and was absent in the neo-epidermis at eight hours (**A''**). The RFP

signal reappeared in the neo-epidermis by four days post wounding (**B'''**). Additionally to the apical side of scales (**B'**) it was also found in a thin layer on the basal side of scales in the scale pocket (**B''**). Anterior is to the left. I wounded and sectioned the fish together with Erica Benard, the immunohistochemistry was done by Erica Benard and Joy Armistead as well as the imaging afterwards.

9.2   <u>Breeding tubercle formation in zebrafish</u>

Zebrafish epidermis is generally not cornified or keratinised like the mammalian epidermis. The exception are specialised appendages called breeding tubercles that are found on the lower jaw of both male and female adult zebrafish as well as the dorsal side of the male pectoral fins. These structures showed differentiation of keratinocytes that resembles the mammalian epidermal cornification in several but not all aspects [7], [229].

For instance, p63, a marker for basal and intermediate keratinocytes of zebrafish, was restricted to the basal layer exclusively under the breeding tubercles, which is highly similar to mammalian epidermis. Proliferation is usually found in both basal and intermediary keratinocytes in regular zebrafish epidermis but was limited to the basal layer as it is the case in mammalian epidermis. Further, the tight junctions were not found in the superficial layer anymore but in the second-tier layer as it is observed in mammalian epidermis. The superficial keratinocytes of breeding tubercles (also termed cap cells) show a high degree of keratinisation and a condensed nucleus, indicating decreased transcriptional activity. However, the terminal differentiation was not as pronounced as it is seen in mammalian epidermis, since the cap cells still had a nucleus and organelles and were still alive [2], [7].

Importantly, the cap cell layer of breeding tubercles was shed and renewed in a continuous manner with constant cell replacement from the basal layer of keratinocytes, implicating a tissue homeostasis that is highly similar to mammalian epidermis. During his work with fish carrying a mutation in the TA isoform of the transcription factor p63 (TAp63), Boris Fischer found that both breeding tubercle size and number is decreased, indicating a defect in regeneration and homeostasis within the tubercles. TAp63 contains an N-terminal transactivation domain that is required for gene transcription. Boris Fischer further observed that this isoform of p63 induces notch signalling and caspase3 activation to initiate the formation of breeding tubercles. He was able to show that the double mutants for *tap63* and *p53* exhibit an even stronger decrease in breeding tubercle size and number. The proposed pathway stated that deltaN p63 (ΔNp63, an isoform lacking the N-terminal TA domain) acts as an inhibitor for the differentiation regulator TAp63 and drives proliferation in both basal and intermediary layers. Due to the limited ΔNp63 domain underneath the breeding tubercles TAp63 could drive differentiation of the upper layers and simultaneously maintain homeostasis in the basal layer by a yet unknown target of caspase3 [7].

During my master thesis, I helped to identify the time point of breeding tubercle development as well as the rhythm of renewal in adult fish. I continued on the proposed pathway and tried to identify the unknown mechanism that restricts ΔNp63 to the basal layer and the downstream mediator by which caspase3 can drive

differentiation cell autonomously and tissue homeostasis in a non-cell autonomous manner. To achieve this, Erica Benard and I collected breeding tubercle-bearing pectoral fins of adult male and tubercle-devoid pectoral fins of adult female zebrafish and extracted the RNA with TRIzol reagent according to the manufacturer. In collaboration with the Cologne Centre for Genomics (CCG), RNA sequencing was performed and evaluated for candidates that were linked to keratinocyte keratinisation or cornification in other systems.

As shown in table T 9.1, genes that were expected according to our own studies, such as p63, notch signalling components, caspase3 [7] appeared in the data and were differentially regulated according to our expectation. *tumour protein p63* was upregulated 2.02-fold, *notch receptor* was upregulated 3.12-fold, notch ligands *jagged* were upregulated between 1.58- and 2.54-fold and *caspase3a* was upregulated 2.42-fold in male pectoral fins compared to female pectoral fins. This demonstrated that the experimental setup was suited for comparison and the sequencing result led to a detection of known breeding tubercle regulators. It did not allow conclusion on whether false-positives are picked up as well and how high the false-positives and breeding tubercle unrelated genes within the dataset was.

Nevertheless, I set out to examine the differential expression levels of putative ΔNp63 regulators and casp3 targets as well as keratinisation- and cornification-associated genes. Table T 9.2 shows all genes which fell into these categories.

Keratins are components of the intermediary filaments [230] and can be used as markers for basal (Krt5 and Krt14) or terminally differentiating suprabasal keratinocytes (Krt1 and Krt10) [231], [232]. Although the cap layer of breeding tubercles is highly keratinised, only one keratin (*krt95*) was strongly upregulated in male pectoral fins (7.21-fold up). Most other keratin family members were downregulated. Alex Kolak performed in situ hybridisation analysis for several differentially expressed genes and found a highly specific staining in breeding tubercles for *krt95*, while neighbouring epidermis was completely lacking the signal (Alex Kolak, Bachelor thesis, Fig. 9.2).

Transglutaminases, envoplakin and S100 proteins have been linked with keratin-crosslinking during the cornification process of mammalian keratinocytes [3], [4], [6], [233], [234]. *transglutaminase1* was found by Boris Fischer already to be upregulated in the breeding tubercles of adult zebrafish, strongly supporting the keratinisation of the suprabasal cells [7]. In the RNA sequencing data set, most transglutaminases were only slightly increased and some, like *tgm8* were downregulated. Envoplakin is a structural protein in the cornified envelope of mammalian keratinocytes and serves in parallel to periplakin and involucrin as a scaffold for other structural components [1], [235]. But aside from periplakin, it is the only cornification-associated protein of the group which is found in the zebrafish genome (zfin.org). To see envoplakin upregulated in our comparison led to the hypothesis that, similar to the mammalian cornification [235], envoplakin might serve as an anchor and base for further keratinisation in zebrafish breeding tubercle differentiation as well. S100 proteins are calcium donors for Transglutaminases that catalyse crosslinking reactions during keratinisation [233], [234] and are conserved in zebrafish as well [236]. Surprisingly, most zebrafish S100 proteins were downregulated in male pectoral fins. During my master thesis I observed as well, that an antibody raised against S100 proteins (DakoCytomation, Z0311) stained superficial keratinocytes of regular epidermis but

was completely absent in developing breeding tubercles (Master thesis Manuel Metzger).

Bone morphogenic proteins (Bmps) are regulators of ΔNp63 [237] and are thereby interesting candidates during breeding tubercle development and maintenance. Bmps are extracellular ligands, that belong to the TGF-ß superfamily [238] and key factors during the specification of the dorsoventral axis during embryogenesis [239]–[241]. Our RNA sequencing demonstrates that bmp16 and bmp7b are upregulated 3.84-fold and 1.52-fold respectively. Additionally, several *bmp receptors* show increased gene expression, while known antagonists of Bmps *gremlin*, *noggin* and *chordin* [242] are downregulated. This opens speculation on whether elevated Bmp signalling could induce ΔNp63 mediated proliferation in basal layers under breeding tubercles, thereby mediating increased tissue turnover in breeding tubercles compared to regular epidermis.

Interleukins (ILs) are extracellular cytokines that regulate several different processes such as cell migration, proliferation and differentiation of mainly leukocytes [243]. Moreover, they have been implicated in both the regulation of keratinocyte proliferation and differentiation via a paracrine loop [244]–[246]. Caspases have been shown to process the pro-peptide version of ILs, thus leading to their activation [247], [248]. Hence, we were interested whether they show differential expression between male and female pectoral fins and thereby might indicate a function in either differentiation or differentiation. *il23* and *il16* were both upregulated 1.7-fold and 2-fold respectively while for example *il4* and *il10* were strongly downregulated (5- and 4-fold). This result indicates a differential use of IL signalling in breeding tubercles and suggests a function in breeding tubercle maintenance that will be intriguing to investigate in future.

In total 4474 genes have been found to be regulated 2-fold or higher between tubercle-bearing and devoid pectoral fins and need to be confirmed in future. But prior to further analysis, the number of candidate genes has to be decreased by excluding sex dimorphism-related genes that are differentially regulated by sex hormones for example. Further, a comparison between *tap63, p53* double mutants and wild type fish is likely to aid the search for downstream regulators of differentiation in breeding tubercles. However, it would not help to find upstream regulators.

T 9.1: RNA sequencing control list

Fold-change	Gene
2,02	tumor protein p63 [Source:ZFIN;Acc:ZDB-GENE-030819-1]
3,12	notch 3 [Source:ZFIN;Acc:ZDB-GENE-000329-5]
2,54	jagged 2 [Source:HGNC Symbol;Acc:HGNC:6189]
2,1	jagged 2b [Source:ZFIN;Acc:ZDB-GENE-011128-3]
1,97	jagged 1b [Source:ZFIN;Acc:ZDB-GENE-011128-4]
1,58	jagged 1a [Source:ZFIN;Acc:ZDB-GENE-011128-2]
2,42	caspase 3, apoptosis-related cysteine peptidase a [Source:ZFIN;Acc:ZDB-GENE-011210-1]

T 9.2: p63 regulators, caspase targets, keratinisation or cornification-associated genes

Fold-change	Gene
7,21	keratin 95 [Source:ZFIN;Acc:ZDB-GENE-040718-88]
-5,02	keratin type 1 c19e [Source:ZFIN;Acc:ZDB-GENE-050506-95]
-3,64	keratin 96 [Source:ZFIN;Acc:ZDB-GENE-030131-221]
-3,72	keratin, type 1, gene 19d [Source:ZFIN;Acc:ZDB-GENE-060316-1]
-3,51	keratin 17 [Source:ZFIN;Acc:ZDB-GENE-060503-86]
-3,26	keratin 18 [Source:ZFIN;Acc:ZDB-GENE-030411-6]
-2,78	keratin 97 [Source:ZFIN;Acc:ZDB-GENE-040718-78]
-2,37	keratin 91 [Source:ZFIN;Acc:ZDB-GENE-040801-181]
-2,36	keratin 15 [Source:ZFIN;Acc:ZDB-GENE-040426-2931]
-2,21	keratin, type 1, gene c5 [Source:ZFIN;Acc:ZDB-GENE-060316-3]
1,79	keratin 222 [Source:ZFIN;Acc:ZDB-GENE-070912-343]
-1,64	keratin 94 [Source:ZFIN;Acc:ZDB-GENE-061027-116]
-1,52	keratin 5 [Source:ZFIN;Acc:ZDB-GENE-991110-23]
-1,44	keratin 4 [Source:ZFIN;Acc:ZDB-GENE-000607-83]
-1,36	keratin 8 [Source:ZFIN;Acc:ZDB-GENE-030411-5]
1,07	keratin 93 [Source:ZFIN;Acc:ZDB-GENE-060421-4592]
-4,45	bone morphogenetic protein 2b [Source:ZFIN;Acc:ZDB-GENE-980526-474]
3,84	bone morphogenetic protein 16 [Source:ZFIN;Acc:ZDB-GENE-100115-1]
2,98	bone morphogenetic protein receptor, type IAb [Source:ZFIN;Acc:ZDB-GENE-040912-150]
3,05	bone morphogenetic protein receptor, type II a (serine/threonine kinase) [Source:ZFIN;Acc:ZDB-GENE-070618-1]
2,16	bone morphogenetic protein receptor, type II b (serine/threonine kinase) [Source:ZFIN;Acc:ZDB-GENE-070618-2]
-2,2	bone morphogenetic protein 8a [Source:ZFIN;Acc:ZDB-GENE-030912-13]
1,99	bone morphogenetic protein receptor, type IAa [Source:ZFIN;Acc:ZDB-GENE-000502-1]
-1,92	bone morphogenetic protein 2a [Source:ZFIN;Acc:ZDB-GENE-980526-388]
-1,8	bone morphogenetic protein 4 [Source:ZFIN;Acc:ZDB-GENE-980528-2059]
-1,96	bone morphogenetic protein 6 [Source:ZFIN;Acc:ZDB-GENE-050306-42]
1,52	bone morphogenetic protein 7b [Source:ZFIN;Acc:ZDB-GENE-060929-328]
1,23	bone morphogenetic protein 15 [Source:ZFIN;Acc:ZDB-GENE-030131-6115]
1,17	bone morphogenetic protein 7a [Source:ZFIN;Acc:ZDB-GENE-000208-25]
1,1	bone morphogenetic protein 3 [Source:ZFIN;Acc:ZDB-GENE-030131-7192]
1,09	bone morphogenetic protein 1b [Source:ZFIN;Acc:ZDB-GENE-060818-2]
1,08	bone morphogenetic protein 10 [Source:ZFIN;Acc:ZDB-GENE-060526-211]
1,01	bone morphogenetic protein 5 [Source:ZFIN;Acc:ZDB-GENE-040426-1413]
-5,41	gremlin 2, DAN family BMP antagonist b [Source:ZFIN;Acc:ZDB-GENE-030911-9]
-4,39	noggin 3 [Source:ZFIN;Acc:ZDB-GENE-990714-8]
-2,99	noggin 2 [Source:ZFIN;Acc:ZDB-GENE-991206-14]
-1,29	noggin 5 [Source:ZFIN;Acc:ZDB-GENE-090618-2]
-1,22	noggin 1 [Source:ZFIN;Acc:ZDB-GENE-991206-8]

-1,01	chordin [Source:ZFIN;Acc:ZDB-GENE-990415-33]
3,28	transglutaminase 1 [Source:HGNC Symbol;Acc:HGNC:11777]
4,13	transglutaminase 1 like 2 [Source:ZFIN;Acc:ZDB-GENE-110408-37]
2,38	transglutaminase 1 like 4 [Source:ZFIN;Acc:ZDB-GENE-050913-29]
-2,32	transglutaminase 8 [Source:ZFIN;Acc:ZDB-GENE-120718-3]
-2,24	transglutaminase 5, like [Source:ZFIN;Acc:ZDB-GENE-110411-176]
2,65	transglutaminase 1 [Source:HGNC Symbol;Acc:HGNC:11777]
1,93	transglutaminase 1 like 1 [Source:ZFIN;Acc:ZDB-GENE-060503-139]
-2,1	transglutaminase 2, like [Source:ZFIN;Acc:ZDB-GENE-050420-97]
1,45	transglutaminase 1 [Source:HGNC Symbol;Acc:HGNC:11777]
1,2	transglutaminase 2b [Source:ZFIN;Acc:ZDB-GENE-030131-2576]
3,44	caspase 8 associated protein 2 [Source:ZFIN;Acc:ZDB-GENE-030826-8]
2,42	caspase 3, apoptosis-related cysteine peptidase a [Source:ZFIN;Acc:ZDB-GENE-011210-1]
2,32	caspase 7, apoptosis-related cysteine peptidase [Source:ZFIN;Acc:ZDB-GENE-050522-506]
-2,27	caspase 6, apoptosis-related cysteine peptidase, like 1 [Source:ZFIN;Acc:ZDB-GENE-041010-48]
2,5	caspase 6, apoptosis-related cysteine peptidase, like 2 [Source:ZFIN;Acc:ZDB-GENE-060312-12]
-1,66	caspase b, like [Source:ZFIN;Acc:ZDB-GENE-090311-53]
-1,6	caspase a [Source:ZFIN;Acc:ZDB-GENE-000616-3]
-1,49	caspase 8, apoptosis-related cysteine peptidase, like 1 [Source:ZFIN;Acc:ZDB-GENE-070608-1]
1,41	caspase 8, apoptosis-related cysteine peptidase [Source:ZFIN;Acc:ZDB-GENE-000713-1]
-1,26	caspase 3, apoptosis-related cysteine peptidase b [Source:ZFIN;Acc:ZDB-GENE-070607-1]
1,23	caspase 8, apoptosis-related cysteine peptidase, like 2 [Source:ZFIN;Acc:ZDB-GENE-070608-2]
1,2	caspase b [Source:ZFIN;Acc:ZDB-GENE-020812-1]
1,19	caspase 2, apoptosis-related cysteine peptidase [Source:ZFIN;Acc:ZDB-GENE-030825-3]
1,05	caspase 9, apoptosis-related cysteine peptidase [Source:ZFIN;Acc:ZDB-GENE-030825-5]
1,02	caspase 6, apoptosis-related cysteine peptidase [Source:ZFIN;Acc:ZDB-GENE-030825-4]
2,55	envoplakin a [Source:ZFIN;Acc:ZDB-GENE-030829-19]
2,96	envoplakin [Source:HGNC Symbol;Acc:HGNC:3503]
-3,05	S100 calcium binding protein Z [Source:ZFIN;Acc:ZDB-GENE-050522-69]
-2,82	S100 calcium binding protein V1 [Source:ZFIN;Acc:ZDB-GENE-080407-1]
-3,23	S100 calcium binding protein W [Source:ZFIN;Acc:ZDB-GENE-080407-2]
-3,05	S100 calcium binding protein V2 [Source:ZFIN;Acc:ZDB-GENE-030131-8909]
-1,97	S100 calcium binding protein, beta (neural) [Source:ZFIN;Acc:ZDB-GENE-040718-290]
-1,76	S100 calcium binding protein A11 [Source:ZFIN;Acc:ZDB-GENE-070717-5]
-1,95	S100 calcium binding protein A10b [Source:ZFIN;Acc:ZDB-GENE-040426-1937]
-1,73	S100 calcium binding protein A1 [Source:ZFIN;Acc:ZDB-GENE-040916-1]
1,32	S100 calcium binding protein U [Source:ZFIN;Acc:ZDB-GENE-030131-3121]
-1,27	S100 calcium binding protein S [Source:ZFIN;Acc:ZDB-GENE-040822-31]
1	S100 calcium binding protein A10a [Source:ZFIN;Acc:ZDB-GENE-041010-35]
-5,07	interleukin 4 [Source:ZFIN;Acc:ZDB-GENE-100204-1]
-3,99	interleukin 10 [Source:ZFIN;Acc:ZDB-GENE-051111-1]
4,75	interleukin 17 receptor A1b [Source:ZFIN;Acc:ZDB-GENE-110914-185]
-3,42	interleukin 10 receptor, beta [Source:ZFIN;Acc:ZDB-GENE-050909-1]
3,15	interleukin 17 receptor A1a [Source:ZFIN;Acc:ZDB-GENE-070705-242]
2,52	interleukin 12 receptor, beta 2a, like [Source:ZFIN;Acc:ZDB-GENE-080107-6]
2,33	interleukin 17 receptor D [Source:ZFIN;Acc:ZDB-GENE-020320-5]
2,08	interleukin 13 receptor, alpha 2 [Source:ZFIN;Acc:ZDB-GENE-030521-10]
2,02	interleukin 16 [Source:ZFIN;Acc:ZDB-GENE-130103-3]
1,7	interleukin 23 receptor [Source:ZFIN;Acc:ZDB-GENE-080107-5]
-1,65	interleukin 34 [Source:ZFIN;Acc:ZDB-GENE-050419-150]
-1,65	interleukin 13 [Source:ZFIN;Acc:ZDB-GENE-100727-2]
1,58	interleukin 10 receptor, alpha [Source:ZFIN;Acc:ZDB-GENE-070905-4]
-1,75	interleukin 17c [Source:ZFIN;Acc:ZDB-GENE-061031-5]
-1,51	interleukin 22 receptor, alpha 2 [Source:ZFIN;Acc:ZDB-GENE-060512-349]
-1,5	interleukin 15, like [Source:ZFIN;Acc:ZDB-GENE-041111-173]
-1,5	interleukin 15, like [Source:ZFIN;Acc:ZDB-GENE-041111-173]
-1,44	interleukin 21 [Source:ZFIN;Acc:ZDB-GENE-120510-4]
-1,4	interleukin 1, beta [Source:ZFIN;Acc:ZDB-GENE-040702-2]
-1,39	interleukin 15 [Source:ZFIN;Acc:ZDB-GENE-060213-2]

1,5	interleukin 11a [Source:ZFIN;Acc:ZDB-GENE-051019-1]
-1,28	interleukin 7 receptor [Source:ZFIN;Acc:ZDB-GENE-080110-7]
1,33	interleukin 26 [Source:ZFIN;Acc:ZDB-GENE-060209-4]
-1,37	interleukin 12a [Source:ZFIN;Acc:ZDB-GENE-060724-1]
-1,2	interleukin 19 like [Source:ZFIN;Acc:ZDB-GENE-071121-1]
1,22	interleukin 11b [Source:ZFIN;Acc:ZDB-GENE-051019-2]
1,21	interleukin 12Ba [Source:ZFIN;Acc:ZDB-GENE-050525-3]
-1,11	interleukin 20 receptor, alpha [Source:ZFIN;Acc:ZDB-GENE-040724-249]
-1,12	interleukin 1 receptor-like 1 [Source:ZFIN;Acc:ZDB-GENE-060621-4]
-1,06	interleukin 22 [Source:ZFIN;Acc:ZDB-GENE-060209-3]
-1,03	interleukin 17d [Source:ZFIN;Acc:ZDB-GENE-061031-4]
-1,02	interleukin 6 receptor [Source:ZFIN;Acc:ZDB-GENE-080107-7]
1	interleukin 17 receptor A2 [Source:ZFIN;Acc:ZDB-GENE-060503-869]
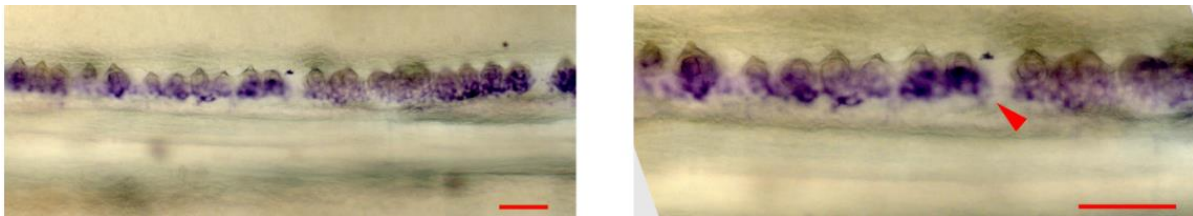
Fig. 9.2: *krt95* expression pattern in pectoral fins of adult male zebrafish. The in situ hybridisation revealed a highly specific expression pattern colocalising with breeding tubercles (red arrow). Staining and pictures were made by Alex Kolak, scale bar 100 µm.

10 Acknowledgements

Seba, you are a brother to me! I'm incredible happy that I have you around me and I'm happy for the distraction you offer. Even though we have gone separate ways over time we are still in contact and that means a lot to me!

Mellie, my dear sister, I love you and I am incredibly proud of you. Even though you have been through tough times you have gone your way and that makes me happy.

Stefan, Angela, Dominic und Sarah. Ihr wurdet zu meiner Familie und ich wäre nicht an der Stelle, an der ich heute bin wenn ihr nicht gewesen wärt. Ohne Fragen und Zögern habt ihr mich in eure Mitte aufgenommen und behandelt, als wäre ich Teil von euch. Ihr habt mir durch turbulente Zeiten geholfen und wart immer für mich da. Ich werde euch das nie vergessen.

The last position in the acknowledgements is reserved for the centre of my life. Nadine, we shared ups and downs and you have supported me in all my decisions. You were the person that always believed in me and thought I can achieve everything I want. Meeting you was the best thing that happened to me. You have been the constant in my life for 17 years now and I hope you will be on my side for years to come because life would only be half as great if you wouldn't be. I love you!

11 Erklärung zur Dissertation

Ich versichere, dass ich die von mir vorgelegte Dissertation selbständig angefertigt, die benutzten Quellen und Hilfsmittel vollständig angegeben und die Stellen der Arbeit - einschließlich Tabellen, Karten und Abbildungen -, die anderen Werken im Wortlaut oder dem Sinn nach entnommen sind, in jedem Einzelfall als Entlehnung kenntlich gemacht habe; dass diese Dissertation noch keiner anderen Fakultät oder Universität zur Prüfung vorgelegen hat; dass sie - abgesehen von unten angegebenen Teilpublikationen - noch nicht veröffentlicht worden ist sowie, dass ich eine solche Veröffentlichung vor Abschluss des Promotionsverfahrens nicht vornehmen werde. Die Bestimmungen dieser Promotionsordnung sind mir bekannt. Die von mir vorgelegte Dissertation ist von Prof. Dr. Matthias Hammerschmidt betreut worden.

_____

Ort, Datum   Manuel Metzger

Teilpublikationen:

R. Richardson *et al.*, "Re-epithelialization of cutaneous wounds in adult zebrafish combines mechanisms of wound closure in embryonic and adult mammals.," *Development*, vol. 143, no. 12, pp. 2077–88, 2016.

12 Lebenslauf

Persönliche Informationen

Name: Manuel Metzger

Geburtstag: 26.01.1985

Geburtsort: Lindau / Bodensee

Staatsangehörigkeit: deutsch

Schulausbildung

09. 1991 - 07. 1993   Grundschule Lindau-Oberreitnau

09. 1993 - 02. 1994   Grundschule Lindau-Reutin

02. 1994 - 07. 1995   Grundschule Lindau-Zech

09. 1995 - 06. 2005   Bodensee-Gymnasium Lindau, Abitur: 3,4

Weiterführende Ausbildung

10.2007 - 02.2011   Biologie-Studium an der Universität zu Köln mit Abschluss:

                              Bachelor of Science: 2,3

04.2011 - 04.2013   Biologie Studium an der Universität zu Köln mit Abschluss:

                              Master of Science: 1,7

Seit 05.2013   Promotion an der Universität zu Köln

                              Institut für Entwicklungsbiologie

                              Betreuer: Prof. Dr. Matthias Hammerschmidt

Publikationen

N. M. Feitosa *et al.*, "Hemicentin 2 and Fibulin 1 are required for epidermal-dermal junction formation and fin mesenchymal cell migration during zebrafish development.," *Dev. Biol.*, vol. 369, no. 2, pp. 235–48, Sep. 2012.

B. Fischer *et al.*, "p53 and TAp63 promote keratinocyte proliferation and differentiation in breeding tubercles of the zebrafish.," *PLoS Genet.*, vol. 10, no. 1, p. e1004048, Jan. 2014.

R. Richardson *et al.*, "Re-epithelialization of cutaneous wounds in adult zebrafish combines mechanisms of wound closure in embryonic and adult mammals.," *Development*, vol. 143, no. 12, pp. 2077–88, 2016.